The involvement of αB-crystallin in cancer

Chantal van de Schootbrugge

The involvement of αB-crystallin in cancer

Chantal van de Schootbrugge

COVER: **JULIE LEUTHOLD (www.flickr.com/julieleuthold)**
"TREE OF HOPE" Breast Cancer Survivor Tree

PRINTED BY: **IPSKAMP DRUKKERS, ENSCHEDE**

ONLINE: **HTTP://BOOKS.IPSKAMPDRUKKERS.NL/THESIS/207528-SCHOOTBRUGGE/**

ISBN: **9789462596399**

The research described in this thesis was performed at the Department of Biomolecular Chemistry, Nijmegen Centre for Molecular Life Sciences, Radboud University Nijmegen, The Netherlands and the Department of Radiation Oncology, Radboud University Nijmegen Medical Centre, The Netherlands. This work was financially supported by the Dutch Cancer Society (project number KUN 2007-3864).

The involvement of αB-crystallin in cancer

Proefschrift

ter verkrijging van de graad van doctor
aan de Radboud Universiteit Nijmegen
op gezag van de rector magnificus prof. dr. Th.L.M. Engelen,
volgens besluit van het college van decanen
in het openbaar te verdedigen op woensdag 8 juli 2015
om 14.30 uur precies

door
Chantal van de Schootbrugge
geboren op 21 augustus 1983
te Nunspeet

PROMOTOREN:
Prof. dr. G.J. Pruijn
Prof. dr. J.H.A.M. Kaanders

COPROMOTOREN:
Dr. W.C. Boelens
Dr. J. Bussink

MANUSCRIPTCOMMISSIE:
Prof. dr. B. Wieringa
Prof. dr. M.A.W. Merkx
Prof. dr. H.H. Kampinga (Universitair Medisch Centrum Groningen)

TABLE OF CONTENTS PAGE

ABBREVIATIONS

αB-STA	Non-phosphorylatable αB-crystallin
αB-STD	Pseudophosphorylated αB-crystallin
αB-WT	Wild-type αB-crystallin
AGO2	Argonaute 2
AKT	Protein kinase B
ANOVA	Analysis of variance
ARCON	Accelerated radiotherapy, carbogen, nicotinamide
ATP	Adenosine Tri-phosphate
BRCA	Breast Cancer susceptibility gene
BSA	Bovine Serum Albumine
CK	Cytokeratin
CRM1	Chromosome region maintenance 1
DFS	Disease-Free Surviva
DMEM	Dulbecco's modified Eagle's medium
DNA	Deoxyribonucleic acid
DOX	Doxycyclin
DTT	Dithiothreitol
EDTA	Ethylenediaminetetraacetic acid
EGF	Epithelial growth factor
EGFP	Enhanced Green Fluorescent Protein
EGFR	Growth factor receptor
EGTA	Ethylene glycol tetraacetic acid
EMEM	Eagle's minimal essential medium
EMT	Epithelial-to-Mesenchymal Transition
ER	Estrogen receptor
ER	Endoplasmic reticulum
ERK1/2	Extracellular regulated protein kinase1/2
ETS-1	E26 transformation-specific-1
FBX4	F-Box protein X4
FCS	Fetal Calf Serum
GFAP	Glial fibrillary acidic protein
GST	Glutathione S-transferase
GTP	Guanosine-5'-triphosphate
HEPES	4-(2-hydroxyethyl)-1-piperazineethanesulfonic acid
HER2	Epidermal growth factor receptor 2
HIF-1	Hypoxia-inducible factor 1
HNSCC	Head and neck squamous cell carcinoma
HSF1	Heat shock factor 1
HSP	Heat shock protein
IGC	Interchromatic granule cluster
IGF-1R	Insulin-like growth factor 1 receptor
LEDGF	Lens epithelial derived growth factor
LRC	Locoregional control
LRR	Locoregional recurrence
LUC	Luciferase
MAPK	Mitogen-activated protein kinase
MEK	Mitogen-activated protein kinase kinase
METS	Mitogenic Ets transcriptional suppressor
MFS	Metastasis-free survival
MK	Mitogen activated protein kinase-activated protein kinase
MOPS	3-(N-morpholino)propanesulfonic acid
MSK1	Mitogen- and stress-activated protein kinase-1
mTOR	Mammalian Target of Rapamycin
NAC	N-acetylcysteine
NADPH	Nicotinamide adenine dinucleotide phosphate
NMR	Nuclear Magnetic Resonance
NRF2	NF-E2-related factor 2
pAKT	phospho-AKT
PBS	phosphate-buffered saline
PHD	Prolyl hydroxylase
pERK1/2	phospho-ERK1/2
pmTOR	phospho-mTOR
POP1	Ribonucleases P/MRP protein subunit
PR	Progesterone receptor
RAS	Oncogene protein P21
ROC	Receiver operating characteristic
ROS	Reactive oxygen species
RT-PCR	Real-time polymerase chain reaction
SDS	Sodium dodecyl sulfate
SF-1	Splicing factor 1
SMA	Smooth muscle actin
SMN	Survival motor neuron
snRNP	Small nuclear ribonucleic particles
TMA	Tumor microarray
TRAIL	Tumor necrosis factor-related apoptosis-inducing ligand
VEGF	Vascular endothelial growth factor
VHL	Von Hippel-Lindau protein

CHAPTER 1
αB-CRYSTALLIN; A VERSATILE SMALL HEAT SHOCK PROTEIN

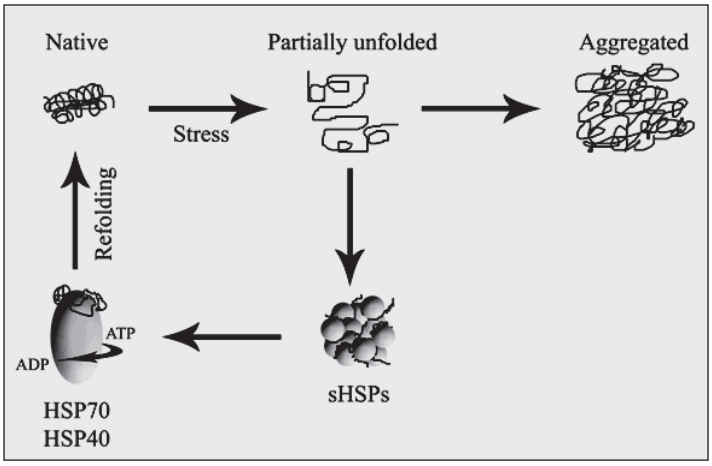

Chapter adapted from:
van de Schootbrugge C., Boelens W.C. (2011): *Introduction to Small Heat Shock Proteins.* Pages 1-27 in: Simon S., Arrigo A.P., editors. Small Stress Proteins and Human Diseases Nova Science Publishers, Inc.

In this thesis, the endeavor to elucidate the steps of cancer formation in which small heat shock protein αB-crystallin can intertwine is described. This introductory chapter is meant to provide background information on this protein to help understand how it can be involved in the development of cancer. Chapter 2 will provide an introduction on cancer formation. The emphasis will be on head and neck squamous cell carcinoma (HNSCC) and breast cancer, since these two types of cancers are the major research subjects in this thesis.

1. EVOLUTIONARY ASPECTS OF SMALL HEAT SHOCK PROTEINS

Back in 1894 α-crystallin, now known to be composed of αA- and αB-crystallin, was discovered as a structural protein in the mammalian eye lens (1). Differentiated lens fiber cells have the unique property, as do erythrocytes, that they lack protein turnover due to the absence of cellular organelles, such as nuclei and mitochondria. Yet, these cells must remain viable and their proteins must keep their functional integrity. To maintain transparency of the lens, aggregation of the ageing lens proteins must be avoided. The role of αA- and αB-crystallin, now also called HSPB4 and HSPB5, was stepwise unraveled in this process. Around 1973, the sequence of bovine αA- and αB-crystallin was determined by direct protein sequencing (2;3). Later, in 1982, it was realized that αA- and αB-crystallin belong to the family of sHSPs based on conspicuous sequence similarities with four *Drosophila melanogaster* sHSPs (4). Ten years later, by virtue of their ability to prevent the aggregation of unfolding proteins, αA- and αB-crystallin were recognized as molecular chaperones (5). However, their activity is generally considered as 'chaperone-like', because of their inability to refold proteins with the help of ATP.

One by one the other human sHSPs were discovered that share conspicuous sequence identity with αA- and αB-crystallin. At present, there are ten HSPB family members known, called HSPB1-10. These possess the α-crystallin domain as the defining feature of their evolutionary relationship (Figure 1 position 113 - 201).

Outside the α-crystallin domain, sHSPs have a low sequence similarity, although a few recurring motifs can be recognized. Noticeable is the "IPI/V" motif, which is localized in the C-terminal extension of a number of sHSPs (Figure 1, positions 218 - 220). This motif is thought to play both a structural and functional role in these proteins (6). In the N-terminal region several sHSPs display a SRLFDQxFG-like motif (Figure 1, positions 51 - 59); this motif has been pinpointed as important as well (7). Deleting this part affects the higher order assembly of the subunits and structural stability, as well as

the chaperone-like activity. The genes encoding HSPB1-10 are scattered over the different chromosomes. Only HSPB2 and αB-crystallin form an exception as they are arranged as a head-to-head gene pair on chromosome 11 (8). The chromosomal dispersal together with the sequence divergence, which amounts to 45 to 85%, suggests that the duplications responsible for these multiple genes occurred before the earliest divergence of present vertebrates. Indeed, in lower vertebrates orthologs of all mammalian sHSPs have been identified, except for HSPB10 (9;10). Based on a sequence alignment of human, mouse and chicken sHSPs, a maximum likelihood tree has been constructed, which facilitates the comparison of the evolutionary relationships between these proteins (Figure 2). It confirms that HSPB4-6 are each other's closest relatives, as are HSPB2 and HSPB3. HSPB9 and HSPB10 are clearly the earliest diverging and most deviating sHSPs.

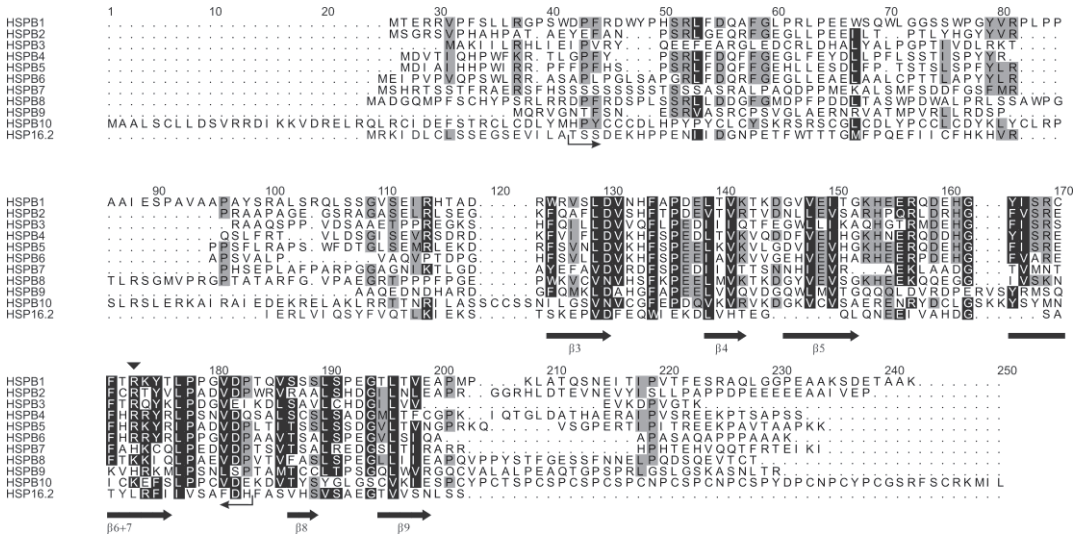

Figure 1. Alignment of the human HSP27 (HSPB1), HSPB2, HSPB3, αA-crystallin (HSPB4), αB-crystallin (HSPB5), HSP20 (HSPB6), cvHSP (HSPB7), HSPB8, HSPB9 and HSPB10. ClustalW v1.83 (11) was used to align the sequences at default settings. The C-terminal part (residues 200-250) was manually edited using GeneDoc (12). Similarity groups used for shading are DN, EQ, ST, KR, FYW and LIVM. Residues in black are conserved in 8-10 sequences and those in grey in 6-7. The β-strands that were identified by solid state NMR in HSPB5 (13) are indicated below the alignment. The arrowhead indicates the structurally and functionally important Arg in the α-crystallin domain. The N-terminal SRLFDQxFG motif is located at positions 51 to 59, the C-terminal IPI/V motif at positions 218 to 220 (14).

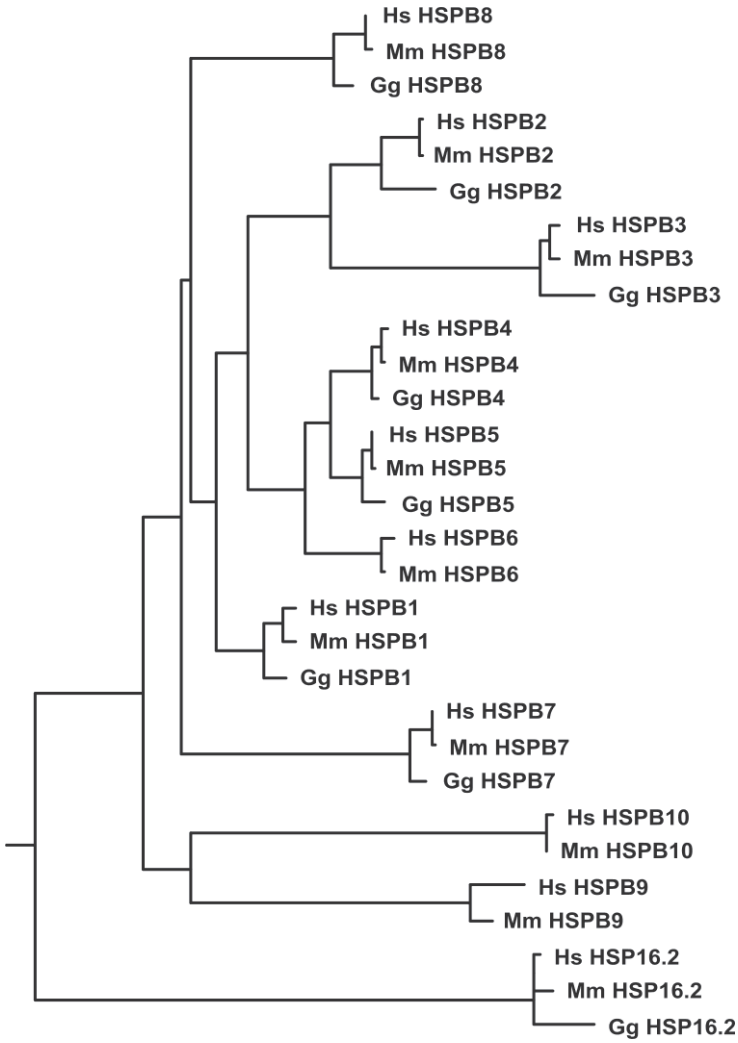

Figure 2. Maximum Likelihood tree of HSP27 (HSPB1), HSPB2, HSPB3, αA-crystallin (HSPB4), αB-crystallin (HSPB5), HSP20 (HSPB6), cvHSP (HSPB7), HSPB8, HSPB9 and HSPB10. The online PhyML program (http://atgc.lirmm.fr/phyml/ (15)) was used to calculate the Maximum Likelihood tree of the human (Hs), mouse (Mm) and chicken (Gg) proteins, using 500 bootstrap sets, the WAG model of substitution, estimated proportion of invariable sites, estimated gamma correction parameter and a BIONJ tree as starting point. The alignment used for this calculation was made with ClustalW v1.83 at default settings.

2. STRUCTURE OF sHSPs

One of the most notable features of sHSPs is their organization as large oligomeric structures. Human sHSPs, such as αB-crystallin, αA-crystallin and HSP27 (HSPB1), exhibit a remarkable polydispersity in their oligomeric states. Through interactions with themselves or with other sHSPs, homo- and hetero-oligomers can be formed containing up to 50 subunits (5;16;17). The quaternary structures are dynamic, which is reflected by rapid subunit exchange under native and stress conditions (18;19). The subunit exchange is markedly enhanced at high temperature, which may be a key factor in preventing protein aggregation during heat denaturation.

The α-crystallin domain plays a central role in sHSP oligomerization across the evolutionary spectrum and is necessary to form the dimeric building blocks of which larger oligomeric structures are composed (20;21). Structurally important residues in the amino acid sequences of the α-crystallin domain are well conserved, and the predicted secondary structure shows a clear conservation of β-strand structures (Figure 1, (10;13;22;23)). These β-strands assemble into a β-sandwich.

The α-crystallin domain is surrounded by a hydrophobic N-terminal region and a rather short and polar C-terminal extension. The last 10-18 residues of the C-terminal extension are highly flexible as determined by NMR studies (24). This extension acts as a solubilizer to counteract the hydrophobicity associated with the target protein sequestration. Many of these C-terminal extensions contain a short β-strand formed by the conserved IPI/V motif. This strand is able to make contact with a hydrophobic patch in the α-crystallin domain of a neighboring subunit, which is critical for the oligomer formation (20;25) and is important for the functioning of sHSPs (26;27). Also, the N-terminal region plays an important role in the stabilization of the assembly and the formation of oligomers (28). This likely occurs via hydrophobic contacts between the N-terminal regions of the subunits that are buried inside the oligomer (25).

In the case of αB-crystallin, a model based on NMR observations reveals that the α-crystallin domain is responsible for dimer formation, that the C-terminal regions are responsible for defining hexameric units, and the N-terminal region and α-crystallin domain are responsible for higher-order multimerization (28). In addition, crystallization studies demonstrated that a highly conserved arginine, position 173 in Figure 1, plays an important role in the formation of intermolecular interactions that mediate the assembly of higher-order structures and substrate binding. Mutations of this residue in human sHSPs are associated with cataract, myopathy and neuropathy.

Delbecq and Klevit reviewed several studies in which the oligomerization of αB-crystallin was addressed. Taken together, these studies indicate that αB-crystallin forms

oligomers composed of 10-40 monomers. They conclude that αB-crystallin exists as a distribution of oligomeric species that include dimers, hexamers, and multiples of hexamers, and that the relatively short lifetime and small population of the smaller species limit their detection under native conditions (29-31).

3. EXPRESSION OF sHSPS

The expression of sHSPs changes during development and may vary depending on the local stress conditions. Under non-stress conditions αB-crystallin, HSP27, HSP20 and HSPB8 are ubiquitously expressed in most tissues, with a high expression level in cardiac and skeletal muscle (32-38). αA-crystallin is abundantly expressed together with αB-crystallin in the eye lens (39;40), but is almost undetectable in other tissues (33;36;41;42). Interestingly, the expression patterns of the head-to-head located genes for HSPB2 and αB-crystallin are not identical, indicating that besides shared, promoter-preferred transcriptional regulatory elements are present as well (43-45).

Several, but not all, members of the sHSP family exhibit a pattern of inducible expression in response to heat or other physiological stimuli. Heat shock is a commonly applied type of stress to determine whether the transcription of a gene is promoted by heat shock transcription factor 1 (HSF1). So far, it has been shown that αB-crystallin, HSP27 and HSPB8 are heat shock inducible, while no induction has been observed for HSPB2, HSPB3, αA-crystallin and HSP20 (46). Many other types of stress, such as osmotic or arsenite stress (47), hypoxia/reoxygenation (48), oxidative stress (49), exposure to heavy metals (50), and enforced exercise (51;52) can increase the expression of different sHSP as well.

Certain diseases are associated with enhanced sHSP expression, especially neurodegenerative disorders and cancer. In brains of Alzheimer's patients, increased expression of αB-crystallin and HSP27 has been observed in the activated glial cells close to the pathological lesions (53). Also, high levels of constitutive HSP27 and αB-crystallin expression have been detected in several cancers, particularly those of carcinoma origin (54).

4. POST-TRANSLATIONAL MODIFICATIONS

Some, if not most, sHSPs can be phosphorylated, allowing to control their functioning by signal transduction pathways (55;56). Most sHSPs have their phosphorylatable serine residues localized in the N-terminal region. Phosphorylation of αB-crystallin

occurs at S19 by an unknown protein kinase, at S45 by ERK1/2 MAPK and at S59 by MK2 (57). In response to a wide variety of stimuli, growth factors, differentiation-inducing agents, tumor necrosis factor, oxidative stress or heat shock, αB-crystallin is rapidly phosphorylated, which modulates its activity (54). Upon phosphorylation the distribution of oligomers shifts from mainly large αB-crystallin oligomers toward higher levels of smaller oligomeric structures (58;59).

Moreover, mimicking phosphorylation enhances chaperone activity, preventing the aggregation of most of the target proteins that were studied (60). The cellular distribution of αB-crystallin can change as well. Phosphorylation of serines 45 and 59 leads to translocation into the cell nuclei. αB-crystallin is localized here in so-called "speckles", which are nuclear bodies that function as storage compartments for splicing factors (61). In response to stress, αB-crystallin is also known to interact with the three major cytoskeletal components, i.e. microtubules, intermediate filaments and microfilaments (62). Phosphorylation is probably important for these interactions, since αB-crystallin phosphorylated at S59 colocalizes with the cytoskeleton components, such as vinculin in focal adhesion and desmin in aggregates (63).

Beside phosphorylation other modifications can occur as well. Deamidation is an aging-related process, resulting in the replacement of an amide group by a carboxylate group. This introduces a negative charge, which has been shown to affect the oligomeric structure and chaperone-like activity of αB-crystallin (64). Other well-known modifications on α-crystallin are truncation (65;66), oxidation (67), glycation (68-71) and racemization/isomerization (72). The structural and functional implications of these modifications are not known yet.

5. INTERACTIONS WITH UNFOLDING PROTEINS

During unfolding of a protein, hydrophobic residues from the interior will be exposed and are responsible for aggregation. These protein aggregates can accumulate over time, which may lead to age-related diseases. Progress in understanding the mechanism of chaperone function of sHSPs has been achieved mainly by a biochemical approach using purified sHSPs and model substrate proteins. The chaperone activity is measured by its ability to prevent thermally or chemically induced aggregation of a substrate. Aggregation is a late step in the unfolding pathway (Figure 3). By interacting with partially unfolded proteins, sHSPs inhibit the aggregation process (25). Both the N-terminal and C-terminal regions have been postulated to be involved in the chaperone function of sHSPs (20). This is based on cross-linking studies with a hydrophobic probe or small substrates. Once formed, complexes between substrates and sHSPs are

very stable. Electron microscopic images have revealed large complexes, of which the morphology depends on the nature of the substrate proteins and the respective sHSPs (73). In addition to these large complexes, still larger assemblies of substrate proteins and sHSPs have been observed when an excess of non-native proteins is present. In patients with aggregation diseases large accumulations of sHSPs with protein aggregates have been observed. Diseases associated with αB-crystallin containing aggregates are, Rosenthal fibers in Alexander disease (74), Lewy bodies in Parkinson's disease (75) and inclusion bodies in myopathies (76). In these situations, the incorporation of sHSPs into protein aggregates is believed to facilitate the reactivation or degradation of substrates. Although the critical role of sHSPs in conferring stress tolerance to cells is well established (77), their role in cellular protein refolding is less clear. The binding capacity can reach one substrate protein per sHSP subunit, indicating that sHSPs can be a major contributor to the chaperoning capacity of a cell. sHSP chaperone activity does not require ATP, and release of the bound substrate with subsequent refolding can be accomplished through interaction with HSP70 (78;79).

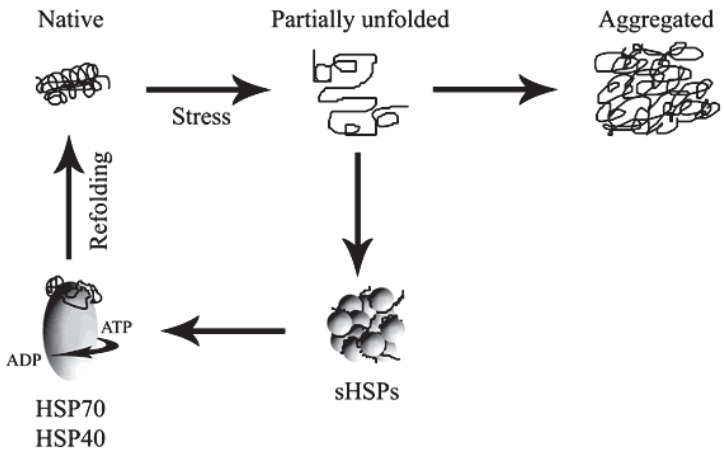

Figure 3. Model for the chaperone functioning of sHSPs under stress conditions. Unfolding of native proteins can lead to (insoluble) aggregations. Partially unfolded proteins can be bound by sHSPs, keeping them in a soluble state, which is accessible for HSP70 and HSP40. These ATP-dependent chaperones can refold the protein to its native state (14).

Studies in *Escherichia coli* and *Saccharomyces cerevisiae* revealed the involvement of a cooperative cellular chaperone network connected to the sHSP-substrate complexes comprised of HSP70-HSP40 (80-83) (Figure 3).

6. INTERACTIONS WITH PARTNER PROTEINS

Interaction between proteins is a key element in building structures and functional protein complexes. These interactions are often transient, and are essential for the activities associated with biological processes. αB-crystallin interacts with other sHSPs to form mixed oligomeric complexes and with unrelated partners to fulfill a broad range of functions, which makes this protein very versatile. Here we focus on four important functions, involving hetero-oligomer formation, cytoskeletal organization, apoptosis and protein degradation.

6.1. INTERACTIONS BETWEEN sHSPS

In muscle cells, seven sHSPs are abundantly expressed (Figure 4). In these cells, hetero-oligomers of sHSPs may form and fulfill specific functions (84). A number of studies describe such mixed sHSP complexes, for example complexes containing αB-crystallin/HSP27 (85) and αB-crystallin/HSP20 (86). Not much is known about the occurrence, composition and dynamics of hetero-oligomeric sHSP complexes *in vivo*, and whether particular compositions are preferred above others. This is in part caused by the difficulty to avoid subunit exchange after cell lysis, which makes it difficult to quantify subunit ratios. Furthermore, the affinity of their interactions is variable and can be regulated in a way that will affect the size of the oligomers (87).
Well-known factors that influence the interaction between different sHSPs are phosphorylation (88) and temperature (89;90). The changes occurring in composition and size of hetero-oligomers may alter the accessibility of particular sites within the complex and could be a way to influence the functioning of sHSPs in the cellular environment. As explained, the expression of sHPSs can vary extensively between different cells types and therefore it is unclear if these interactions are muscle cell specific or more broadly occurring.

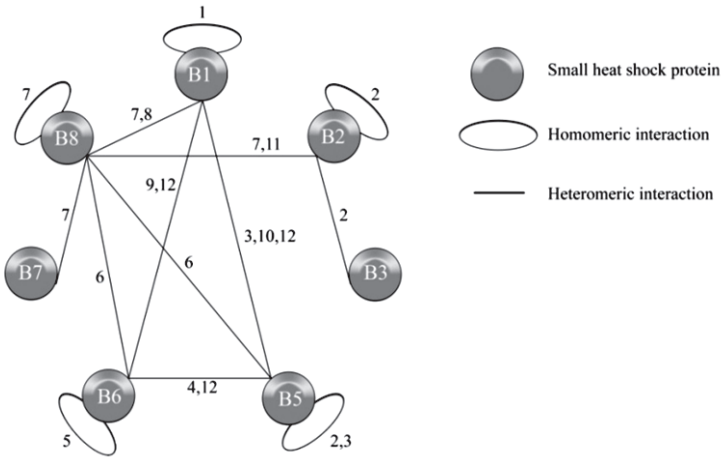

Figure 4. Interactions between the seven sHSPs expressed in muscle cells. Several complexes can be formed through interactions of sHSPs with themselves (homomeric interaction) or with other sHSPs (heteromeric interaction). 1: homomeric interaction HSP27 (HSPB1) (91), 2: homomeric interaction HSPB2, homomeric interaction αB-crystallin (HSPB5) and interaction between HSPB2 and HSPB3 (87), 3: homomeric interaction αB-crystallin (HSPB5) and interaction between HSP27 (HSPB1) and αB-crystallin (HSPB5) (92), 4: interaction between αB-crystallin (HSPB5) and HSP20 (HSPB6) (93), 5: homomeric interaction HSPB6 (59), 6: interaction between αB-crystallin (HSPB56 and HSPB8 and interaction between HSP20 (HSPB6) and HSPB8 (94), 7: homomeric interaction HSPB8, interaction between cvHSP (HSPB7) and HSPB8, interaction between HSP27 (HSPB1) and HSPB8 and interaction between HSPB2 and HSPB8 (95), 8: interaction between HSP27 (HSPB1) and HSPB8 (96), 9: interaction between HSPB6 and HSP27 (HSPB1) (90), 10: interaction between αB-crystallin (HSPB5) and HSP27 (HSPB1) (97), 11: interaction between HSPB2 and HSPB8 (98), 12: interaction between αB-crystallin (HSPB5) and HSP27 (HSPB1) (14;17).

6.2. INTERACTIONS WITH THE CYTOSKELETON

sHSPs binds and thereby modulates the structure of the cytoskeleton, an activity which is linked to their protective function. αB-crystallin, as well as HSP27, are able to associate with actin (99). The interaction appears to be vital for the stability of the actin network and is important for cardiac and skeletal muscle development (100). Moreover, αB-crystallin associates with intermediate filaments, especially type III filaments such as vimentin (101), desmin (102) and glial fibrillary acidic protein (GFAP) (103) and regulates the assembly of intermediate filaments and assists in their recovery from stress by preventing untimely filament–filament interactions that would

otherwise lead to aggregation. The missense mutation R120G in αB-crystallin, which reduces the chaperone-like activity (104), leads to accumulation of desmin-positive sarcomeric inclusions (105). αB-crystallin also plays a critical role in Alexander disease to prevent aggregation of GFAP and the formation of Rosenthal fibers (106). In the absence of stress, αB-crystallin interacts directly with tubulin and microtubule-associated proteins to promote microtubule assembly and under stress protects against microtubule depolymerization (107-109). This action is dependent on the oligomeric state of αB-crystallin (110).

6.3. INTERACTION WITH APOPTOSIS-INDUCING PROTEINS

Apoptosis is a controlled way of cell death and several stimuli can trigger this process. There are two pathways leading to apoptosis: the intrinsic (mitochondrial) pathway and the extrinsic (death receptor) pathway. Increased expression of sHSPs during a stress response correlates with better cell survival after the stress, which might be an effect of the inhibition of the apoptotic process. αB-crystallin interacts with pro-apoptotic factors interfering with their function and therefore leading to inhibition of the intrinsic pathway (111). *In vitro*, αB-crystallin is capable of binding procaspase 3 cleavage products (112) and thus may inhibit the intrinsic apoptosis pathway *in vivo* (113). Posttranslational modifications are important as well for the protective function of αB-crystallin, as phosphorylation of S45 and S59 protects against C2-ceramide and staurosporine-induced cell death (114).
It is clear that αB-crystallin and also other sHSPs aid in cell survival in several different ways. However, the significance and physiological importance of each interaction in the regulation of the apoptotic process is still not well understood and needs further investigations.

6.4. INTERACTION WITH THE DEGRADATION MACHINERY

sHSPs have been implicated in the ubiquitin-proteasome pathway, a process in which ubiquitin ligases mark substrate proteins for degradation by the proteasome. This is executed by covalent addition of multiple ubiquitin molecules. αB-crystallin can interact with F-Box protein X4 (FBX4), which forms an E3 ubiquitin ligase, together with Skp1 and Cullin1 (115). One of the targets of this FBX4/αB-crystallin E3 ligase is phosphorylated cyclin D1 (116). This protein accounts for the G1 to S phase transition in the cell cycle and its degradation leads to diminished cell proliferation. Thus by

interacting with FBX4, αB-crystallin may interfere with cell growth. αB-crystallin can also bind to one of the fourteen subunits of the 20S proteasome, possibly guiding the substrate to the proteasome (117).

7. INVOLVEMENT OF sHSPS IN DISEASE

As molecular chaperones, sHSPs protect protein structure and activity, thereby counteracting the deleterious effects of disease processes. The expression of various sHSPs is therefore upregulated under different pathological conditions. sHSPs guard against ischemic and reperfusion injury caused by myocardial infarction or stroke, prevent cataract in the mammalian eye lens and protect against aggregation and/or toxicity of α-synuclein in Parkinson's disease, huntingtin in Huntington's disease and amyloid in Alzheimer's disease. The exact role of sHSPs in these diseases might be linked to their chaperone activity in providing a first line of defense against misfolded proteins (118-121), and in modulating the aberrant protein interactions that trigger pathogenic cascades.

On the other hand, mutated sHSPs contribute to cell malfunctioning. For instance, mutants of sHSPs are implicated in diseases such as myofibrillar myopathy, cardiomyopathy, neuropathies and cataract. These pathologies result from the misfolding and progressive aggregation of the mutated sHSP, although the molecular mechanism is likely to be different for each type of disease (54;122). The myofibrillar myopathy associated R120G mutation in αB-crystallin has been found to modify the properties of αB-crystallin, such as oligomerization and *in vitro* chaperone-like activity (104), and to increase its affinity to desmin (123). This mutation in αB-crystallin results in misfolding and progressive aggregation, and subsequent association with desmin filaments to form αB-crystallin /desmin/amyloid-positive aggresomes (124). The D109H mutation found in a family with five affected individuals, results in the same clinical phenotype as the R120G mutation (125). Interestingly, molecular modelling shows that D109 and R120 interact with each other during dimerization of αB-crystallin, which might explain why these mutations give the same phenotype. Several members of the HSPB family have been implicated in cancer development, of which αB-crystallin and HSP27 are most well studied. αB-crystallin can act as an oncoprotein in breast cancer and its expression is correlated with a poor clinical outcome (126). High expression induces neoplastic changes and invasive properties in human mammary epithelial cells, which are inhibited by αB-crystallin phosphorylation. Phosphorylation affects oligomerization and anti-apoptotic activities of αB-crystallin.

Remarkably, αB-crystallin does not increase the tumorigenic potential under all circumstances. In fact, the protein can reduce cancer progression by forming, together with FBX4, an E3 ligase able to ubiquitinate and subsequently degrade cyclin D1 (see 6.4) (116). Cyclin D1 is a well-known oncoprotein, and decrease in αB-crystallin levels likely lead to elevated cyclin D1 levels, which may drive tumor formation. Studies by Lin and co-workers show that in a subset of breastcancer-derived cell lines the expression of αB crystalline is decreased, which indeed coincided with cyclin D1 stabilization (116).

The expression of sHSPs is also involved in another aspect of cancer biology. sHSP expression is associated with cellular resistance to cytostatic anticancer drugs (127;128). Some of these drugs, in particular cisplatin (129), vincristine and colchicine (108) have been demonstrated to enhance αB-crystallin and HSP27 expression, leading to even higher resistance to these drugs. Thus, high expression of sHSPs may impair the efficiency of the clinical treatments using chemotherapeutic agents and could ultimately affect the survival of the patient.

CHAPTER 2
CANCER FORMATION

Title: Clara Jacobi
Image from the History of Medicine (NLM)
Copyright Statement: The National Library of Medicine believes this item to be in the public domain.

Clara Jacobi was a Dutch woman who, in 1689, had a tumor removed from her neck.

In this thesis the research is focused on two types of solid tumors; head and neck squamous cell carcinoma (HNSCC) and breast cancer. This chapter will provide an introduction on how solid tumors are generally formed and describes the major characteristics of these two kinds of tumors. Moreover, metastasis formation and the presence of hypoxic regions in solid tumors will be discussed.

1. SOLID TUMORS

A tumor is formed when cells exhibit uncontrolled cell division. If the tumor is benign, the lump of cells can often be removed and in most cases does not regrow. If the tumor is able to intrude and destroy adjacent tissues, it is termed malignant and cancerous (130).

There are different kinds of cancer, depending on the type of cell from which the cancer originates. *Carcinomas* begin in epithelial cells of the skin or in endothelial cells that cover internal organs. *Sarcomas* develop from bone, muscle, cartilage, fat, muscle, blood vessels or connective or supportive tissue. *Lymphoma* and *leukemia* start in the blood-forming (hematopoietic) cells. There are *central nervous system cancers*, which begin in the brain or spinal cord. *Blastoma* originates from precursor cells and usually occurs in children.

A solid tumor, the type of tumors on which this chapter will be focused, consists of two distinct compartments: the *parenchyma*, which are the neoplastic cells and the *stroma*, which is comprised of nonmalignant supporting tissue, connective tissue, inflammatory cells and blood vessels (131).

High throughput sequencing data reveal that numerous mutations are involved in tumorigenesis (132-134). All kinds of point mutations, translocations, amplifications and deletions may contribute to cancer development (132-134). Using bioinformatic analysis, it has become clear that many core signaling pathways and processes are affected by these mutations (135). Most cells require alterations on at least six important areas of cell signaling and functioning, which collectively make transformation to a cancer cell feasible: self-sufficiency in growth signaling, insensitivity to anti-growth signaling, evasion of programmed cell death, limitless replication, sustained angiogenesis and tissue invasion and metastasis (Figure 1) (136). All these alterations uncouple cell growth from extracellular stimuli (137;138) and cells obtain characteristics that promote growth and cell survival, ultimately leading to evolution of a tumor (139;140). The affected genes can be subdivided into two categories. The first category is formed by the tumor suppressor genes, which become

inactivated upon so called loss-of-function mutations. Normally, these genes encode for proteins that function in the inhibition of the cell cycle or inhibit proliferation, like p53 and pRb (141;142). The other category consists of the proto-oncogenes, which after 'gain of function' mutations become oncogenes. Example are the cell cycle regulator cyclin D1 and Epidermal Growth Factor Receptor 2 (HER2, also known as HER2/neu or ERBB2), an epidermal growth factor receptor able to activate several signaling pathways (143;144).

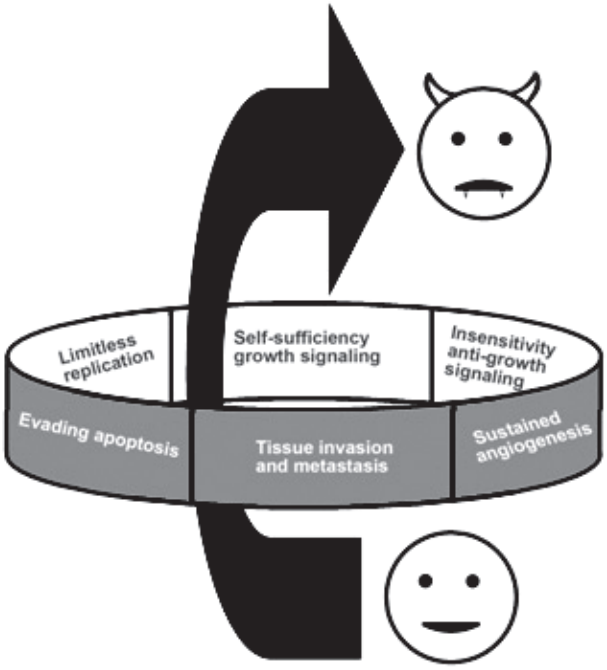

Figure 1. Physiological alterations required for cellular transformation into a cancerous cell. Cells need to become self-sufficient in growth signaling, insensitive to antigrowth signaling, unable to die by apoptosis and perform limitless replications, stimulate sustained angiogenesis and ultimately able to invade tissues to form metastasis. Figure is based on (136).

Mutations usually increase the activity of the encoded protein or increase expression of the gene. Novel mutations can arise for example due to errors during DNA replication or mutations can be acquired via exposure to a broad range of environmental and occupational carcinogens (145;146). The accumulation of mutations also drives tumor progression, meaning that cancers can become more and more malignant over time (147;148) (Figure 2).

2. HNSCC AND BREAST CANCER

Head and neck squamous cell carcinoma (HNSCC) is the sixth most common cancer worldwide and accounts for 6% of all cancers (149;150). Although prognosis gradually improved over the past 40 years, the overall 5 year survival rate is still only around 50%. Most important risk factors for the development of HNSCC are tobacco use, alcohol consumption (151) and viral infections, most notably with HPV (152;153). Genetic predisposition plays a role as well (154).

Several oncogenic mutations specific for oral cancer, a subtype of HNSCC, have been established. An effect of these mutations can be an elevated production of growth factor TGF-α, which binds to epidermal growth factor receptor (EGFR, also termed HER1) (155-157). Also, EGFR itself can be constitutive activated by mutations, like deletion of the N-terminal ligand-binding domain, deletion of the C-terminus, preventing downregulation after ligand binding or overexpression (158-162). Also intracellular messengers (like the RAS family members) and transcription factors (for example cyclin D1) are altered. Moreover, mutations in tumor suppressor genes like p53, p16 and doc-1 have been described (157;163).

Breast cancer is a leading cause of death from cancer among women. Using gene expression profiling, the heterogeneous group of breast cancer tumors can be divided in several subsets, of which the most well-known are normal breast-like, luminal A and B, HER2-enriched and basal-like breast tumors (164). An immunohistochemical difference between these groups can be found in expression of the estrogen receptor (ER), progesterone receptor (PR) and HER2 receptor (Table 1). The group of breast cancers lacking the expression of the three receptors, ER, PR and HER2, but with overexpression of for example EGFR, is referred to as triple negative. These tumors often show the basal-like gene expression pattern, including expression of basal-like marker CK5/6 and smooth muscle actin (SMA) and this type accounts for 15% of all breast cancer cases. The different tumor subtypes vary in their prognosis and is the worst for patients with the triple negative/basal-like subtype (165).

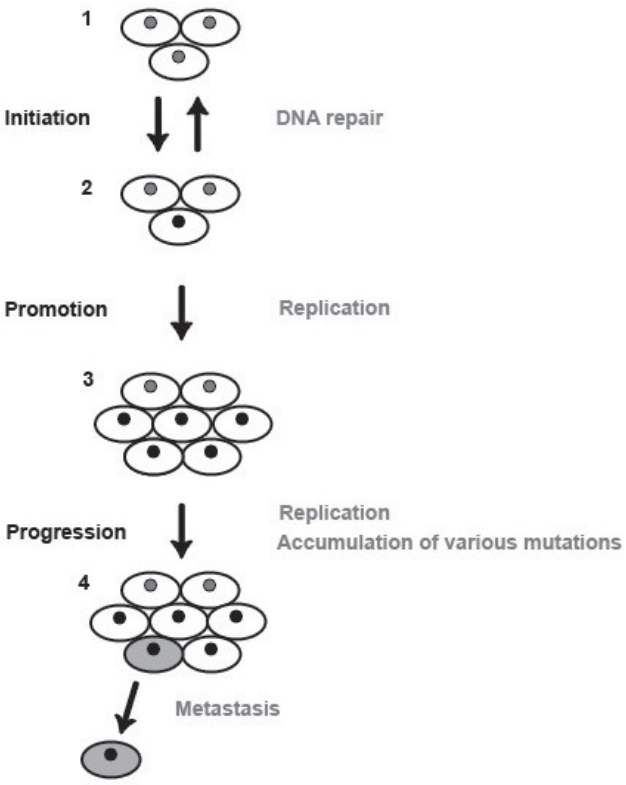

Figure 2. Cellular transformation leading to formation of a malignant tumor. Due to DNA replication errors and effects of exogenous carcinogens, mutations can arise (initiation, 2, black nucleus). If a cell is able to repair the mutation, the cell is again unaffected (DNA repair, 1, all nuclei have the normal grey phenotype). If the mutation is not repaired and inactivates a tumor suppressor gene or activates a proto-oncogene, a phenotype can arise causing uncontrolled replication of the affected cell, leading to solid tumor formation (promotion, 3). Ultimately, genomic instability can lead to the accumulation of even more mutations, leading to a tumor showing genomic heterogeneity between cells (progression, 4) and presenting more malignant behavior (metastasis). Figure is adapted from (148).

Many mutations are described to be present in breast cancer tissue. In 80% of the familial hereditary breast cancers, BRCA1 or BRCA2 are affected. These proteins are functioning in the DNA damage response pathway and malfunctioning causes susceptibility to an instable genome (166). Also mutations of signal transduction mediators (oncogenes as mTOR and RAS, cell cycle modulators as cyclin D1 and

tumor suppressor genes p53, p27 and PTEN) have been described (167). Overexpression of EGFR has been described as well, especially in the basal-like subtype (Table 1), only overexpression is not as common as for example in HNSCC (168).

Table 1. Receptor status of different breast cancer subtypes (168).

Breast cancer subtype	Receptor
Luminal A	ER+ and/or PR+, HER2-
Luminal B	ER+ and/or PR+, HER2+
Normal breast-like	ER-, PR-, HER2-
Basal-like	ER-, PR-, HER2-, EGFR+*
HER2-enriched	ER-, PR-, HER2+

* Expression of basal-like markers

3. METASTASIC MECHANSIMS OF SOLID TUMORS

Some types of cancer cells are prone to spread to other parts of the body through the blood and lymph systems. This process is termed metastasis formation (130). Organs to which solid tumors preferentially spread and in which secondary tumors are generally formed are the lungs, liver, brain and bone. Both HNSCC and breast cancer are prone to metastasis formation (169). Generally, many steps are necessary for cell spreading to occur from the primary tumor site to a distant site. This process is known as the metastatic cascade. First, the so-called Epithelial-to-Mesenchymal Transition (EMT) occurs. During EMT, epithelial cells acquire characteristics similar to less specialized mesenchymal cells (170;171). Secondly, tumor cells become dissociated from the tumor. Normally, cells would undergo anoikis, which is cell death induced by inappropriate loss of cell adhesion. Hence, anoikis suppression is required for tumor cells to be able to metastasize to distant sites (172;173). As a third step, neighboring tissue is invaded. In many tumors, a basal lamina separates nests of tumor cells from stroma and at sites where the lamina is incomplete, often tumor invasion occurs (174). Thus, tumor cells must acquire the ability to invade and migrate (130). Many proteins are involved in the process of cell migration, and in metastasizing tumors mutations in the genes encoding for example integrins, which are transmembrane receptors that mediate the attachment between cells and their surroundings, can be found (175-177). The fourth step entails intravasation into pre-existing and newly formed blood and

lymph vessels. Normally, angiogenesis is rare and occurs mainly during wound healing and the female reproductive cycle. The growth of new vessels is controlled by a balance of angiogenic activators and angiogenic inhibitors (130;178;179). During the "angiogenic switch", upon which a tumor activates vascularisation, this balance is disturbed (137). A major player in angiogenesis is vascular endothelial growth factor (VEGF) (180). Tumor cells are transported to distant sites in the body through blood- or lymph vessels (fifth step). In the sixth step of the metastatic cascade, cells extravasate from vessels. In the seventh and final step, outgrowth of metastases occurs (130). There are differences between the different types of cancer regarding the propensity to metastasize, the extent of metastasis and the sites to which tumors metastasize. The last few years there has been much focus on the discovery of gene targets that regulate metastasis or can act as biomarkers for metastasis formation.

4. HYPOXIC REGIONS AND REACTIVE OXYGEN SPECIES IN SOLID TUMORS

When a tumor reaches a size of 1-2 mm, tumor formation is hampered due to the limitation of diffusion of O_2 and nutrients. If growth occurs beyond this limit without formation of new blood vessels, another phenomenon arises, which is the development of hypoxic regions within these tumors. Hypoxia is a condition in tissues were oxygen pressure is less than 5 to 10 mmHg (0.66 – 1.32% O_2) (181).

The best-characterized hypoxia response pathway is via hypoxia-inducible factor-1 (HIF-1). HIF-1 consists of the constitutively expressed HIF-1β and HIF-1α, of which the latter is regulated in an oxygen dependent way. In normoxic areas of the tumor, prolyl hydroxylases (PHD) modify Pro-402 and Pro-564 of HIF-1α in a reaction that uses O_2 as a substrate. Hydroxylated HIF-1α interacts with the Von Hippel-Lindau protein (VHL). This protein is part of an E3 ubiquitin ligase complex, of which binding ultimately leads to proteasomal degradation of HIF-1α (182).

In hypoxic regions, HIF-1α is stabilized by suppressed breakdown and subsequently transported to the nucleus, where it dimerizes with HIF-1β, forming the HIF-complex. This binds to hypoxia response element (5'-G/ACGTG-3') with help of coactivator CBP/p300. Binding of HIF-1 to CBP/p300 is regulated by the factor inhibiting HIF-1 (FIH-1), which uses O_2 as a substrate to hydroxylate HIF-1α at Asn-803, thereby preventing the binding to CBP/p300 (181). Targets of HIF-1 signaling can be divided into the categories: glucose transporters and glycolysis, angiogenesis, survival and proliferation (183). The presence of hypoxia is correlated to worse clinical outcome (184-186) and is associated with therapeutic resistance and metastatic progression

(183;187-193). Moreover, HIF-1α is overexpressed in many cancers (182). There are two different kinds of hypoxia: acute and chronic. Chronic hypoxia arises when the vasculature provides limited blood flow capacity. Acute hypoxia arises, when enough blood vessels are present only these are leaking or partially blocked, thereby preventing O_2-rich blood from reaching the inner part of the tumor (181). Multiple studies have shown that the blood flow in tumors can be irregular. This is responsible for hypoxia and reoxygenation phases, which is called intermittent hypoxia (194-198). Tumor cells exposed to cyclic hypoxia/reoxygenation showed much greater upregulation of metastasis-related genes (187), thus not only hypoxia itself, but reoxygenation as well can have detrimental effects.

In vivo studies have demonstrated that hypoxia/reoxygenation transitions are associated with transient increased levels of reactive oxygen species (ROS) (199;200). Underlying molecular mechanisms are not completely characterized yet. Both the respiratory system of the mitochondria, as well as NADPH oxidases have been implicated as sources of elevated ROS levels in situations of hypoxia/reoxygenation (201). Other mechanisms could lead to ROS formation as well. In the middle of a hypoxic region, often a necrotic centre is present (181;202), especially in HNSCC, which may stimulate ROS formation (202). Elevation of ROS levels has an important role in tumor development (203;204). Moderate increase in ROS levels that, lethal to a cell, lead to enhanced DNA oxidation. As a result, genetic instability and accumulation of oncogenic mutations in proto-oncogenes, tumor suppressor genes, and other genes will occur, leading to dysfunction and neoplastic cell transformation and/or further tumor progression (203) (Figure 2).

5. CANCER TREATMENT OPTIONS

To assess the prognosis of the patient, tumors are pathologically classified. For a long time been this was mainly based on histopathologic classification where characteristics seen upon light microscopy of biopsy specimens are studied (205). Another well-known classification method to predict tumor progression is tumor staging using the TNM system. Staging attempts to measure the extent of tumor spread within a patient on the basis of parameters as the size of the primary tumor (T), the degree of spread to lymphnodes (N) and the presence of distant metastasis (M) (206), though these methods do have shortcomings. A different TNM scale is required for every type of tumor and scoring is subjective and not always reproducible. Moreover, tumors are heterogeneous, thus a risk of sampling error exists for the histopathological

classification. Also, as a result of tumor progression, predictions of tumor behavior are not straightforward (147). Therefore there is a need of biomarkers, which can help in determining prognosis and customizing anti-cancer treatment as well.

For patients with solid tumors surgery and radiotherapy are the most effective treatment options. These are often combined with systemic treatments such as chemotherapy and targeted therapies. Although these treatment combinations are frequently associated with significant toxicity rates, the quality of life of cancer patients has increased thanks to more advanced radiotherapeutic techniques as well as organ-preservation protocols (207;208).

Using radiotherapy, cell death is mainly induced by direct ionization of DNA or indirectly by radiation-induced ROS formation; these include hydroxyl radicals, superoxide anion radicals and other molecules such as hydrogen peroxide. Additional destructive radicals are formed through various chemical interactions (209-211).

One important cause of radiation resistance is the occurrence of hypoxia, as oxygen is essential for the generation of ROS and thus the cell damaging effects (212). Therefore, hypoxic regions in solid tumors are 2 to 3 times more radio-resistant than well-oxygenated tumor cells (186). To increase treatment options, several approaches are used to take hold of the hypoxic tumor regions. To raise tumor oxygen levels, oxygen enhanced gas mixtures and pharmacologic modification of blood flow are used, for example using "accelerated radiotherapy, carbogen, nicotinamide" (ARCON) therapy (213). Moreover, specific killing of hypoxic tumor cells could be achieved by hypoxia-selective cytotoxins, like tirapazamine (214).

To further improve treatment, targeted drugs were developed and implemented in combination with radiotherapy. Monoclonal antibodies are used, which through several mechanisms raise a response against cancer cells. A well-known example is cetuximab, an EGFR-specific human/mouse chimeric antibody. The affinity of this antibody to the receptor is much higher than the affinity of the endogenous ligands, thereby blocking EGF-based cellular signaling and leading to receptor internalization (215;216). EGFR is a member of the epidermal receptor (HER)/Erb-B family, which contain tyrosine kinase domains able to activate two pathways: RAS-Raf-MEK1/2-ERK1/2 and RAS-PI3K-Akt-mTor (Figure 3). Ultimately, blocking signaling can influence cell proliferation, apoptosis, angiogenesis and metastasizing potential (217). Another receptor that often is targeted by drugs is the vascular endothelial growth factor receptor (VEGFR). VEGF and VEGFR are associated with tumor progression, changes in microvessel density, development of lymphnode metastasis, distant metastasis and treatment failure. Thus, interference in signaling mediates a broad anti-tumorigenic response (218).

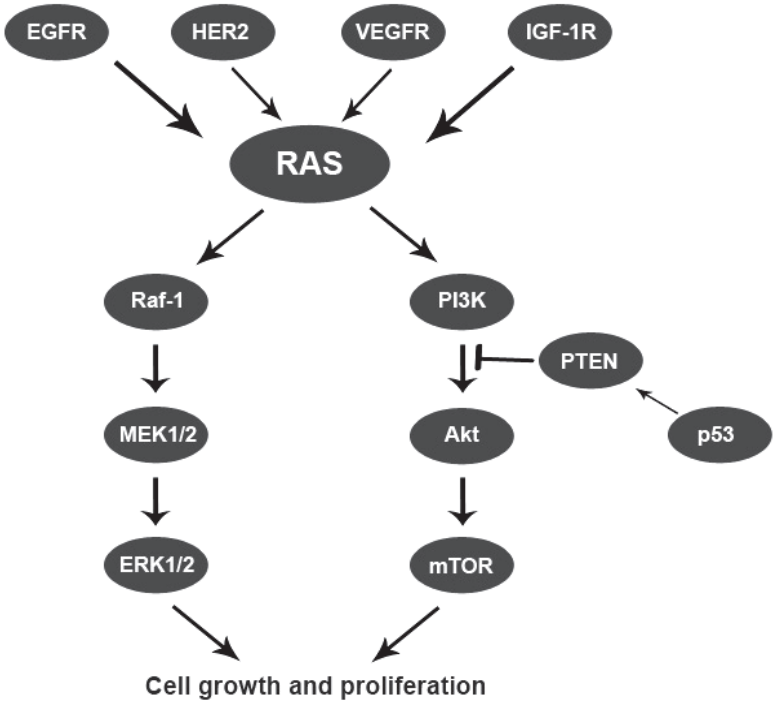

Figure 3. Ras-Raf-MEK1/2-ERK1/2 and PI3K-Akt-mTor pathways. Dysregulation of growthfactor receptors (EGFR, HER2, VEGFR and IGF-1R) and/or downstream kinases (RAS, Raf-1, MEK1/2, ERK1/2, PI3K, Akt and mTOR) or tumor suppressor genes (PTEN or p53) can result in uncontrolled cell growth and proliferation. Figure is adapted from (219).

6. OUTLINE OF THIS THESIS

Using a semi- quantitative method of analysis, Chin and co-workers showed that small heat shock protein αB-Crystallin is a promising biomarker in HNSCC, predicting lower disease-free survival rates for patients with tumors expressing high levels of αB-Crystallin (220). Interestingly, in another study that was performed semi- quantitatively in HNSCC biopsies by Boslooper and co-workers, these results were not confirmed (221). Results from both these semi-quantitative studies are difficult to compare, therefore, in ***Chapter 3*** other approaches are followed to determine whether αB-crystallin expression in HNSCC is correlated with worse prognosis. αB-crystallin expression in HNSCC biopsies is studied in a computer-aided quantitative way, where percentage of αB-crystallin-positive surface was calculated per biopsy. A division is made between low and high αB-crystallin expression. These data are correlated to patient data regarding local and regional recurrence and distant metastasis formation to find which specific component in cancer formation is affected by αB-crystallin expression. Moreover, siRNA mediated knockdown of αB-crystallin in HNSCC cell lines is used to determine the effect of αB-crystallin expression on VEGF secretion and cell motility, which both are linked to metastasis formation.

As described in the introduction, in most solid tumors areas are present containing hypoxic-stressed cells. Since aB-crystallin can become upregulated by several types of stress, an analysis was performed of the relationship between the presence of hypoxia in HNSCC tumors and αB-crystallin expression. Findings are described in ***Chapter 4***. Also the influence of hypoxia on αB-crystallin mRNA and protein expression levels in HNSCC cell lines is studied and it is determined whether hypoxia-stimulated ROS generation plays a role in αB-crystallin induction during hypoxia/reoxygenation. Furthermore, it is investigated whether αB-crystallin, as chaperone protein, is able to enhance survival of cells exposed to hypoxic stress.

In ***Chapter 5*** the correlation of αB-crystallin expression with several signaling molecules is studied, including pERK1/2, pAKT, pmTOR, EGFR and IGF-1R (Chapter 2, Figure 3) in a breast tumor tissue microarray. These molecules are known to be involved in cancer formation, thus an interaction of αB-crystallin with these signaling pathways could be of importance. Also the correlation of αB-crystallin expression with triple negativity, thus the absence of ER, PR and HER2 expression, and expression of basal markers CK5/6 and SMA is studied. To determine whether αB-crystallin directly effects the expression of pERK1/2 and ERK1/2, the influence of αB-crystallin knockdown on ERK1/2 expression levels and phosphorylation levels are studied in a triple negative breast cancer cell line.

αB-Crystallin is mainly a cytoplasmic protein, but can accumulate in the nucleus when it is phosphorylated at specific positions. However, it is not known how αB-crystallin enters the nucleus and whether the protein has a nuclear function. ***Chapter 6*** is focused on these two aspects**.** The nuclear chaperoning activity of αB-crystallin is measured by its ability to refold heat-shock denatured nuclear luciferase in HeLa cells. Yeast two-hybrid screening shows that (especially pseudophosphorylated) αB-crystallin interacts with the C-terminus of Gemin3, which is part of the SMN complex. Using an *in vitro* and *in situ* nuclear import assay it is determined whether the nuclear import of αB-crystallin is facilitated by the SMN complex.
Finally, in ***Chapter 7*** a discussion on findings in the research chapters and suggestions for further research is provided.

CHAPTER 3
αB-CRYSTALLIN STIMULATES VEGF SECRETION AND TUMOR CELL MIGRATION AND CORRELATES WITH ENHANCED DISTANT METASTASIS IN HEAD AND NECK SQUAMOUS CELL CARCINOMA

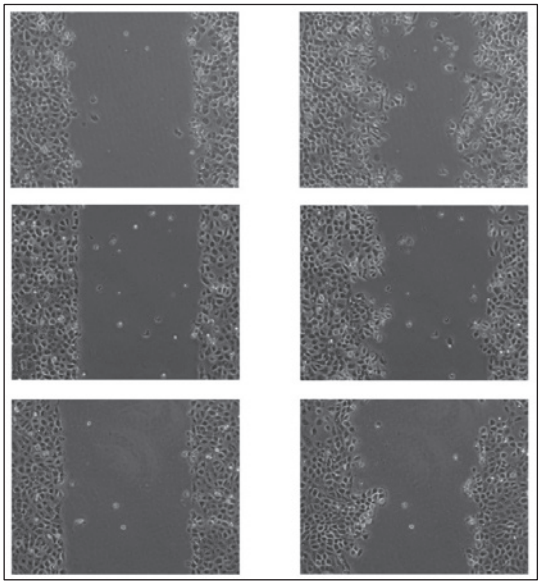

Van de Schootbrugge *et al.*, BMC Cancer 2013

ABSTRACT

αB-crystallin is able to modulate vascular endothelial growth factor (VEGF) secretion. In many solid tumors VEGF is associated with angiogenesis, metastasis formation and poor prognosis. We set out to assess whether αB-crystallin expression is correlated with worse prognosis and whether this is related to VEGF secretion and cell motility in head and neck squamous cell carcinoma (HNSCC). αB-crystallin expression was determined immunohistochemically in tumor biopsies of 38 HNSCC patients. Locoregional control (LRC) and metastasis-free survival (MFS) of the patients were analyzed in relation to αB-crystallin expression. Additionally, the effects of αB-crystallin knockdown on VEGF secretion and cell motility were studied *in vitro*. Patients with higher staining fractions of αB-crystallin exhibited a significantly shorter MFS (Log-Rank test, $p < 0.005$). Under normoxic conditions αB-crystallin knockdown with two different siRNAs in a HNSCC cell line reduced VEGF secretion 1.9-fold and 2.1-fold, respectively. Under hypoxic conditions, a similar reduction of VEGF secretion was observed, 1.9-fold and 2.2-fold, respectively. The effect on cell motility was assessed by a gap closure assay, which showed that αB-crystallin knockdown decreased the rate by which HNSCC cells were able to close a gap by 1.5- to 2.0-fold. Our data suggest that αB-crystallin expression is associated with distant metastases formation in HNSCC patients. This association might relate to the chaperone function of αB-crystallin in mediating folding and secretion of VEGF and stimulating cell migration.

BACKGROUND

The small heat shock protein αB-crystallin (HspB5) is expressed in several types of cancer, including head and neck squamous cell carcinomas (HNSCC) (220;221) and breast carcinomas (126;222;223). The expression is often correlated with a poor prognosis, but the reason for this is not fully understood (54;224). αB-crystallin plays a role in many different cellular processes such as proliferation, cell migration and apoptosis (54;126;225). The expression of this protein is increased during various stresses, like heat shock and oxidative stress (14). A well-known function of αB-crystallin is molecular chaperoning, allowing the prevention of aggregation of proteins (14). Recently, it has been shown that αB-crystallin chaperones the hypoxia-induced VEGF protein to the endoplasmic reticulum, leading to more properly folded and thus secreted VEGF (226;227). VEGF is a major player involved in tumor angiogenesis

(228) and increased VEGF secretion is often correlated with metastasis formation (229) and worse outcome for the patient (230).

HNSCC is the sixth most common cancer worldwide and accounts for 6% of all cancers (150). The majority of these patients are treated with radiotherapy, alone or in combination with surgery or chemotherapy (231). Based on the improved understanding of the molecular pathways underlying HNSCC, targeted drugs (e.g. EGFR-specific antibodies) and other modifications have been implemented in treatment protocols (231). However, only a subset of patients profit from these combined modality strategies. Therefore, there is a great demand for biomarkers to customize treatment.

In the present study the value of αB-crystallin as a biomarker in HNSCC was investigated. αB-crystallin expression levels were immunohistochemically determined in HNSCC biopsies and correlated with clinicopathological characteristics and outcome. Moreover, the effect of knockdown of αB-crystallin on VEGF secretion and cell migration was studied.

METHODS

Patients

Biopsy material from a cohort of HNSCC patients with stage II to IV primary squamous cell carcinoma of the oral cavity, oropharynx, hypopharynx or larynx was used. The inclusion criteria of patients with HNSCC have been described before (232). Approval from the ethics committee of Radboud University Nijmegen Medical Centre was obtained and all patients provided written informed consent. Of 13 patients no biopsy materials were left and were excluded from this study. The median duration of follow-up for all patients was 29 months and for surviving patients 85 months. During follow-up, LRC and MFS were registered.

Immunohistochemical staining of αB-crystallin of HNSCC biopsies

Oral cavity tumor sections (233) were incubated with 100-fold diluted polyclonal rabbit αB-crystallin antiserum (38) and subsequently stained with diaminobenzidine (DAB) according to a standard protocol. Sections of the 38 available biopsies (5 μm) were mounted on poly-L-lysine coated slides, fixed for 10 minutes in acetone at 4°C and rehydrated in PBS. The sections were incubated overnight at 4°C with 100-fold diluted αB-crystallin antiserum (38) and subsequently incubated for 30 minutes at 37°C with 600-fold diluted goat-α-rabbit-FabCy3 (Jackson Immuno Research Laboratories Inc) in PBS, for 45 minutes at 37°C with 10-fold diluted endothelium antibody PAL-E

(Euro Diagnostica BV) in PAD, for 60 minutes at 37°C with 100-fold diluted chicken-α-mouse Alexa647 (Molecular probes) in PBS and finally for 5 minutes at room temperature with 0.5 ng/ml Hoechst (Sigma) in PBS. Between the incubation steps, 3 times 2 minutes washing steps in PBS were performed. The sections were mounted using fluorostab (ProGen Biotechnik GmbH).

Image acquisition

Scanning of the tumor sections was performed with a fluorescence microscope (Axioskop, Zeiss) and a computer-controlled motorized stepping stage, using IP-lab software (Scanalytics) (234). Each section was completely scanned for αB-crystallin staining. The resulting grey scale images were subsequently binarized. Thresholds were set just above the background staining for each staining. Manually, the total tumor area was contoured, excluding surrounding tissue, large necrotic areas and artifacts. The percentage of αB-crystallin was determined as the tumor area positive for αB-crystallin relative to the total tumor area.

Cell culture, siRNA treatment, hypoxia exposure and VEGF secretion measurement

The HNSCC cell line, UT-SCC-5 (described in (235)), was maintained in DMEM + Glutamax^{tm} (Invitrogen) supplemented with 10% fetal calf serum (Gibco-BRL) in a standard humidified 37°C incubator. At 40% confluency, cells were transfected using Lipofectamine^{tm} 2000 Reagent according to the manufacturers' protocol (Invitrogen). The siRNAs used were si-Luciferase (siRNA LUC) as negative control, sequence: CGUACGCGGAAUACUUCGAdTdT, si-αB-crystallin1 (siRNA αB1) sequence: GCACCCAGCUGGUUUGACAdTdT and si-αB-crystallin2 (siRNA αB2) sequence: CCCUGAGUCCCUUCUACCUdTdT. After 5 hours, cells were reseeded ($9.0x10^3$ cells in 0.3 cm^2 wells in 12-fold, for VEGF secretion measurements, and $2.5x10^5$ cells in 10 cm^2 wells in 4-fold, for RNA expression measurements (see below)). Hypoxia treatment was performed 24 hours after siRNA transfection cells in a humidified 37°C H35 Hypoxystation (Don Whitley Scientific) with 0.1% O_2. Cells cultured under normoxic (6-fold) and hypoxic (6-fold) conditions were maintained for 48 hours. The culture media of the samples were collected and VEGF levels were determined using a quantitative enzyme-linked immunosorbent assay (ELISA). The details of this assay have been described previously by Span and coworkers (236). The assay is based on the combination of four polyclonal antibodies raised in four different animal species, duck, chicken, rabbit and goat, and are employed in a sandwich assay format. The assay measures $VEGF_{165}$ and $VEGF_{121}$, the main isoforms of VEGF. There is no cross-reactivity with VEGF B, VEGF C and VEGF D (236;237).

Gap closing assay

The HNSCC cell line UT-SCC-15 (235) was transfected with siRNA as described above. Twenty-four hours after transfection, cells were seeded at $1.0x10^5$ cells per side of the Culture-Inserts (Ibidi, N = 6 per condition). For quantitative RT-PCR, $0.5x10^6$ cells were seeded in parallel in 10 cm^2 wells (N = 5). 24 Hours later cells were washed with PBS, fresh medium was added and the insert was removed. Time lapse imaging was performed for 24 hours in a microscope stage incubator (Oko-Lab) on a Nikon DiaPhot microscope equipped with a Hamamatsu C8484-05G digital camera. Images were taken every 10 min using TimeLapse Software (Oko-Lab), version 2.7, with a 10x objective. Analysis of gap closing was performed using TScratch (238).

RNA analysis by quantitative PCR

Total RNA from UT-SCC-5 and UT-SCC-15 cell lysates was extracted using standard Trizol isolation. After DNAse I treatment (Amplification grade, Invitrogen) mRNAs were reverse transcribed using oligo(dT) primers and the Reverse Transcription System (Promega) according to manufacturer's protocol starting with 1 µg of RNA in a total volume of 20 µl. Subsequently quantitative PCR reactions were performed with 10 µl Power SYBR Green (Applied BioSystems), 5 µM of primers and 2 µl cDNA in a total volume of 20 µl. The sequence of the used αB-crystallin primers is: 5'-ATCTTCTTTTGCGTCGCCAG-3' and 5'-TTCCCCATGGTGTCTGAGC-3', and of the GAPDH primers: 5'-GATTGAGGTGCATGGAAAAC-3' and 5'-AGGACCCCATCAGATGACAG-3'. The fluorescent signal intensities were recorded with the ABI Prism 7000 system (Applied Biosystems). Samples were kept for 10 minutes at 95°C, followed by 40 cycles of 15 seconds at 95°C and 1 minute at 60°C. Data analysis was performed with 7000 System SDS software (Applied BioSystems).

Statistics

Statistical analyses were performed using Graphpad Prism 5.00 software. To test for differences in αB-crystallin expression using binary patient data, the unpaired *t*-test was used. For survival analyses, receiver operating characteristic (ROC) curves were made to determine the cut-off value with the highest sensitivity and specificity for discriminating between patients with or without locoregional recurrence (LRR) or distant metastasis with at least 24 months of follow-up or an LRR or distant metastatic event before that. Survival rates were calculated starting at the date of diagnosis. The Kaplan-Meier method and the log-rank test were used to test for differences in LRC and MFS rates in all patients. P-values below 0.05 were considered *a priori* to indicate a significant difference. Differences in VEGF secretion and gap closure speed were tested using One-way ANOVA and Tukey's Multiple Comparison Test.

RESULTS

The presence of αB-crystallin in the tumors was analyzed by immunohistological staining. In most tumors cells αB-crystallin could be detected. In stromal cells, no or only very low levels of nuclear staining were found (Figure 1a). The αB-crystallin expression was determined in 38 primary HNSCC biopsies, which were histologically confirmed to contain tumor tissue (232). The characteristics of the tumors at the time point of biopsy collection are listed in Table 1. To quantify the fraction of the tumor section expressing αB-crystallin, fluorescently labeled secondary antibodies were used and the images were analyzed with a digital image analysis system. Only, the tumor area was used for the analysis by excluding the surrounding stromal tissue, large necrotic areas and artifacts. The results showed that the αB-crystallin expressing tumor areas varied from 0 to 69%. Examples of biopsies having marginal and extensive αB-crystallin expression are shown in Figure 1b and c.

αB-crystallin expression in HNSCC biopsies is associated with distant metastasis

Patients with at least 24 months of event-free follow up or with a locoregional recurrence (LRR) or distant metastatic event before 24 months were dichotomized in groups with and without LRR (N = 16 and N = 12, respectively), or with and without metastasis (N = 17 and N = 10, respectively). Figure 2 shows that the mean percentage of the tumor area expressing αB-crystallin was not significantly different between biopsies from patients with or without LRR (Figure 2a). However, the mean percentage of the tumor area expressing αB-crystallin was significantly higher in biopsies from patients who developed distant metastasis during follow up as compared to those without (two-tailed unpaired *t*-test, $p < 0.05$, Figure 2b). The highest sensitivity and specificity for discriminating between patients with or without metastasis was determined by receiver operating characteristic (ROC) curve to be at a cut-off value of 20%. At this cut-off value the Kaplan-Meier estimates for LRC did not show any significant differences (Figure 2c), and the same result was obtained with other cut-off values (results not shown). For MFS a significant difference was observed (Log-Rank, $p < 0.005$, Figure 2d), which was especially clear after 22 months; at that time point MFS was 86% for the patients with relatively low fractions of tumor area expressing αB-crystallin, whereas this was only 36% for the patients with extensive αB-crystallin expression in the tumors. These results suggest that the levels of αB-crystallin expression inversely correlate with MFS.

Table 1. Characteristics of 38 head and neck squamous cell carcinomas

Characteristics	Number of biopsies
Site of tumor	
Oral cavity	1
Hypopharynx	12
Larynx	15
Oropharynx	10
T classification	
1	1
2	13
3	16
4	8
N classification	
0	10
1	10
2	18
M classification	
0	38
Differentiation grade	
1	2
2	21
3	14
Unknown	1

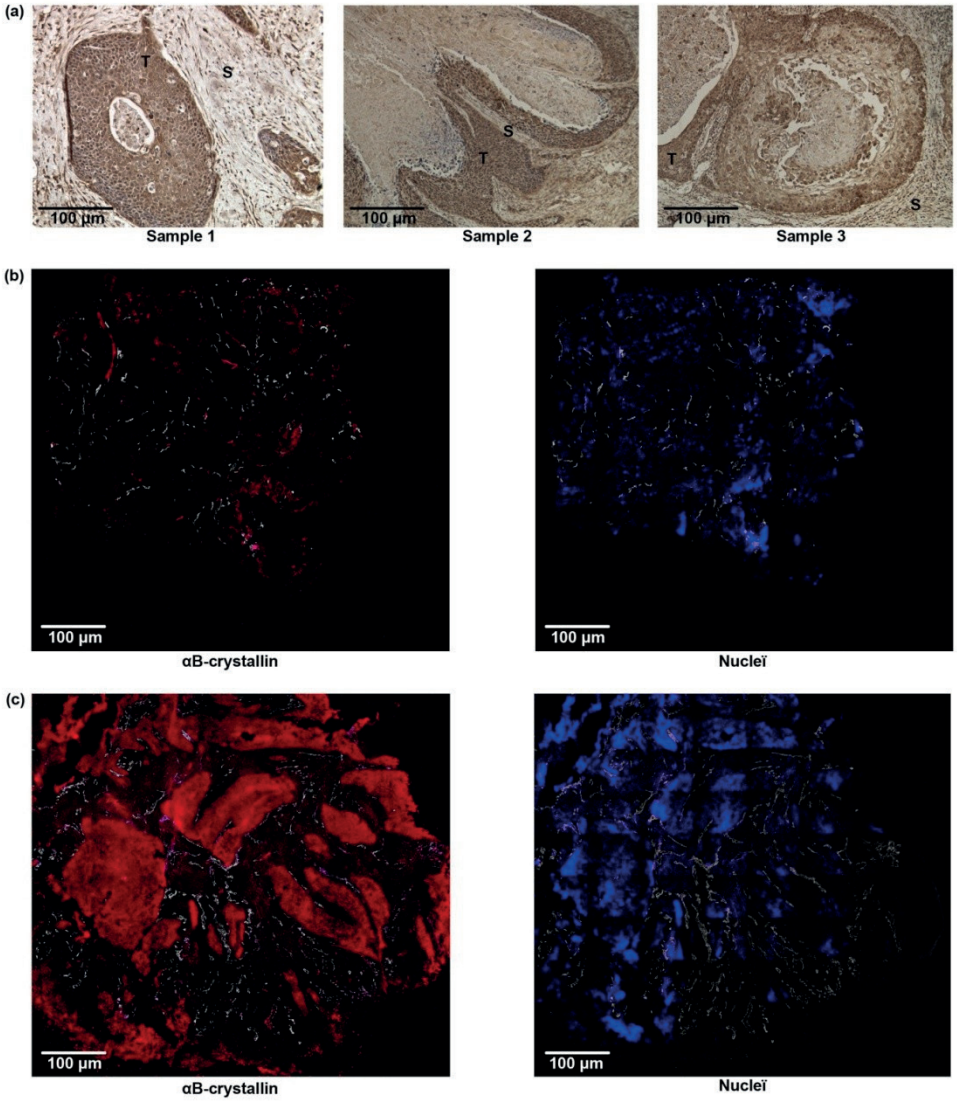

Figure 1. Immunohistochemical staining of tumor tissues with polyclonal anti-αB-crystallin antibody. DAB staining of three oral cavity tumor sections. Tumor cells are indicated with T, surrounding stromal cells with S (**a**). Immunofluorescent staining of biopsies with low αB-crystallin expression (red, **b** left panel) and high αB-crystallin expression (red, **c** left panel) and the corresponding Hoechst stainings (blue, **b** and **c** right panels). Blood vessels are indicated in white.

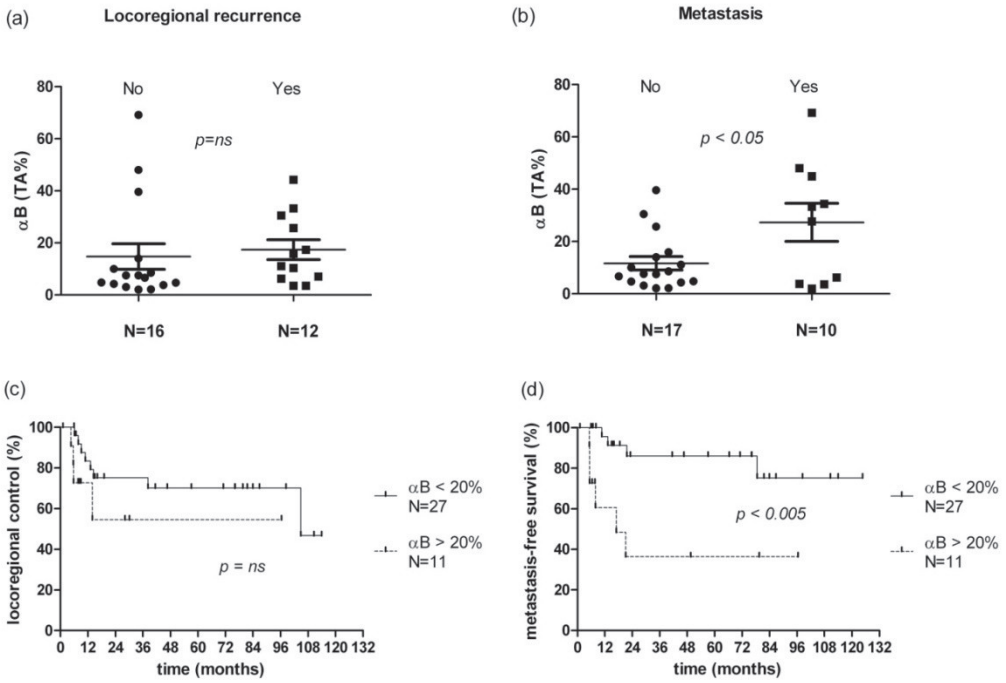

Figure 2. Relation between αB-crystallin expression and locoregional recurrence and metastasis. αB-crystallin expression per biopsy and the mean αB-crystallin expression of each group with standard error of the mean (SEM) in biopsies from patients without or with locoregional recurrence (**a**) or metastasis (**b**) and Kaplan-Meier analysis of locoregional control (**c**) and metastasis-free survival (**d**) for patients with high (>20% of tumor area) and low (<20% of tumor area) αB-crystallin expression. TA: Tumor area, ns: not significant.

αB-crystallin expression enhances VEGF secretion

The recently reported involvement of αB-crystallin in VEGF production prompted us to investigate the effects of αB-crystallin expression on VEGF secretion by HNSCC cells. For these experiments the HNSCC cell line UT-SCC-5 was used and the levels of αB-crystallin were reduced by siRNA-mediated knock-down. Two distinct αB-crystallin siRNAs, αB1 and αB2, resulted in a 1.3-fold and 1.8-fold reduction of αB-crystallin mRNA levels, respectively (Figure 3a). Downregulation of αB-crystallin significantly decreased VEGF secretion (1.9-fold and 2.1-fold reduction, respectively). Since hypoxia leads to elevated VEGF production, we next assessed the effects of αB-crystallin knock-down under hypoxic conditions. Indeed, VEGF secretion appeared to

be increased in UT-SCC-5 cells by hypoxia (Figure 3b, 1.6-fold) and also under these conditions αB-crystallin depletion resulted in decreased VEGF expression (1.9-fold and 2.2-fold reduction, respectively). These results show that αB-crystallin expression can affect VEGF secretion both at normoxia and hypoxia.

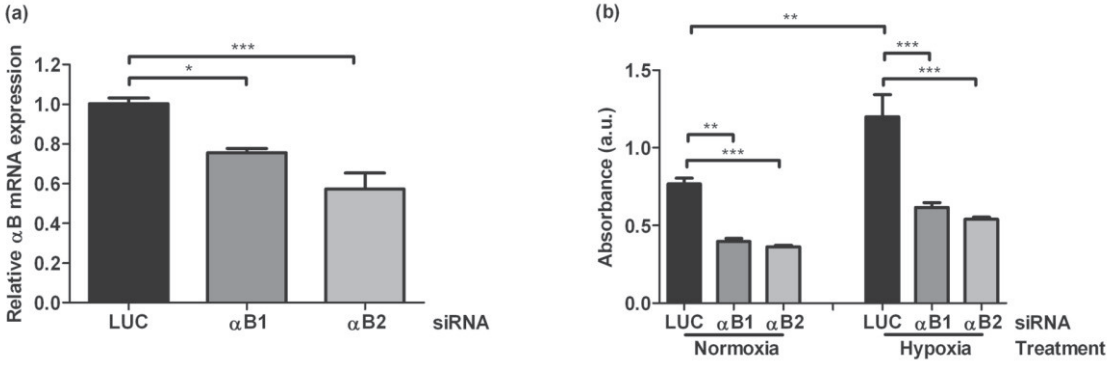

Figure 3. Influence of αB-crystallin knock-down on VEGF secretion. Knockdown of αB-crystallin mRNA expression in UT-SCC-5 cells by two different siRNAs, αB1 and αB2, compared to negative control siRNA LUC (Luciferase) as measured by quantitative PCR (**a**). VEGF secretion levels in UT-SCC-5 cells transfected with the αB1, αB2 or LUC siRNA under normoxic and hypoxic conditions determined by ELISA (**b**). Statistical analysis was performed using One-way ANOVA and Tukey's Multiple Comparison Test. *** $P < 0.001$, ** $0.001 < P < 0.01$, * $0.01 < P < 0.05$; a.u: absorbance units

Effect of αB-crystallin expression on cell migration

The association of αB-crystallin expression with metastasis may also be due to effects on cell motility (126). To investigate whether motility of HNSCC cells is affected by reduced αB-crystallin a gap closure assay was applied. Since the UT-SCC-5 cells were easily damaged during gap preparation, disturbing migration, the related cell line UT-SCC-15 was used. Also in this HNSCC cell line αB-crystallin mRNA levels could be reduced by siRNA-mediated knock-down, although the efficiency appeared to be much higher than that in the UT-SCC-5 cells (Figure 4a). Depletion of αB-crystallin resulted in decreased gap closure rates compared to mock treated cells (Figure 4b). The cell

migration rate was reduced 2.0-fold and 1.5-fold after treatment with the siRNA αB1 and αB2, respectively (Figure 4c).

DISCUSSION

Here, we show that αB-crystallin expression in HNSCC tumors correlates with MFS, but not with LRC. Clues for the mechanism by which αB-crystallin might affect distant metastasis formation in patients were obtained by the depletion of αB-crystallin in HNSCC cell lines, which showed that both VEGF secretion and cell motility were decreased when αB-crystallin expression was reduced. Previously, two studies have addressed the prognostic value of αB-crystallin in HNSCC. Chin and coworkers have shown that αB-crystallin is a marker for poor prognosis (220), which is substantiated by our data. However, they noted that none of the patients lacking αB-crystallin had LRR, while 37% of the patients with tumors stained positive for αB-crystallin had LRR. In the current study, the difference in prognosis was mainly caused by a higher rate of distant metastasis in the high αB-crystallin group and not by a difference in LRR. Boslooper and colleagues did not find αB-crystallin to be a prognostic marker for HNSCC (221). These researchers observed the highest concentrations of αB-crystallin in the centre of tumor cell nests and not the more diffuse localization observed in this study and the study of Chin and coworkers (220). This difference in αB-crystallin localization may have been caused by a difference in staining procedure and could be the reason why this study led to a different conclusion. αB-crystallin was also found to be associated with a poor prognosis in several other types of cancers, such as breast cancer (126;222;223;239;240) and was downregulated in a breast cancer cell line by breast cancer metastasis suppressor 1, which specifically suppresses metastasis (241). αB-crystallin is a molecular chaperone able to prevent protein aggregation and can confer protection to cells under stress conditions. αB-crystallin inhibits apoptosis in response to different anti-cancer agents, such as DNA-damaging drugs, TNFα and Fas ligand (54) and has been shown to be a predictor of resistance to chemotherapy (242). However, since our data do not support an association of αB-crystallin expression with local recurrence after treatment of the patients, the cytoprotective activity is likely not the sole reason why αB-crystallin is associated with poor prognosis. Metastasis formation occurs via a series of steps, also known as the “metastatic cascade” (130). One of the factors associated with metastatic spread is VEGF (243;244). Several studies have demonstrated roles for αB-crystallin in VEGF-dependent angiogenesis (245;246). Tumor vasculature in αB-crystallin-deficient mice displays high levels of

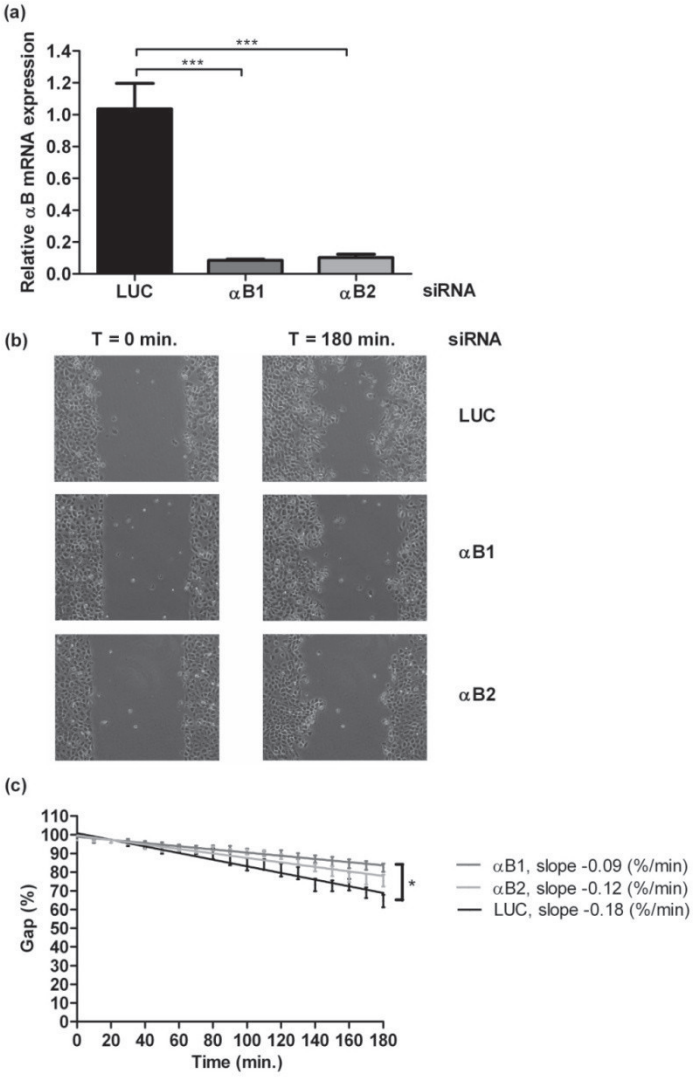

Figure 4. Influence of αB-crystallin knock-down on cell migration determined with gap closure assay. Knockdown of αB-crystallin mRNA expression in UT-SCC-15 cells by two different siRNAs, αB1 and αB2, compared to negative control siRNA LUC (Luciferase) as measured by quantitative PCR (**a**). Representative micrographs of the gap closure by UT-SCC-15 cells after 0 and 180 minutes at 10x magnification (**b**). Relative gap size between 0 and 180 minutes of UT-SCC-15 cells transfected with the αB1, αB2 or LUC siRNA (**c**). Statistical analysis was performed using One-way ANOVA and Tukey's Multiple Comparison Test. *** $P < 0.001$, * $0.01 < P < 0.05$.

endothelial apoptosis and decreased vessel formation. αB-crystallin has been shown to associate with VEGF-A (the most well-known member of the VEGF protein family) (225;246) and colocalizes with VEGF at the endoplasmic reticulum (227). Furthermore, VEGF-A expression remained low in αB-crystallin-deficient mice during retinal revascularization after artificially-induced retinopathy (226). Here we have shown that in a HNSCC cell line αB-crystallin is also involved in secretion of VEGF and in this way may influence tumorigenic blood vessel formation and metastasis formation in HNSCC. For the growth of metastatic tumors in lymph nodes neoangiogenesis is not absolutely needed (247;248), which might explain why no correlation was found between αB-crystallin expression and LRC. Migration-associated proteins may also correlate with worse outcome, as has been shown for patients with squamous cell carcinoma of the tongue (249). αB-crystallin can affect cell migration as well. Overexpression of αB-crystallin led to higher cell motility in several studies (126;239;250). Here we have shown that depletion of αB-crystallin decreased the motility of UT-SCC cells, indicating also in these types of cells αB-crystallin may affect cell migration. VEGF also plays a role in cell migration (251), potentially by enhancing invadopodia formation (252). The effect of αB-crystallin on cell migration may thus be mediated by VEGF, although other mechanisms are also possible, as for example by the influence of αB-crystallin on actin filaments dynamics (252;253). Further research is needed to reveal the molecular mechanisms by which αB-crystallin affects cell migration.

CONCLUSIONS

High αB-crystallin expression is associated with metastasis formation in HNSCC but not with locoregional recurrence. αB-crystallin could be a useful biomarker to help fine-tune treatment, possibly by targeting αB-crystallin-induced VEGF secretion or cell motility. Validation in a larger HNSCC cohort is required to confirm the significance of this finding.

CHAPTER 4
EFFECT OF HYPOXIA ON THE EXPRESSION OF αB-CRYSTALLIN IN HEAD AND NECK SQUAMOUS CELL CARCINOMA

Van de Schootbrugge *et al.*, BMC Cancer 2014

ABSTRACT

The presence of hypoxia in head and neck squamous cell carcinoma (HNSCC) is associated with therapeutic resistance and increased risk of metastasis formation. αB-crystallin (HspB5) is a small heat shock protein, which is also associated with metastasis formation in HNSCC. In this study, we investigated whether αB-crystallin protein expression is increased in hypoxic areas of HNSCC biopsies and analyzed whether hypoxia induces αB-crystallin expression *in vitro* and in this way may confer hypoxic cell survival. In 38 HNSCC biopsies, the overlap between immunohistochemically stained αB-crystallin and pimonidazole-adducts (hypoxiamarker) was determined. Moreover, expression levels of αB-crystallin were analyzed in HNSCC cell lines under hypoxia and reoxygenation conditions and after exposure to reactive oxygen species (ROS) and the ROS scavenger N-acetylcysteine (NAC). siRNA-mediated knockdown was used to determine the influence of αB-crystallin on cell survival under hypoxic conditions. In all biopsies αB-crystallin was more abundantly present in hypoxic areas than in normoxic areas. Remarkably, hypoxia decreased αB-crystallin mRNA expression in the HNSCC cell lines. Only after reoxygenation, a condition that stimulates ROS formation, αB-crystallin expression was increased. αB-crystallin mRNA levels were also increased by extracellular ROS, and NAC abolished the reoxygenation-induced αB-crystallin upregulation. Moreover, it was found that decreased αB-crystallin levels reduced cell survival under hypoxic conditions. We provide the first evidence that hypoxia stimulates upregulation of αB-crystallin in HNSCC. This upregulation was not caused by the low oxygen pressure, but more likely by ROS formation. The higher expression of αB-crystallin may lead to prolonged survival of these cells under hypoxic conditions.

BACKGROUND

In solid tumors, hypoxic regions can be present when cells are exposed to an oxygen pressure below 5 to 10 mmHg (0.66 – 1.32% O_2) (181). Hypoxia can be a result of insufficient oxygen transportation to remote parts of a tumor, caused by deficient blood vessel formation (chronic, diffusion-limited hypoxia) or leaking or partially blockage of blood vessels (acute, perfusion-limited hypoxia) (181). Hypoxia might be intermittent when the blood flow is restored after temporary vascular shutdown, which can result in a cycling pattern of hypoxia and reoxygenation (194;196;197). The presence of hypoxic regions in the tumor is detrimental for the patient, since hypoxic

tumor cells are associated with therapeutic resistance and metastatic progression (187;188;254). Despite the low oxygen levels, hypoxia is also associated with the presence of reactive oxygen species (ROS) (199;200;255). As ROS are conventionally thought to be cytotoxic and mutagenic, they could lead to cancer progression and might be one of the reasons why the presence of hypoxia is as a bad prognostic factor (256).
αB-crystallin is a small heat shock protein, which can bind to partially unfolded proteins, thereby keeping them in a soluble state to prevent their aggregation (54;224). It may protect cells from death induced by accumulation of unfolded proteins (257). Furthermore, αB-crystallin may confer stress resistance to cells by inhibiting the processing of the pro-apoptotic protein caspase-3 (258). Besides being mainly expressed in eye lens and muscle tissues (259), αB-crystallin can also be found in several types of cancer, among which head and neck squamous cell carcinoma (HNSCC) (220;260;261) and breast carcinomas (126;222;262). αB-crystallin expression is associated with metastasis formation in HNSCC and in breast carcinomas (14;223) and in other types of cancer, expression is often correlated with poor prognosis as well (54;224). The expression of αB-crystallin can be increased during various stresses, like heat shock, osmotic stress or exposure to heavy metals (14). Moreover, in tissues from newborn piglets, αB-crystallin has been shown to be upregulated by hypoxia (263;264). In this study, we analyzed whether the expression of αB-crystallin protein is affected in hypoxic regions of HNSCC's and whether αB-crystallin knockdown influences cell survival under hypoxic stress.

METHODS

Patients

Biopsy material of 38 HNSCC patients with stage II to IV primary squamous cell carcinoma of the oral cavity, oropharynx, hypopharynx or larynx was used (not all biopsies of the available cohort could be used due to the lack of material) (232;261). Two hours before biopsies were taken (1 per patient), patients received 500 mg/m^2 body surface of the hypoxia marker pimonidazole (intravenously, dissolved in 100 ml 0.9% NaCl) over 20 minutes. The obtained biopsies were snap-frozen and stored in liquid nitrogen until immunohistochemical processing. Approval from the ethics committee of Radboud University Nijmegen Medical Centre was obtained and all patients provided written informed consent.

Immunohistochemisty

Sections of the biopsies (5 μm) were mounted on poly-L-lysine coated slides, fixed for 10 minutes in acetone at 4 °C and rehydrated in PBS. The sections were incubated overnight at 4 °C with 100-fold diluted αB-crystallin antiserum (38) and subsequently incubated for 30 minutes at 37 °C with 600-fold diluted FabCy3 goat-α-rabbit IgG (Jackson Immuno Research Laboratories Inc) in PBS for 45 minutes at 37 °C with 10-fold diluted endothelium antibody PAL-E (Euro Diagnostica BV) in Primary Antibody Diluent (PAD, Dako) and for 60 minutes at 37 °C with 100-fold diluted Alexa 647 chicken-α-mouse IgG (Molecular probes) in PBS. For visualization of the pimonidazole adducts, the sections were stained with 1000-fold diluted rabbit-α-pimonidazole (gift from Dr. James A. Raleigh, University of North Carolina), diluted in PAD for 30 minutes at 37 °C and subsequently stained with 600-fold diluted Alexa 488 donkey-α-rabbit IgG (Molecular probes) in PBS 30 minutes at 37 °C. During the latter step only the rabbit antibodies directed to pimonidazole were stained (265). Between the incubations, 3 times 2 minutes washing steps in PBS were performed. The sections were mounted using fluorostab (ProGen Biotechnik GmbH).

Image acquisition

Scanning of the biopsy sections was performed with a fluorescence microscope (Axioskop, Zeiss) and a computer-controlled motorized stepping stage, using IP-lab software (Scanalytics), as described previously (266). Each section was completely sequentially scanned for αB-crystallin, pimonidazole and blood vessel staining at 100x magnification. The resulting composite grey scale images were converted to binary images for further analysis. Thresholds were set just above the background staining for each individual staining. The total tumor area was contoured manually, excluding nontumor tissue, large necrotic areas and artifacts. The percentage of αB-crystallin in the normoxic area was determined as the pimonidazole-negative tumor area containing αB-crystallin relative to the total pimonidazole-negative tumor area. The percentage of αB-crystallin in the hypoxic area was determined as the tumor area positive for αB-crystallin and pimonidazole relative to the total pimonidazole-positive area.

αB-crystallin mRNA expression upon hypoxia

The HNSCC cell line UT-SCC-5 (described in (235)), maintained in DMEM + GlutaMAX (Invitrogen) supplemented with 10% fetal calf serum (Gibco-BRL) was seeded on 6-wells plates, $0.5x10^6$ cells per well, N = 4 per time point, and transferred after 24 hours from a standard humidified 37 ºC incubator to a humidified 37 ºC H35 hypoxystation (Don Whitley Scientific) with 0.1% O_2. Samples were harvested after 0–22 hours of hypoxic incubation for quantitative RNA analysis.

αB-Crystallin mRNA expression upon hypoxia, reoxygenation and N-acetylcysteine

The HNSCC cell lines UT-SCC-5 and UT-SCC-15 (described in (235)), maintained in DMEM + GlutaMAX supplemented with 10% fetal calf serum, were seeded in 6-wells plates, $0.3x10^6$ cells per well, N = 4 per condition, and transferred after 24 hours from a standard humidified 37 ºC incubator to a H35 hypoxystation with 0.1% O_2 (Don Whitley Scientific), or maintained in a standard incubator. Normoxic and hypoxic samples were harvested after 48 hours for quantitative RNA analysis. The reoxygenation samples were transferred after 24 hours of hypoxic incubation to a standard incubator again for 24 hours and subsequently harvested. To reduce ROS, cells were incubated after 24 hours of hypoxia or normoxia with 0.05 mM NAC (Sigma). After NAC was added, the reoxygenation samples were transferred from the hypoxystation to a standard humidified 37 ºC incubator and incubated for 24 hours and subsequently harvested.

αB-crystallin protein expression upon hypoxia and reoxygenation

The UT-SCC-5 cell line was seeded in T25 flasks, 0.9x106 cells per flask, N = 3 for the normoxic condition and N = 4 for the hypoxic and reoxygenation condition, and incubated for 5 hours in a standard humidified 37ºC incubator. The cells were transferred to the hypoxystation maintained at 0.1% or kept in the standard incubator and harvested after 48 hours. The reoxygenation samples were transferred after 24 hours of hypoxic incubation to the standard incubator again for 24 hours and subsequently harvested. The cells were harvested in 2% sodium dodecyl sulfate (Gibco), heated for 5 minutes at 100 °C and sonicated 5x 30 seconds on and 30 seconds off with Bioruptor (Diagenode). The protein concentrations were determined with BCA Protein Assay Kit (Thermo Scientific) according to manufacturer's protocol. Protein samples (60 µg/sample) were separated by electrophoresis on a 12.5% polyacrylamide gel and transferred to a nitrocellulose membrane (Protran). The membranes were blocked with 5% Elk (Campina) in PBS for an hour and washed 3 times for 10 minutes with PBS + 0.0025% v/v Nonidet P-40. The membranes were incubated for an hour with the 200-fold diluted monoclonal mouse-α-human-αB-crystallin (RIKEN) and 6000-fold diluted mouse-α-human-γ-tubulin as reference (Sigma-Aldrich) diluted in 0.025% w/v Nonidet P-40 and completed with 2% Elk in PBS. After washing, blots were incubated for 1 hour with a 6000-fold dilution of IRDye 800CW goat-α-mouse IgG (LI-COR). The proteins were visualized with the Odyssey scanner (LI-COR). Analysis was performed using Odyssey 2.1 software.

αB-crystallin mRNA expression upon H_2O_2-induced oxidative stress

UT-SCC-5 cells were seeded in 6-wells plates, $0.5x10^6$ cells per well; N = 4 per concentration maintained in DMEM + GlutaMAX supplemented with 10% fetal calf serum. After 24 hours, cells were incubated with 0 mM (mock), 0.3 mM, 1.5 mM or 3.0 mM H_2O_2 for 1 hour after which they were incubated again in normal medium and harvested after 7 hours for quantitative RNA analysis.

Hypoxia survival upon siRNA-mediated knock-down of αB-crystallin

$4.4 x10^6$ UT-SCC-5 cells were seeded in a T175 culture flask and maintained in DMEM + GlutaMAX supplemented with 10% fetal calf serum. After 24 hours, cells were transfected with siRNA using Lipofectamine 2000 Reagent according to manufacturers' protocol (Invitrogen). The siRNA's were directed against luciferase (siRNA LUC, sequence: CGUACGCGGAAUACUUCGAdTdT) and EGFP (si-EGFP, sequence: CGAGAAGCGCGAUCACAUGdTdT) as negative controls and αB-crystallin (si-αB1, sequence: GCACCCAGCUGGUUUGACAdTdT, si-αB2 sequence: CCCUGAGUCCCUUCUACCUdTdT and si-αB3, sequence: CCGGAUCCCAGCUGAUGUAdTdT). After 5 hours, cells were reseeded $4.0x10^4$ cells/well in 96-wells plates (6-fold per condition) and $1.25 x10^5$ cells/well in 6-wells plates (4-fold per condition). The next day, the cells in the 96-wells plates were washed twice with PBS and DMEM (supplemented with GlutaMAX, 1 mM sodiumpyruvate and 10% fetal calf serum) was added containing 0 mM or 5 mM Glucose (Dextrose D(+), Invitrogen). After one hour, cells were kept in the standard incubator or transferred to the H35 hypoxystation maintained at 0.1% O_2 and incubated for 24 hours. All 96-wells plates were subsequently incubated in the standard incubator for 3.5 hours and washed twice with PBS and incubated for two hours in 10-fold diluted Cell Counting Kit-8 solution (Sigma-Aldrich) in Optimem (Invitrogen). The absorbance at 450 nm was measured using an ELISA-reader (Tecan). The cells in the 6-wells plates were harvested 48 hours after siRNA transfection for quantitative RNA analysis to determine the efficiency of αB-crystallin mRNA knockdown.

RNA analysis by quantitative RT-PCR

Total RNA from the harvested UT-SCC-5 and UT-SCC-15 cells was extracted using standard Trizol isolation. After DNAse I treatment (Amplification grade, Invitrogen) mRNAs were reverse transcribed using oligo(dT) primers and the Reverse Transcription System (Promega) according to manufacturer's protocol starting with 1 µg of RNA in a final volume of 20 µl. Subsequently, quantitative PCR (qPCR) reactions were performed with 10 µl Power SYBR Green (Applied BioSystems), 5 µM primers and 2 µl cDNA in a final volume of 20 µl. The used primer sequences for αB-

crystallin are: ATCTTCTTTTGCGTCGCCAG and TTCCCCATGGTGTCTGAGC, and for GAPDH: GATTGAGGTGCATGGAAAAC and AGGACCCCATCAGATGACAG. The fluorescent signal intensities were recorded with the ABI Prism 7000 system (Applied Biosystems). Samples were kept for 10 minutes at 95 °C, followed by 40 cycles of 15 seconds at 95 °C and 1 minute at 60 °C. Data analysis was performed on the CFX96 (Biorad). Analysis was performed with CFX Manager Software (Biorad).

Statistics

Statistical analyses were performed using Graphpad Prism 5.00 software. Statistical analysis was performed using One-way ANOVA and Tukey's Multiple Comparison.

RESULTS

αB-crystallin protein is increased in the hypoxic areas of HNSCC biopsies

The expression of αB-crystallin protein was analyzed in the hypoxic and normoxic regions present in sections of HNSCC biopsies of 38 different patients. To detect the hypoxic regions, the hypoxia marker pimonidazole was used. Figure 1 shows a representative binarized staining of αB-crystallin and pimonidazole (Figure 1a and 1b). Most of the hypoxic areas (Figure 1c, depicted in green) are located in tumor areas at larger distance from blood vessels (Figure 1c, depicted in blue). Interestingly, areas showing αB-crystallin expression (Figure 1c, depicted in red) are largely overlapping with hypoxic areas, though αB-crystallin can be detected in normoxic areas as well. By digital analysis of the scanned images the percentages of αB-crystallin-positive areas in the normoxic tumor areas and in the hypoxic tumor areas were determined for each biopsy. In case hypoxia does not affect αB-crystallin expression, the percentages of αB-crystallin-positive areas present in normoxic and hypoxic areas would be similar (Figure 2, grey line). However, as shown in Figure 2, the percentages of αB-crystallin-positive areas were found to be higher in the hypoxic than in the normoxic areas in all analyzed HNSCC biopsies.

αB-crystallin expression is upregulated by reoxygenation, not hypoxia

The increased presence of αB-crystallin in the hypoxic areas might be the result of two different processes: a stress-induced upregulation of αB-crystallin and/or a longer survival of the cells expressing αB-crystallin. It has been shown that hypoxia stimulates upregulation of αB-crystallin in piglet stomach, colon and heart tissue (263;264). For this reason we first tested whether hypoxic incubation is able to increase

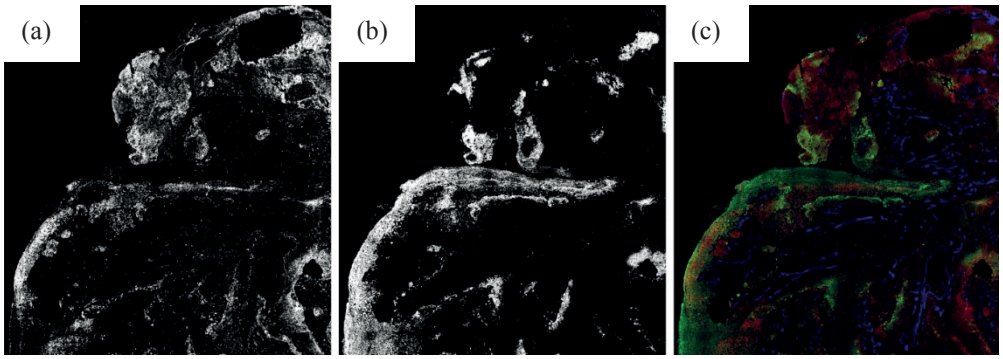

Figure 1. Immunofluorescent staining of human HNSCC for αB-crystallin, pimonidazole-modified proteins and PAL-E. Shown is a representative biopsy section. The fluorescent grey scale images were binarized, resulting in black and white images for αB-crystallin staining and pimonidazole-modified proteins staining, indicating the hypoxic areas (**a** and **b**). The merged image with αB-crystallin staining (assigned red), pimonidazole staining (assigned green) and PAL-E blood vessel staining (assigned blue) shows a substantial overlap between αB-crystallin and hypoxic regions. Hypoxic regions are mostly located in areas at greater distance from vessels (**c**).

αB-crystallin mRNA expression levels of HNSCC cell lines by using quantitative RT-PCR. The HNSCC cell line UT-SCC-5 was maintained for 22 hours under 0.1% O_2 conditions and every 2 hours (except t = 12 hours), αB-crystallin mRNA expression levels were determined. Surprisingly, αB-crystallin mRNA levels were found not to be upregulated, but actually 2.3-fold downregulated after 22 hours (Figure 3, $P < 0.001$), which suggests that the increased expression of αB-crystallin in the hypoxic areas of HNSCC is not directly caused by low oxygen levels. Reoxygenation can also lead to αB-crystallin upregulation, as has been shown in cultured optic nerve astrocytes (48). Since in some areas hypoxia can be intermittent, resulting in periods with higher oxygen (194;196;197), we assessed the effect of reoxygenation on αB-crystallin expression. Consistent with the previous experiment, after 48 hours of hypoxic incubation, αB-crystallin mRNA expression was downregulated in UT-SCC-5 as well as in the HNSCC cell line UT-SCC-15 (Figure 4). However, upon reoxygenation, αB-crystallin expression levels were significantly higher than in the cells which were only incubated under normoxic conditions. A similar response was also observed in HeLa cells (data not shown), indicating that this might be a general response. Next we tested if a similar effect of the reoxygenation could be found on the protein level. For this we could only use the UT-SCC-5 cell line, since αB-crystallin expression in UT-SCC-15

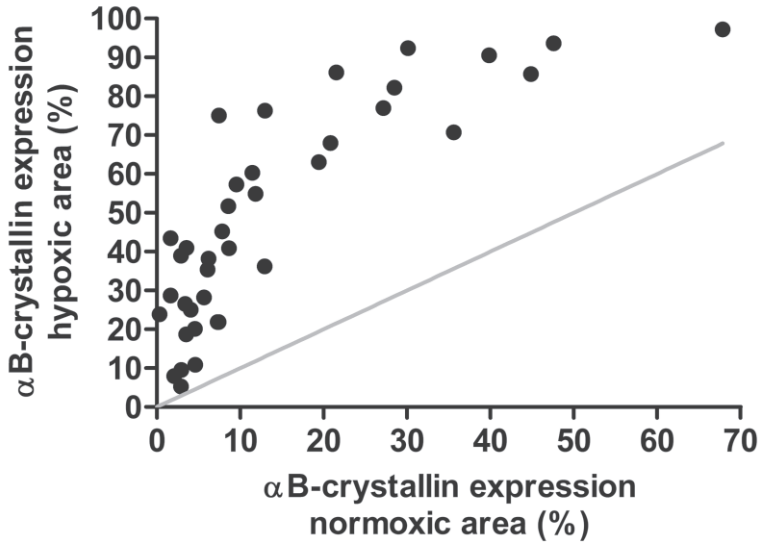

Figure 2. αB-crystallin expression is increased in hypoxic areas. The symbols represent the relative amount of αB-crystallin staining in the normoxic areas and in the hypoxic areas for each individual HNSCC. Equal staining of αB-crystallin in the normoxic and hypoxic areas would be according to the grey line.

cells was too low to allow detection by western blotting. After 48 hours of hypoxic conditions, αB-crystallin protein levels were decreased 2.0-fold (Figure 5, $p < 0.001$) and upon reoxygenation the αB-crystallin level was raised 1.5-fold compared to the hypoxic level ($p < 0.01$). Although the level after reoxygenation did not reach the level observed at normoxic conditions ($p < 0.01$), these results show that also the αB-crystallin protein was upregulated upon reoxygenation after hypoxia.

αB-crystallin mRNA overexpression during reoxygenation is induced by ROS

Reoxygenation stimulates the production of ROS (267), which at a high concentration is stressful for cells. As a reaction, cells can protect themselves by increasing the level of stress proteins (48). To test whether ROS induces αB-crystallin expression in HNSCC cells, UT-SCC-5 cells were treated with H_2O_2. The cells were incubated for 1 hour with a H_2O_2 concentration series between 0 and 3.0 mM H_2O_2 and subsequently harvested after 7 hours (Figure 6). At the protein level no effect could be detected, because the protein expression was too low to allow accurate measurement by western blotting (data not shown). However, a significant increase in αB-crystallin mRNA

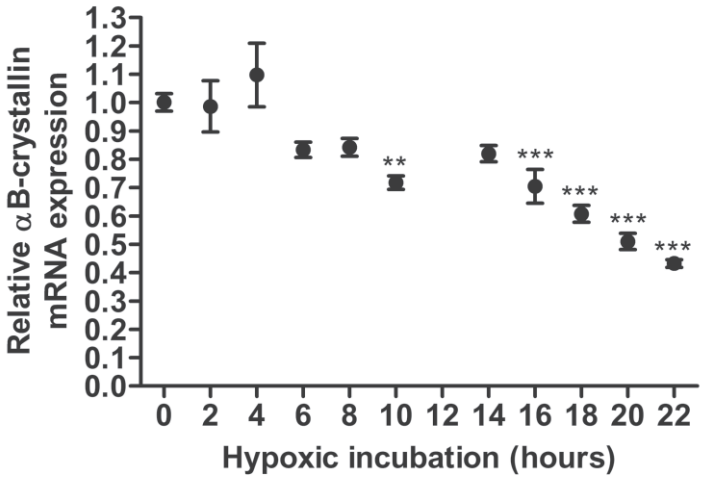

Figure 3. Relative αB-crystallin mRNA expression during hypoxia. αB-crystallin mRNA expression levels in UT-SCC-5 cells after incubation in a humidified 37 ºC H35 hypoxystation at 0.1% O_2 for the indicated time points. αB-crystallin mRNA expression levels were assessed via RT-qPCR (N = 4) *** $p < 0.001$, ** $0.001 < p < 0.01$

expression could be observed at 1.5 mM and 3.0 mM H_2O_2, compared to incubation with mock ($P < 0.001$). Next, it was tested whether induction of αB-crystallin upon reoxygenation can be reduced with the ROS scavenger NAC. UT-SCC-5 cells were incubated without and with NAC during normoxia, hypoxia and reoxygenation. Without NAC, αB-crystallin mRNA levels were again downregulated during hypoxia and upregulated during reoxygenation, as expected (Figure 7). In the presence of NAC, the hypoxia-induced αB-crystallin mRNA downregulation remained the same, whilst the upregulation upon reoxygenation was reduced 1.7-fold, compared to reoxygenation without NAC. These results suggest that the ROS produced upon reoxygenation is at least in part responsible for the upregulation of αB-crystallin in UT-SCC-5 cells.

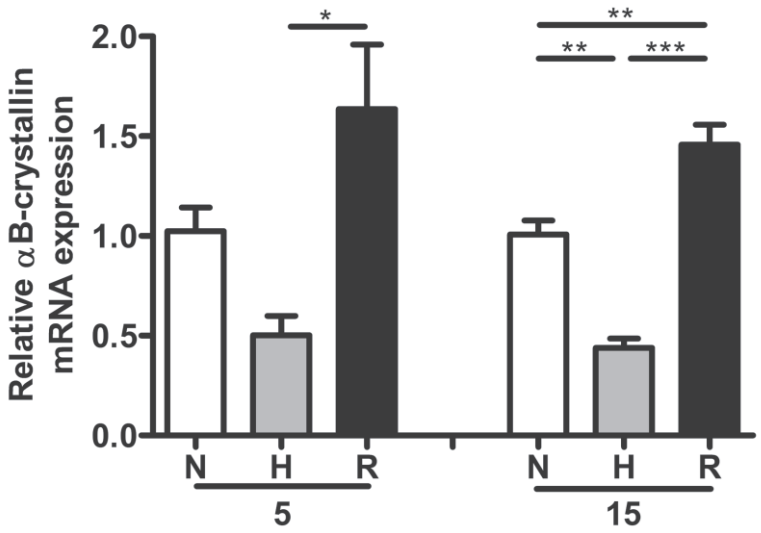

Figure 4. Relative αB-crystallin mRNA levels after hypoxia and reoxygenation. αB-crystallin mRNA levels in UT-SCC-5 and UT-SCC-15 cells under 48 hours normoxia (N), hypoxia (H, 0.1% O_2) and after reoxygenation (R, 24 hours 0.1% O_2/24 hours normoxia). αB-crystallin mRNA expression levels were assessed via RT-qPCR (N = 4). *** $p < 0.001$, ** $0.001 < p < 0.01$, * $0.01 < p < 0.05$.

αB-crystallin knockdown leads to diminished cell survival under hypoxic and hypoglycemic stress

Next, it was investigated whether cells expressing αB-crystallin were able to survive longer under hypoxic conditions. In hypoxic areas, not only a shortage in oxygen, but hypoglycemia as well is a physiological stressor (268). Since glucose is able to protect cells under hypoxic conditions (269) and glucose is the main energy source required for HNSCC cell survival (270;271), medium without glucose was used as an additional stress condition. Reduction of αB-crystallin expression in UT-SCC-5 cells was obtained by siRNA-mediated knockdown. Cells with normal and reduced levels of αB-crystallin were exposed to a hypoxic oxygen level of 0.1% for 24 hours, after which the survival was determined by analyzing the cell number with Cell Counting Kit-8. The knockdown of αB-crystallin was performed with 3 different siRNAs and compared with 2 different control siRNAs (Figure 8a). Under normoxic conditions in the presence of 5 mM glucose, knockdown of αB-crystallin did not significantly alter cell survival, although with all three siRNAs a trend in survival reduction was observed

(Figure 8b). Hypoxic stress in the presence of 5 mM glucose, led to a significant lower cell survival, compared to normoxic conditions (67% for siEGFP and siLUC). Cell survival could be further reduced significantly, by knockdown of αB-crystallin (57% for si-αB1 and 58% for si-αB2 and si-αB3). Under normoxic conditions, 0 mM glucose led to lower cell survival rates (66% for siEGFP and 63% for si-LUC), which was

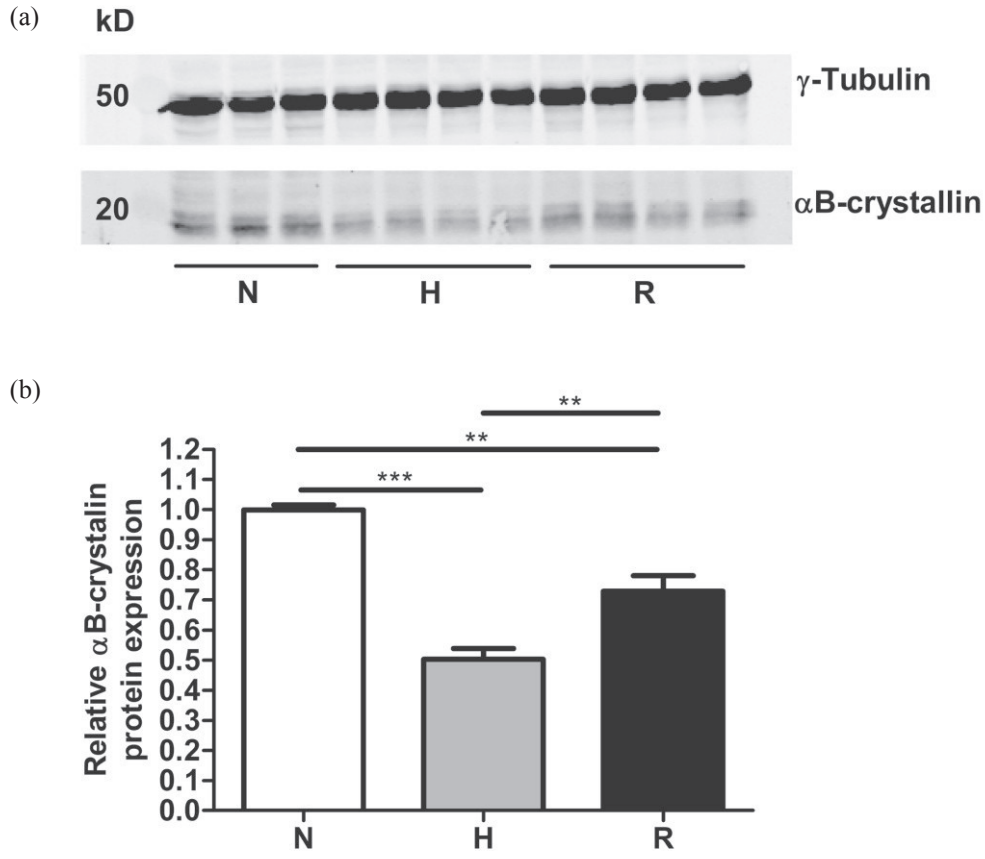

Figure 5. Relative αB-crystallin protein levels after hypoxia and reoxygenation. αB-crystallin protein expression levels in UT-SCC-5 cells under 48 hours normoxia (N), hypoxia (H, 0.1% O_2) and after reoxygenation (R, 24 hours 0.1% O_2/24 hours normoxia). αB-crystallin protein expression was analyzed of 3–4 independent incubations via western blotting (**a**) and quantified (**b**). ***$p < 0.001$, ** $0.001 < p < 0.01$.

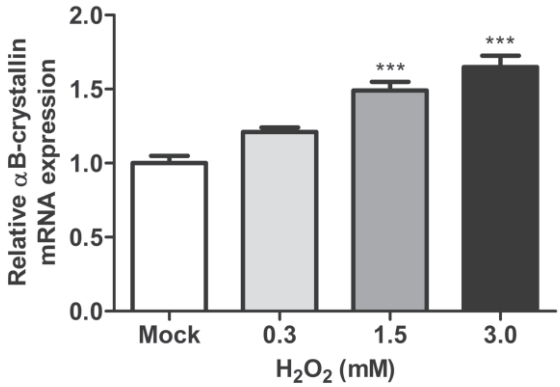

Figure 6. Relative αB-crystallin mRNA levels upon H_2O_2-incubation. Relative αB-crystallin mRNA levels in UT-SCC-5 cells after incubation with 0.0 mM (mock), 0.3 mM, 1.5 mM or 3.0 mM H_2O_2 for 1 hour and 7 hours of recovery. αB-crystallin mRNA expression levels were assessed via RT-qPCR (N = 4). *** $p < 0.001$.

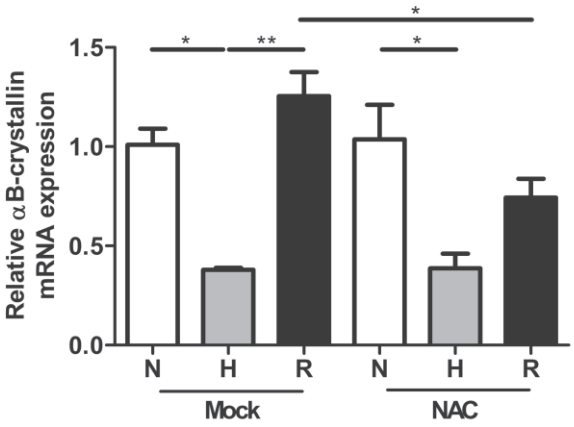

Figure 7. Effect of the ROS-scavenger NAC on αB-crystallin mRNA levels during reoxygenation. UT-SCC-5 cells after incubation with mock or NAC under 48 hours normoxia (N), hypoxia (H, 0.1% O_2) and after reoxygenation (R, 24 hours 0.1% O_2/24 hours normoxia).** $0.001 < p < 0.01$, * $0.01 < p < 0.05$.

further reduced as well after knockdown of αB-crystallin (57% for si-αB1 and 55% for si-αB2 and si-αB3). Combining hypoxic as well as hypoglycemia stress was detrimental resulting in 0% cell survival. Since all 3 different αB-crystallin siRNAs gave similar results, it is very unlikely that these observations are due to off-targets effects. These results show that reduction of the αB-crystallin level decreases the survival of hypoxia-exposed and glucose-deprived cells.

DISCUSSION

In the current study, we show that more αB-crystallin protein is present in hypoxic HNSCC tumor areas than in normoxic areas. Since an increased αB-crystallin expression might be the result of a stress-induced transcriptional upregulation, we investigated whether hypoxic stress is able to induce αB-crystallin expression in HNSCC cell lines. Remarkably, under hypoxic conditions αB-crystallin mRNA expression was found to be downregulated in UT-SCC-5 and UT-SCC-15 cells. It is not clear how αB-crystallin is downregulated, but this could be due to a general transcription shutdown caused by epigenetic modifications (272;273). Only after reoxygenation, a significant upregulation of αB-crystallin mRNA in the HNSCC cell lines was found. The same trend was observed at the protein level. The upregulation of αB-crystallin has also been observed in other cell types and by different forms of reoxygenation stress, such as chemical ischemic/recovery stress and ischemic/reperfusion injury (274;275), although from those studies it appeared that the upregulation of αB-crystallin is not a general mechanism since not all cell types show this effect (274). The reoxygenation-induced upregulation of αB-crystallin also fits with the studies performed with the piglets, where hypoxia-induced αB-crystallin upregulation was detected (263;264). In these studies piglets were maintained in a hypoxic chamber for either 1 or 4 hours and were allowed to recover over periods of 1 to 68 hours under normoxic condition and thus underwent a period of reoxygenation.
The reoxygenation-induced upregulation of αB-crystallin mRNA is at least partially caused by ROS, based on the inhibitory effect of the ROS-scavenger NAC (Figure 7). Despite the low level of oxygen, significant levels of ROS can be present in hypoxic areas and thus can be responsible for the induction of αB-crystallin expression. ROS-levels in hypoxic areas can be increased by moments of reoxygenation due to intermittent, perfusion-limited hypoxia (200) or produced by necrotic cells which are often present in hypoxic tumor areas (202;268;276;277). Also ROS can be produced by a synergistic effect of oncogenic-induced stimulation of increased mitochondrial

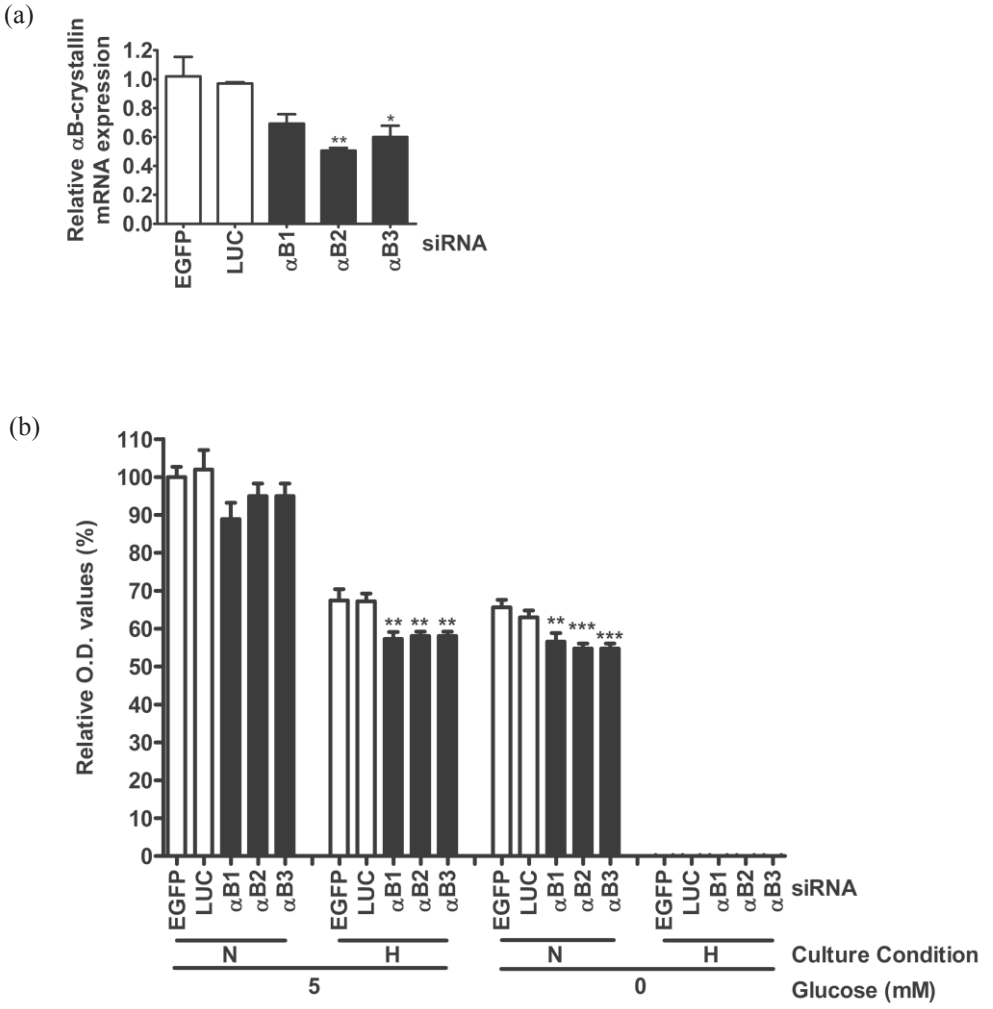

Figure 8. Knockdown of αB-crystallin expression reduces hypoxia and hypoglycemia survival. Expression of αB-crystallin mRNA in UT-SCC-5 cells was reduced by three different αB-crystallin siRNAs (αB1, αB2 and αB3). LUC and EGFP were used as negative control siRNAs (**a**). Survival of siRNA-treated UT-SCC-5 cells under normoxic (N) and hypoxic (H, 0.1% O_2 for 24 hours) conditions in the presence of 5 mM or 0 mM glucose (**b**). Cell survival was assessed via a colorimetric assay using cell counting kit-8. The optical density (O.D.) of siEGFP-treated cells was set at 100%. *** $p < 0.001$, ** $0.001 < p < 0.01$, * $0.01 < p < 0.05$.

capacity and low oxygen levels, which causes an ineffective functioning of mitochondrial respiratory complexes (255). For this a hypoxia-induced downregulation of thioredoxin reductase 1 seems to be important in maintaining high levels of ROS under hypoxic conditions (278). As mentioned earlier, some normoxic areas may also contain significant levels of αB-crystallin. These local αB-crystallin expressions might be explained by intermittent hypoxia as well. As shown by Bennewith and colleagues a substantial proportion of tumor cells can go through cycles of hypoxia and normoxia (279;280). If the intervals of hypoxia are too short or if pimonidazole is not present at the hypoxic moments, erroneously no staining by this marker will be detected (279;280). Nevertheless, αB-crystallin induced by the ROS formed during the reoxygenation periods might still be present.

αB-crystallin is a stress protein which may enhance cell survival upon ROS exposure, as shown for H_2O_2 treated mouse retinal pigment epithelium cells (281). Based on knockdown experiments, we showed that αB-crystallin is able to play a role in the survival of cells coping with hypoxia and glucose-deprivation stress as well. It is thus possible that the αB-crystallin present in hypoxic tumor areas plays a role in tumor cell survival during hypoxic stress (268;282). This protective activity of αB-crystallin may further increase the number of αB-crystallin-positive cells in hypoxic tumor areas. In summary, the relative higher levels of αB-crystallin in HNSCC hypoxic tumor areas might be caused by a combination of ROS-induced αB-crystallin upregulation and an enhanced survival of αB-crystallin-positive cells exposed to this stress.

The enhanced expression of αB-crystallin in HNSCC may have a negative effect on the prognosis of the patient. We have recently found that αB-crystallin expression is associated with distant metastases formation in HNSCC patients (261). This association might relate to the chaperone function of αB-crystallin in mediating folding and secretion of VEGF. αB-crystallin is able to bind misfolded vascular endothelial growth factor (VEGF), leading to enhanced VEGF secretion (226;227). VEGF is specifically upregulated by hypoxia-inducible factor 1 (HIF1) and is important for tumor vascularization. VEGF induction is thus a mechanism to alleviate hypoxic circumstances (228;283). Cycling hypoxia-induced VEGF expression has been shown to increase pulmonary metastasis formation in mice (284). Since αB-crystallin can increase hypoxic cell survival and can help in the (re)folding of hypoxia-induced VEGF expression, αB-crystallin expression could ultimately increase the risk of hypoxic tumors to become metastasis-prone (285). Furthermore, by increasing hypoxic cell survival αB-crystallin may also decrease the sensitivity of a tumor to cancer treatments, such as radiation or other cancer treatments, as shown by the effect of αB-crystallin on tumor necrosis factor-related apoptosis-inducing ligand (TRAIL) as well

as cisplatin-induced apoptosis in human ovarian cancer cells (286). Because of its potential to interfere with anti-tumor therapies, αB-crystallin might be a promising target for anti-cancer treatment.

CONCLUSIONS

Enhanced αB-crystallin expression in HNSCC and also in other kind of tumors correlates with poor prognosis of the patients. The underlying stress that induces αB-crystallin expression in HNSCC was not known. Here we show that αB-crystallin is most abundantly present in the hypoxic areas of the tumor, likely caused by ROS stress. The increased expression of αB-crystallin may lead to prolonged survival of hypoxic cells, thereby protecting those cells which are most resistant against cancer treatments.

CHAPTER 5
αB-CRYSTALLIN EXPRESSION IS CORRELATED WITH PHOSPHO-ERK1/2 EXPRESSION IN HUMAN BREAST CANCER

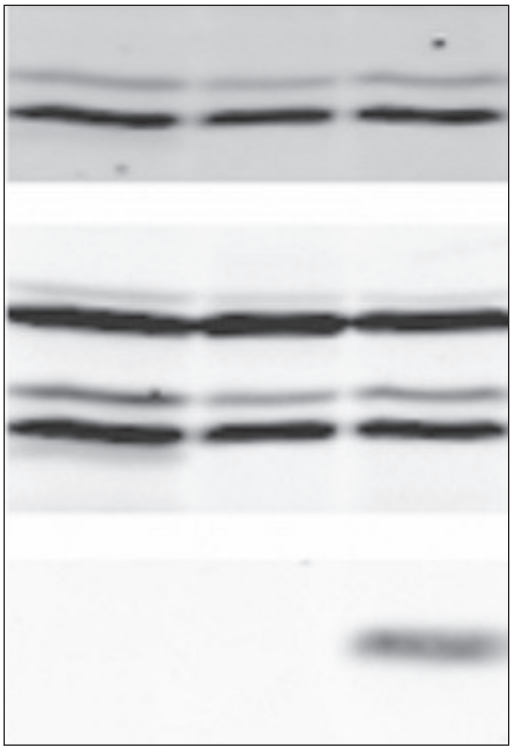

Van de Schootbrugge *et al.*, Int J Biol Markers 2013

ABSTRACT

αB-crystallin is regarded as a biomarker for triple negative/basal-like breast cancer. In normal breast cells overexpression of αB-crystallin leads to neoplastic-like changes, which likely relates to enhanced expression of phosphorylated ERK1/2 (pERK1/2). In this study, we investigated whether αB-crystallin expression is correlated to pERK1/2 expression in breast cancer. In a balanced tissue microarray the expression of αB-crystallin and pERK1/2 kinase were determined immunohistochemically, together with triple negativity and basal-like markers CK5/6 and SMA and the signaling molecules pAKT, pmTOR, EGFR and IGF-1R. αB-crystallin expression significantly correlated with triple negativity and basal-like markers CK5/6 and SMA (Pearson Chi-square test $p=0.004$, $p=0.001$, $p<0.001$, respectively). A significant correlation was observed with pERK1/2 expression ($p=0.002$). siRNA-mediated knockdown of αB-crystallin in triple negative breast cell line MDA-MB468 did not show an effect on pERK1/2 expression levels, indicating that lowering the level of αB-crystallin does not reduce pERK1/2 expression. Our results confirm that αB-crystallin can be used as a biomarker for triple negative and/or basal like breast cancer. The expression of αB-crystallin correlates with pERK1/2 expression in breast cancer tissue suggesting that therapies targeting αB-crystallin might be considered for treatment of triple negative or basal-like breast cancer.

INTRODUCTION

Breast cancer consists of a heterogeneous group of tumors with varying histological appearances and prognoses (164). Using gene expression profiling, breast cancer can be categorized in several subsets, of which the most well known are normal breast-like, luminal A and B, epidermal growth factor receptor 2 (HER2)-enriched, and basal-like breast tumors (164;287). Because of the clinically aggressive nature, basal-like breast cancers have the worst prognosis (287).

Triple negative breast cancers are defined by the absence of immunohistochemical staining for estrogen receptor (ER), progesterone receptor (PR) and HER2. This tumor type accounts for 15% of all breast cancer cases (288). Around 75% of the triple negative cases have the basal-like gene expression profile showing expression of, amongst other markers, high-molecular weight basal cytokeratins (CKs) and smooth muscle actin (SMA) (166;289-291).

Expression of αB-crystallin, a molecular chaperone able to interfere with several cellular processes resulting in cell maintenance under stress conditions (77;122;257), is enhanced in triple negative and basal breast cancer, and is a marker for poor prognosis (126;166;222;223;292). αB-crystallin may directly contribute to malignant progression as overexpression of wild type αB-crystallin in MCF-10A immortalized mammary epithelial cells leads to the formation of abnormal mammary acini and induction of neoplastic changes (126). Constitutive overexpression of αB-crystallin in MCF-10A cells was found to upregulate expression of extracellular regulated protein kinase1/2 (ERK1/2) and phospho-ERK1/2 (pERK1/2), AKT and phospho-AKT (pAKT). Only inhibition of the ERK1/2 pathway could oppose the abnormal acini formation induced upon αB-crystallin overexpression. In cell lines and tumor models, AKT and/or ERK1/2 are implicated in cancer progression and metastasis formation (293). However, it is not known whether αB-crystallin expression in breast tumors is correlated to enhanced activity of these kinases. Therefore, we have studied whether endogenous αB-crystallin expression levels in breast tumors are correlated with the expression of phosphorylated, thus activated, forms of ERK1/2, AKT and mTOR in breast cancer tissue and with the expression of epidermal growth factor receptor (EGFR) and insulin-like growth factor 1 receptor (IGF-1R), which can activate these kinases (294;295). Furthermore, the direct effect of αB-crystallin depletion on pERK1/2 expression was studied *in vitro*, using siRNA mediated knockdown of αB-crystallin.

MATERIAL AND METHODS

Patients

The study population was selected from a cohort of breast cancer patients that was surgically treated between January 1991 and December 1996 at the University Medical Centre St. Radboud. Selection criteria were: no axillary lymph node invasion, no adjuvant systemic treatment, and at least 5 years follow up or an earlier recurrence during follow-up (296;297). In order to increase the power of our analysis, we designed a TMA with a high percentage of triple negatives and approximately equally sized groups of breast cancer subtypes were obtained. This ultimately led to a cohort of 122 patients. As approved by the institutional review board and according to national law, coded tumor tissues were used.

Immunohistochemistry on breast cancer TMAs

Immunohistochemical analyses were performed on 4 µm thick formalin-fixed, paraffin-embedded human tissue micro array (TMA), containing sections of human breast tumors. The specifications for each IHC assay are listed in Table 1. The tissue sections were deparaffinized in xylol and rehydrated through a graded ethanol into water series. All sections were pretreated with a 10 mM citrate buffer (pH 6.0) in a microwave oven for 3 minutes at 800W, followed by 10 minutes at 180W. After cooling for 1.5 hours at room temperature (RT), slides were washed in distilled water. To block endogenous peroxidase activity slides were treated with 3% hydrogen peroxide in distilled water for 10 minutes at RT followed by washing in distilled water and Tris buffered saline (TBS). The primary antibodies were diluted in 1% BSA-TBS and applied overnight in a humidified chamber at 4°C. The following day, the sections were washed with TBS and incubated with PowerVision (ImmunoLogic) for 30 minutes at RT. Subsequently, the sections were washed with TBS and the antibody binding was visualized by incubating 5 minutes at RT with PowerVision DAB (3,3'-diaminobenzide) (ImmunoLogic). After rinsing in distilled water, the sections were counterstained with

Table 1. Antibodies used for immunohistochemical staining

Antigen	Antibody	Dilution	Control tissue
αB-crystallin	mAb mouse IgG (RIKEN Cell Bank)	1/1600	Kidney
SMA	mAb mouse IgG (#A2547, SIGMA)	1/30000	Muscle
CK5/6	mAb mouse IgG (#M7237, DAKO)	1/40	Skin
EGFR	pAb rabbit IgG (#sc-03, Santa Cruz)	1/50	Placenta
IGF-1R	pAb rabbit IgG, (#3027, Cell Signaling Technology)	1/250	Squamous cell carcinoma and mamma carcinoma
pAKT	mAb rabbit IgG (#3787, Cell Signaling Technology)	1/100	Squamous cell carcinoma and mamma carcinoma
pmTOR	mAb rabbit IgG (#2976, Cell Signaling Technology)	1/50	Mamma carcinoma
pERK1/2	mAb rabbit IgG, (#4376, Cell Signaling Technology)	1/100	Melanoma

Mayer's hematoxylin solution, dehydrated through graded ethanol, cleared in xylol and enclosed with Permount (Fisher Scientific). Control tissues were used as a positive control for each IHC assay as listed in Table 1. Negative control included substitution of the primary antibody with 1% BSA-TBS.

Scoring of IHC results

Scoring of the stainings was performed by eye according to a scoring system where a score of '0' is a negative staining and '1' is positive staining. Cut-off points were determined for each staining. For pAKT, pERK1/2, pmTOR, EGFR en IGF-1R any observable staining was regarded as positive, for CK5/6 and SMA above 5% and for αB-crystallin above 15% of the cells expressing the protein were regarded as positive staining.

Statistical Analysis

Analysis of results was done in SPSS 16.0 using the Pearson Chi-square test.

Cell culture of triple negative cell lines

MDA-MB231, MDA-MB436 and MDA-MB468 cells were seeded into T25 flasks and maintained in DMEM + Glutamax^{tm} (Invitrogen) supplemented with 10% fetal calf serum (Gibco-BRL). At 80% confluency, the cells were harvested and, after trypsinization and two times washing with PBS, 40 µl 2% sodium dodecyl sulfate (SDS, Gibco) was added. Samples were twice heated for 5 minutes at 100°C and sonicated for 10 minutes (1 minute cycles, 30 seconds on, 30 seconds off, Bioruptor®, Diagenode). The samples were stored at -20^{o}C.

αB-crystallin knockdown in triple negative breast cancer cells

7.75*10^{5} MDA-MB468 cells were seeded into T25 flasks, N = 2 per condition and maintained in DMEM + Glutamax^{tm} (Invitrogen) supplemented with 10% fetal calf serum (Gibco-BRL). After 24 hours, confluency was 40% and cells were transfected with 1.25 ng siRNA/flask using Lipofectamine^{tm} 2000 Reagent according to manufacturers' protocol (Invitrogen). One mock transfection and five different siRNA's were used: Mock transfection using MQ, two negative control siRNAs: si-EGFP (CGAGAAGCGCGAUCACAUGdTdT) and si-LUC (CGUACGCGGAAUACUUCGAdTdT), and three αB-crystallin specific siRNA's: si-αB1 (GCACCCAGCUGGUUUGACAdTdT), si-αB2 (CCCUGAGUCCCUUCUACCUdTdT) and si-αB3(CCGGAUCCCAGCUGAUGUAdTdT). The medium was refreshed 5 hours after

transfection. Forty-eight hours after transfection, the cells were harvested, and protein was isolated as described above. The samples were stored at -20 ^{o}C.

Western blotting

The protein concentrations of the lysates were determined with BCA Protein Assay Kit (Thermo Scientific) according to manufacturer's protocol. Protein samples were separated by electrophoresis on a 12.5% SDS-polyacrylamide gel and transferred to a nitrocellulose membrane (Protran). The membranes were blocked with 5% non-fat dry milk (Elk, Campina) in 1x PBS for an hour and washed 3 times for 10 minutes with 1x PBS + 0.0025% v/v Nonidet P-40. The membranes were incubated with the monoclonal mouse-anti-human-αB-crystallin antibody (undiluted, RIKEN), mouse-anti-human-gamma-tubulin as reference (1:3000, Sigma-Aldrich), mouse-anti-human-ERK1/2 (1:200, Cell Signaling) and rabbit-anti-human-phospho-ERK1/2 (1:200, Cell Signaling) diluted in 0.025% w/v Nonidet P-40 and completed with 2% Elk in 1x PBS. After washing, blots were incubated for 1 hour with a 6000-fold diluted goat-anti-mouse IRDye® 800CW (LI-COR) and 6000-fold diluted goat-anti-rabbit IRDye® 680CW (LI-COR). The proteins were visualized with the Odyssey scanner (LI-COR). Analysis was performed using Odyssey 2.1 software.

RESULTS

αB-crystallin expression is correlated with triple negative and basal-like markers

In this study, a balanced breast cancer tissue TMA was used of which 69% of the sections were negative for ER expression, 81% were negative for PR expression, 70 % were negative for HER2 expression and 43% were triple negative. Endogenous αB-crystallin expression was assessed by immunohistochemistry and 39% of the sections were scored positive. αB-crystallin expression appeared to correlate with triple negativity (Table, 2, $p = 0.004$), and not or less well with the lack of expression of one the three receptors *per se* (ER $p = 0.103$, PR $p = 0.859$ and HER2 $p = 0.018$). Moreover, a correlation was found with basal-like markers SMA ($p < 0.001$), and CK5/6 ($p = 0.001$) (Table 2). These results suggest that αB-crystallin is a good biomarker for triple negative tumors and/or basal-like tumors.

Table 2. Tumor markers and kinases correlated with αB-crystallin expression in a balanced breast cancer TMA

Tumor marker	N=	αB-crystallin		p-value
		Negative	Positive	
Triple negativity	113			0.004
Yes		22	27	
No		46	18	
ER	113			0.103
Negative		43	35	
Positive		25	10	
PR	113			0.859
Negative		55	37	
Positive		13	8	
HER2	115			0.018
Negative		43	37	
Positive		27	8	
SMA	111			<0.001
Negative		69	29	
Positive		0	13	
CK5/6	113			0.001
Negative		42	13	
Positive		27	31	
EGFR	120			0.563
Negative		35	20	
Positive		38	27	
IGF-1R	113			0.455
Negative		41	23	
Positive		28	21	

Tumor marker	N=	αB-crystallin		p-value
		Negative	Positive	
pAKT	89			0.648
Negative		27	15	
Positive		28	19	
pmTOR	108			0.291
Negative		22	10	
Positive		44	32	
pERK1/2	105			0.002
Negative		31	7	
Positive		34	33	

αB-crystallin expression is correlated with pERK1/2 expression

As constitutive overexpression of αB-crystallin in the immortalized mammary epithelial cell line MCF-10A was found to upregulate expression of pERK1/2 and pAKT (13), we determined whether a correlation does exist between αB-crystallin and pAKT and pERK1/2 in the TMA. Besides pERK1/2 and pAKT, also pmTOR, which is an AKT substrate was analyzed and IGF-1R and EGFR, which both are able to activate the pERK1/2 and pAKT pathways (16;17) (Table 2). Remarkably, only pERK1/2 expression showed significant correlation with αB-crystallin expression ($p = 0.002$), whereas pAKT ($p = 0.648$), pmTOR ($p = 0.291$), IGF-1R ($p = 0.455$) and EGFR ($p = 0.563$) did not.

αB-crystallin depletion does not affect pERK1/2

The results described above suggest that αB-crystallin may directly or indirectly affect pERK1/2 expression. To investigate the effects of a reduction of αB-crystallin expression on pERK1/2, triple negative breast cell lines MDA-MB231, MDA-MB436 and MDA-MB468, were selected for αB-crystallin knock-down experiments. All three cell lines showed expression of pERK1/2 and ERK1/2, but αB-crystallin was only detected on Western blot in MDA-MB468 cells (Figure 1). Therefore, αB-crystallin was depleted in MDA-MB468 cells, which was done by transfection with three different αB-crystallin-specific siRNAs. As controls, mock-transfected cells and cells

transfected with unrelated siRNAs (si-LUC and si-EGFP) were included. Although αB-crystallin levels were successfully reduced (Figure 2a), the results show that reduction of αB-crystallin in the triple negative breast cell line MDA-MB468 did not detectably affect total pERK1/2 levels (Figure 2b).

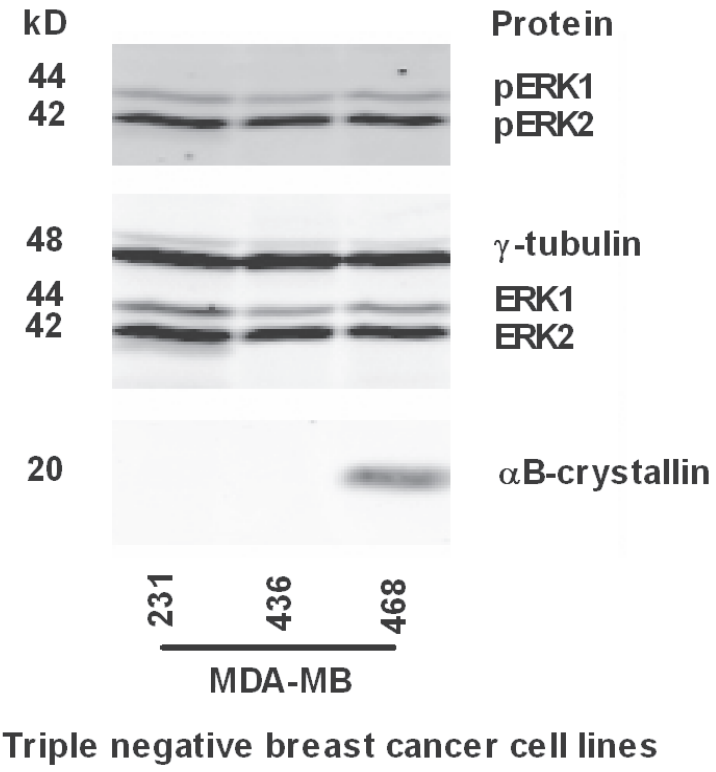

Figure 1. αB-crystallin expression in three cell lines derived from triple-negative breast tumors. Western blot analysis of αB-crystallin, ERK1/2 and pERK1/2 expression in the three triple negative breast cancer cell lysates MDA-MB231, MDA-MB436 and MDA-MB468. α-γ-Tubulin was used as loading control.

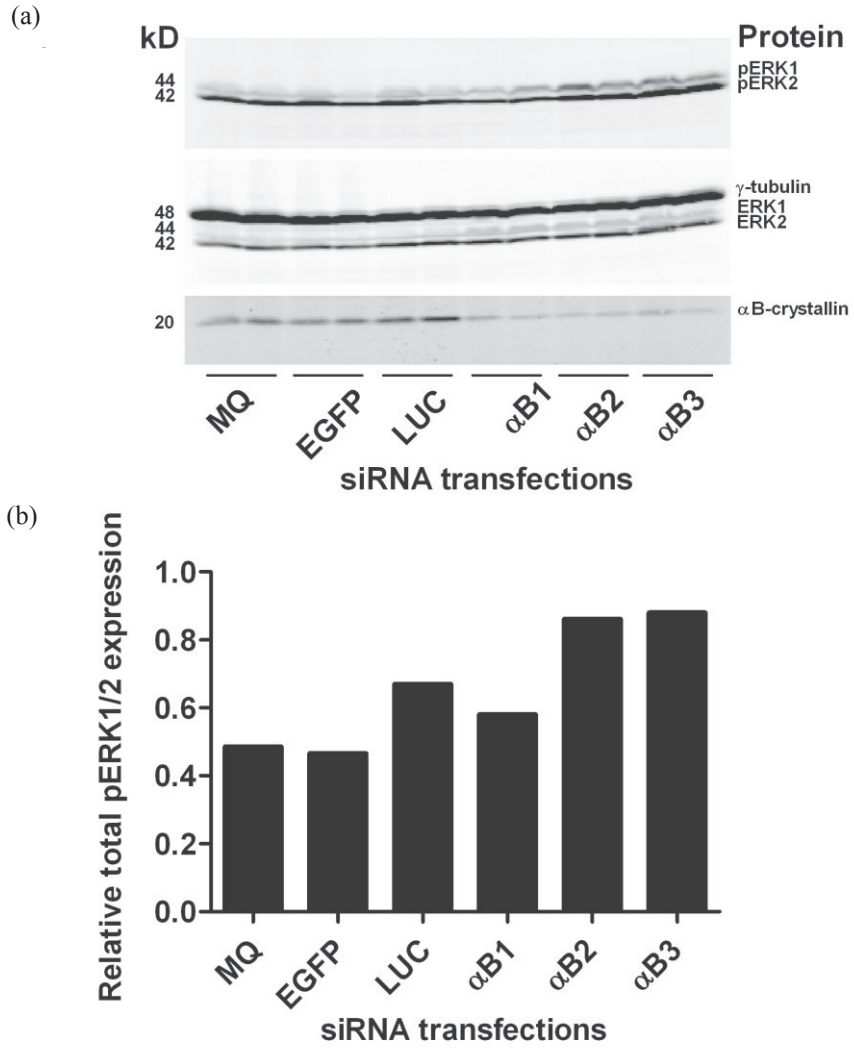

Figure 2. pERK 1/2 and ERK1/2 expression upon αB-crystallin depletion. siRNA-mediated αB-crystallin knockdown was performed in MDA-MB468 and analyzed by western blotting using an antibody to αB-crystallin. pERK1, pERK2, ERK1 and ERK2 expression was detected by using anti-pERK1/2 and anti-ERK1/2 antibodies. α-γ-Tubulin was used as a loading control (**a**). Quantification of total pERK1/2 expression levels, relative to γ-Tubulin expression. The bars in the graph are the mean of the two adjacent samples on Western blots (**b**).

DISCUSSION

Here we describe how, in human breast cancer tissues, αB-crystallin is related to triple negativity and the basal-like markers CK5/6 and SMA. This relation of αB-crystallin with basal-like breast cancers is in line with other studies, that also reported that αB-crystallin is related to poor prognosis in breast cancer (126;166;222;223;292). EGFR, which is also often used as a basal-like marker (290), did not correlate with αB-crystallin in our study, which is contrary to the findings described by Tsang and coworkers (292). This discrepancy, however, might be explained by the lack of a well-documented standard assay for this marker protein (298).

Patients with triple negative breast cancers have a poor prognosis (287), partly as particular treatments are not available for these patients. Anti-breast cancer treatments targeting the estrogen, progesterone or HER2 receptors are ineffective in triple negative breast cancers that do not express these receptors. Other strategies in cancer treatment involve the use of small molecule kinase inhibitors, which target the intracellular downstream signaling pathways (299). Assessing which kinases are specifically enhanced in triple negative breast cancers might therefore reveal new targets for treatment using kinase inhibitors in these tumors. For triple negative tumors, increased activation of the AKT and ERK1/2 pathways has been described (300), suggesting that targeting these pathways might be beneficial in the treatment of triple negative breast cancer. Disruption of the RAS/RAF/MEK/ERK1/2 pathway could be an alternative strategy in particular breast cancer subtypes (301;302). Alternatively, proteins or mechanisms involved in the upregulation of these kinases might be a potential target for alternative treatment options. Reportedly, αB-crystallin could have an effect on the aggressiveness of tumor cells via upregulation of the AKT or ERK1/2 signaling pathways (126). The correlation, observed in the present study, between αB-crystallin and pERK1/2 expression suggests that αB-crystallin expression specifically influences the ERK1/2 pathway and not the AKT pathway, which is in agreement with the observations of Moyano and coworkers (126). However, in the triple negative cell line MDA-MB468 knockdown of αB-crystallin did not detectably change pERK1/2 expression. Moyano and coworkers reported an upregulation of pERK2 in MCF-10A breast cells upon αB-crystallin overexpression in MCF-10A breast cells (126) (pERK1 is not expressed in this cell line (301)) and thus downregulation of at least pERK2 was expected upon siRNA treatment. Why αB-crystallin knockdown did not show an effect on ERK1/2 phosphorylation is not clear. Since αB-crystallin is a heat shock protein which expression is specifically enhanced during stress situations, it is possible that αB-crystallin affects pERK1/2 expression only when the protein is overexpressed. The correlation of αB-crystallin with triple negative tumors and ERK1/2 suggests that

therapies targeting αB-crystallin might be considered for treatment of triple negative or basal-like breast cancers. Our data suggest that not αB-crystallin downregulation but preventing αB-crystallin upregulation might be an option for such an alternative treatment.

CHAPTER 6
PSEUDOPHOSPHORYLATED αB-CRYSTALLIN IS A NUCLEAR CHAPERONE IMPORTED INTO THE NUCLEUS WITH HELP OF THE SMN COMPLEX

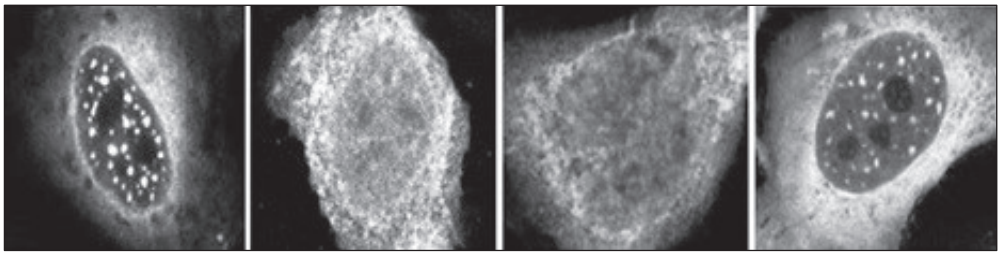

Den Engelsman, Van de Schootbrugge *et al.*,
PLOS ONE 2013

ABSTRACT

The human small heat shock protein αB-crystallin (HspB5) is a molecular chaperone which is mainly localized in the cytoplasm. A small fraction can also be found in nuclear speckles, of which the localization is mediated by successional phosphorylation at Ser-59 and Ser-45. αB-crystallin does not contain a canonical Nuclear Localization Signal sequence and the mechanism by which αB-crystallin is imported into the nucleus is not known. Here we show that after heat shock pseudophosphorylated αB-crystallin mutant αB-STD, in which all three phosphorylatable serine residues (Ser-19, Ser-45 and Ser-59) were replaced by negatively charged aspartate residues, is released from the nuclear speckles. This allows αB-crystallin to chaperone proteins in the nucleoplasm, as shown by the ability of αB-STD to restore nuclear firefly luciferase activity after a heat shock. With the help of a yeast two-hybrid screen we found that αB-crystallin can interact with the C-terminal part of Gemin3 and confirmed this interaction by co-immunoprecipitation. Gemin3 is a component of the SMN complex, which is involved in the assembly and nuclear import of U-snRNPs. Knockdown of Gemin3 in an *in situ* nuclear import assay strongly reduced the accumulation of αB-STD in nuclear speckles. Furthermore, depletion of SMN inhibited nuclear import of fluorescently labeled recombinant αB-STD in an *in vitro* nuclear import assay, which could be restored by the addition of purified SMN complex. These results show that the SMN-complex facilitates the accumulation of hyperphosphorylated αB-crystallin in nuclear speckles, thereby creating a chaperone depot enabling a rapid chaperone function in the nucleus in response to stress.

INTRODUCTION

αB-Crystallin is a member of the small heat shock protein (sHSP) family and is regarded as a molecular chaperone with an important role in cellular protection against diverse stress stimuli (77;122;257;258;303). This is consistent with its high expression in stress-sensitive tissues, like eye lens and muscle (304). There are numerous examples of its protective function, varying from protecting cytoskeletal components to preventing cell death in general (305;306). The primary mode of action is to keep partially unfolded substrate proteins in a folding-competent state, allowing quick recovery after stress stimuli (78). αB-crystallin can be phosphorylated at three different sites: Ser-19, for which the kinase is not known, and Ser-45 and Ser-59, which are phosphorylated by p44/42 mitogen-activated protein kinase and MAP kinase activated

protein kinase 2, respectively (56). Different forms of stress, like heat shock and oxidative ischemic stress, may increase the phosphorylation of αB-crystallin, especially at Ser-59. Ser-19 and Ser-45 are preferentially phosphorylated during the mitotic phase of the cell cycle (57;303). Phosphorylation of αB-crystallin induces conformational changes which affect the interaction with substrate proteins (307). The changes in αB-crystallin increase the chaperone activity by preventing heat shock- and reduction-induced aggregation of target proteins, although for some substrates the chaperone activity might be decreased depending on the nature and concentration of the substrates (56;60;307;308).

Previously, we and others have found that a small subset of the αB-crystallin population can be found in the nucleus, where it predominantly is localized in nuclear speckles (309-312). These nuclear speckles, also known as interchromatin granule clusters (IGCs), are thought to be sites for storage and recycling of splicing factors (313). The subnuclear localization of αB-crystallin is modulated by differential phosphorylation of Ser-45 and Ser-59, as demonstrated by the substitution of these serine residues by negatively charged aspartate residues to mimic phosphorylation, or by non-phosphorylatable alanine residues, as well as by immunocytochemical staining with antibodies directed to endogenously phosphorylated αB-crystallin (311). In interphase cells, phosphorylation at Ser-59 is required for nuclear import, whilst phosphorylation at Ser-45 is crucial for nuclear speckle localization (311). Furthermore, nuclear import of αB-crystallin might be facilitated by the Survival Motor Neuron (SMN) complex, as suggested by the interaction and co-localization of (pseudo)phosphorylated αB-crystallin with a subunit of this complex (311). The SMN complex is involved in the biogenesis and nuclear import of small nuclear ribonucleoparticles (snRNPs) (314;315) and contains, in addition to SMN, at least seven other proteins, named Gemin2-8 (316).

The highly regulated nuclear import of αB-crystallin and its specific subnuclear localization suggest that this protein has a nuclear function in addition to its activities in the cytoplasm. Here we show that upon heat shock pseudophosphorylated αB-crystallin moves from the nuclear speckles to the nucleoplasm, allowing protection of a broad range of nuclear proteins, and we identified the SMN complex as an important factor that facilitates the nuclear import of αB-crystallin.

MATERIALS AND METHODS

Cell culture, plasmids, transfections and two-hybrid screen

HeLa cells were grown at 37°C in Dulbecco's modified Eagle's medium (DMEM; Invitrogen) supplemented with 10% fetal calf serum (FCS; PAA laboratories), 100 units/ml penicillin and 200 µg/ml streptomycin, in the presence of 5% CO_2 in a humidified 37ºC incubator. The doxycyclin-inducible T-REx™-HeLa-pcDNA4-αB-STD cell line (61) was kept in Eagle's minimal essential medium **(**EMEM, Lonza) supplemented with Glutamax^{tm} (Invitrogen), 10% fetal calf serum (Gibco-BRL), 5 ug/ml Blasticidin (Invitrogen) and 200 ug/ml Zeocin (Invitrogen). The DNA fragments encoding the sequence of αB-crystallin wild-type, STD (Ser-19, Ser-45 and Ser-59 replaced by Asp) and STA (Ser-19, Ser-45 and Ser-59 replaced by Ala) have been described elsewhere (61;115). The nuclear luciferase DNA, present in the pEGFP-N2 vector from Clontech has been described by Nollen and coworkers (317). A β-galactosidase expression vector was used to measure the transfection efficiency in the nuclear luciferase assay (318). Transfections of HeLa cells with the plasmids were performed by lipofection using the FuGENE^{tm} 6 system (Roche Molecular Biochemicals), as described by the manufacturer. The yeast two-hybrid screen was performed with αB-crystallin-LexA fusion protein (bait) to select for proteins (preys) able to interact with αB-crystallin by screening a cDNA library from HeLa cells as has been described before (117).

Heat shock assay

HeLa cells (1 x 10^6) were seeded on coverslips (18 x 18 mm^2) one day prior to transfection with 1 µg DNA. Two days after transfection cells were untreated or heat shocked for 45 minutes at 45^{o}C and recovered at 37^{o}C for the indicated time. The cells were fixed in 3% paraformaldehyde for 15 minutes and permeabilized for 10 minutes in 0.2% Triton X-100 in phosphate-buffered saline (PBS). The cells were subsequently incubated with undiluted monoclonal antibody to αB-crystallin (RIKEN Cell Bank) and a 1:20 dilution of TRITC-conjugated rabbit anti-mouse antibody (DAKO Corp.). All images were obtained by confocal laser scanning microscopy (BIO-RAD MRC1024).

Nuclear luciferase refolding assay

HeLa cells (1 x 10^5) were transfected with 0.2 µg of the transfection control vector expressing β-galactosidase, 0.2 µg pN-luc-EGFP vector coding for nuclear luciferase and 0.6 µg of the pIRES vector either empty or with an αB-crystallin isoform. Three days after transfection, cells were supplemented with 100 µg/ml cycloheximide and 20

mM 3-(N-morpholino)propanesulfonic acid (MOPS) pH 7.4, 1 hour prior to heat shock. Cells were incubated at 45°C for 45 minutes, followed by recovery at 37°C in the presence of 5% CO_2. Cells were washed 3 times with PBS and lysed by scraping the cells in 100 µl nuclear luciferase lysis buffer (25 mM Tris/H_3PO_4, pH 7.8, 10 mM $MgCl_2$, 1% Triton X-100, 15% glycerol and 1 mM EDTA) per 10^6 cells. Luciferase activity was measured by adding 50 µl of luciferase reagent (Promega) to 10 µl of lysate and subsequent analysis on a Lumat LB 9507 luminometer. β-Galactosidase activity was determined by first incubating 10 µl lysate for 30 minutes with 100 µl of β-galactosidase reagent buffer (1:100 Galacton (Tropix) in 100 mM phosphate buffer pH 8.1, 5 mM $MgCl_2$) and then adding 150 µl light emission accelerator (Tropix) for the analysis on a Lumat LB 9507 luminometer.

Co-Immunoprecipitations

HeLa cells (1 x 10^6) were transfected with 1 µg pIRES vector either empty or with an αB-crystallin isoform. Cells were harvested by trypsinization and washed once with DMEM containing 10% fetal calf serum and twice with cold PBS, and suspended in 1 ml lysis buffer (50 mM Tris-HCl pH 7.5, 100 mM NaCl, and 0.5% Nonidet P-40) at 4°C. Cell lysates were cleared by centrifugation at 16,000 g for 30 minutes at 4°C and subsequently incubated with protein G-agarose beads (Roche Molecular Biochemicals) coupled with monoclonal antibody to αB-crystallin (RIKEN Cell Bank). After incubation at 4°C, beads were washed three times with buffer (50 mM Tris-HCl pH 7.5, 100 mM NaCl, and 0.05% Nonidet P-40) and boiled in sample buffer (1% SDS, 0.063 M Tris-HCl pH 6.8, 10% glycerol, 0.01% β-mercaptoethanol, 0.02% bromophenol blue) and analyzed by western blotting.

***In vitro* import assay (319)**

HeLa cells grown on coverslips to 80-90% confluence were washed twice with PBS and once with P-buffer (50 mM HEPES/KOH pH 7.5, 50 mM KAc, 8 mM $MgAc_2$, 2 mM EGTA, 1 mM DTT, protease inhibitors cocktail (Roche)). The cells were permeabilized for 5 minutes at room temperature with 40 mg/ml digitonin (Sigma) in T-buffer (20 mM HEPES/KOH pH 7.5, 50 mM KAc, 4 mM $MgAc_2$, 1mM DTT, protease inhibitors cocktail (Roche) and subsequently washed three times with T-buffer. The permeabilized cells were incubated with 50 µl reaction buffer (T-buffer containing 1 mM ATP, 0.2 mM GTP, 5 mM phosphocreatine, 0.2 mg/ml creatinephosphokinase, 10 mg/ml BSA, 0.25 M sucrose), which was mixed with 5 µl reticulocyte lysate (Promega) and 400 µg purified recombinant αB-crystallin (117), labeled with FITC (Fluorescein isothiocyanate, Pierce) according to the protocol described by the manufacturer, and incubated for 60 minutes at room temperature.

After incubation, the cells were washed three times with T-buffer and fixed with 3% paraformaldehyde and mounted on glass slides with Fluorescent Mounting Medium (Dakocytomation). Images of the cells were obtained by confocal laser scanning microscopy (Bio-Rad MRC1024). Immunodepletion reticulocyte lysate was performed by incubating 20 µl lysate for 30 minutes with protein G beads alone or with protein G beads coupled with Gemin3 or SMN protein antibodies, after which the beads were removed by centrifugation. Nuclear import was reconstituted by adding 50 ng SMN complex, which was purified from HeLa cells stably overexpressing Flag-tagged SMN (320) (see Figure S2).

siRNA transfection assay

T-REx™-HeLa-pcDNA4-αB-STD cell line was seeded on coverslips (10 mm^2) in the absence of antibiotics. At 40% confluency, cells were transfected with 0.1 ng siRNA per coverslip (n=2 per sample) using Lipofectamine^{tm} 2000 Reagent according to manufacturers' protocol (Invitrogen). Six different siRNA's were used: two negative control siRNAs: si-Luciferase (CGUACGCGGAAUACUUCGAdTdT), si-Pop1 (GAAUUUAACCGUAGACAAAdTdT) (321), two Gemin2 specific siRNA's: si-Gemin2.1 (CCCAACACUUCAAUGGCAAdTdT), si-Gemin2.2 (CUGGAAUAGAUUAUGUACAdTdT) and two Gemin3 specific siRNAs: si-Gemin3.1 (GAGGAGUACUGGAGAGCUUdTdT), si-Gemin3.2 (GCAAAGGAAAUAAGUCAUAdTdT). The medium was refreshed 5 hours after transfection and 24 hours after transfection 1 µg/µl doxycyclin (Invitrogen) was added. After 16 hours culturing with doxycyclin, cells were washed twice with PBS and fixed for 20 minutes at RT in 2% paraformaldehyde (Merck) in PBS and subsequently washed with PBS-G (PBS supplemented with 1.5 g/l glycine (MP Biomedicals)). Cells were permeabilized by 10 minutes incubation at RT with 0.1% Triton X100 (USB) in PBS-G. Slides were incubated with monoclonal antibody to αB-crystallin (RIKEN Cell Bank) for 1 hour at 37^{o}C, 10-fold diluted in PBS-GT, (PBS-G, containing 0.05% Tween-20 (Fluka)), washed three times with PBS-G and incubated with goat-α-mouse-Alexa Fluor 488 (LI-COR) for 1 hour at 37^{o}C, 1:150 diluted in PBS-GT. Coverslips were washed three times with PBS-G and mounted using MOWIOL (Calbiochem). Analysis was performed with a fluorescence microscope (Axioskop, Zeiss). Per glass slide, 3 fields were selected randomly and per siRNA an average of 110 cells were counted. Speckle positive and negative nuclei were scored by eye by two independent evaluators. Statistical analysis was performed using One-way ANOVA and Tukey's Multiple Comparison Test. To check for transfection efficiency, cells were transfected using 1.25 ng siRNA/T25 flask. The cells were harvest by trypsinization, washed two

times with PBS and denatured by 5 minutes heating in 40 µl sample buffer and analyzed by western blotting.

Western blotting

Protein samples were separated by electrophoresis on a 12.5% SDS-polyacrylamide gel and transferred to nitrocellulose membranes (Protran) or Hybond-P membranes (Amersham Biosciences). The membranes were blocked with 5% non-fat dried milk (Campina) + 0.05% Tween-20 (Merck) in PBS for an hour. The membranes were incubated O/N in 2% non-fat dried milk in PBS containing monoclonal mouse-anti-human-αB-crystallin (RIKEN), mouse-anti-human-gamma-tubulin (Sigma-Aldrich), mouse-anti-human-gemin2 (E6, Santa Cruz Biotechnology), mouse-anti-human-gemin3 (12H12, Santa Cruz Biotechnology), rabbit-anti-human-αB-crystallin (38), rabbit-anti-human-SMN (Santa Cruz Biotechnology) or rabbit-anti-human-Skp1 (Neomarkers). After washing three times ten minutes with PBS complemented with 0.1% Tween-20, blots were incubated for one hour with goat-anti-mouse IRDye® 800CW (LI-COR) or horseradish peroxidase conjugated goat-anti-mouse secondary antibodies or swine-anti-rabbit secondary antibodies (DAKO Corp.) to allow visualization of the bound antibodies with the Odyssey scanner (LI-COR) or by enhanced chemoluminescence (Pierce Chemical Co.).

RESULTS

Speckle-localized pseudophosphorylated αB-crystallin serves as a chaperone depot

Under normal physiological conditions αB-crystallin is mainly present in the cytoplasm, but upon phosphorylation at Ser-59 and Ser-45 accumulates in nuclear speckles (311). To investigate whether αB-crystallin remains in the nuclear speckles upon heat shock, the pseudophosphorylated αB-crystallin mutant αB-STD was used. This mutant, besides being present in the cytoplasm, abundantly accumulates in the nuclear speckles (311). HeLa cells transfected with pIRES αB-STD vector were subjected to a heat shock (45 min) and subsequently allowed to recover for 0, 6 and 24 hours at 37°C. As expected, nuclear αB-STD of non-heat shocked cells was found predominantly in speckles. However, heat-shocked cells examined directly or 6 hours after the heat shock showed diffuse nuclear staining (Figure 1). Speckle localization was restored 24 hours after heat shock. These results suggest that during heat stress nuclear αB-crystallin exerts its chaperone function in the nucleoplasm.

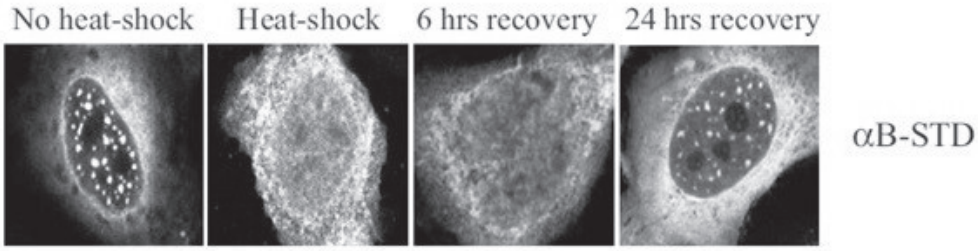

Figure 1. Relocalization of nuclear pseudophosphorylated αB-crystallin in response to heat-shock. Transiently transfected HeLa cells expressing αB-STD were mock-treated or subjected to heat-shock and allowed to recover for 6 or 24 hours. The localization of αB-STD was visualized by immunofluorescence, using a monoclonal antibody against αB-crystallin.

Pseudophosphorylated αB-crystallin is a nuclear chaperone

To determine whether αB-crystallin can assist in the refolding of proteins present in the nucleus we used a nuclear targeted luciferase-EGFP fusion protein (N-luc-EGFP) (317) as a heat-sensitive reporter. This reporter protein shows a diffuse nuclear staining in non-stressed cells. HeLa cells were transfected with the empty pIRES vector or with pIRES constructs coding for αB-crystallin or mutants thereof, together with the nuclear luciferase construct. In every transfection a β-galactosidase construct was included to be able to correct for variations in transfection efficiency. After three days the cells were exposed to a heat shock to denature the luciferase. The luciferase activity was measured before, directly after and six hours after heat shock. During the recovery period the translation inhibitor cycloheximide was present to prevent *de novo* synthesis of luciferase. As can be seen in Figure 2, directly after heat shock the activity of luciferase was strongly reduced in cells transfected with pIRES, wild-type or non-phosphorylatable αB-crystallin (αB-STA) and somewhat less pronounced in the cells transfected with αB-STD. Six hours after heat shock a significant recovery of luciferase activity was observed in the αB-STD transfected cells (8.7%), whereas the pIRES, wild-type or αB-STA transfected cells showed almost no or much less recovery of luciferase activity (0.3, 2.2 and 1.0%, respectively). These data demonstrate that pseudophosphorylated αB-crystallin participates in nuclear chaperoning activity during and directly after heat shock.

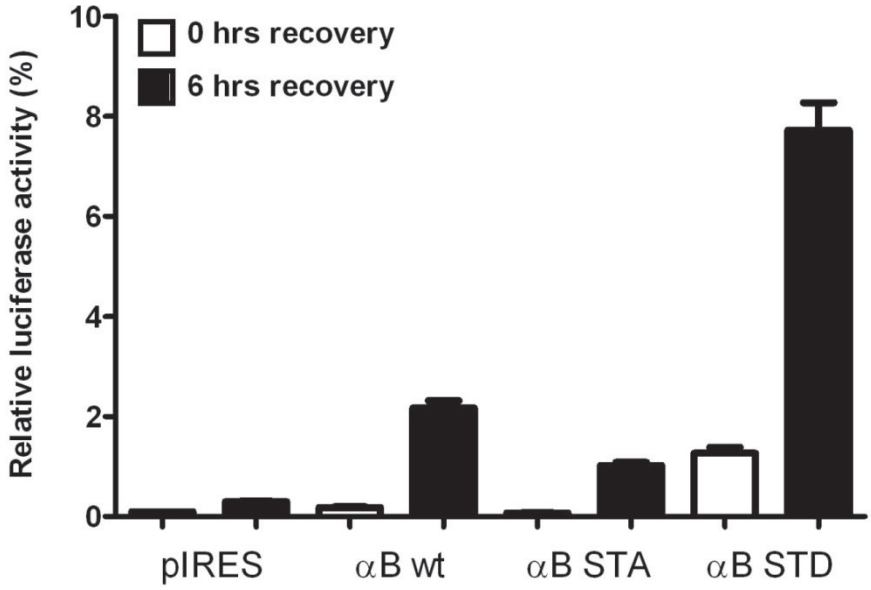

Figure 2. Pseudophosphorylated αB-crystallin enhances refolding of heat-inactivated nuclear luciferase. Transiently transfected HeLa cells expressing nuclear luciferase were heated (45 min at 45°C) and subsequently lysed directly or 6 hours thereafter. Cycloheximide was added just prior to heating to prevent de novo luciferase synthesis. Recovery of luciferase activity is indicated for cells cotransfected with empty pIRES vector (pIRES), or constructs encoding wild-type (WT), non-phosphorylatable αB-crystallin (αB-STA) or pseudophosphorylated αB-crystallin (αB-STD). The luciferase activity was determined and compared with the initial luciferase activity before heat shock. All transfections were corrected for the transfection efficiency as measured by the β-galactosidase activity resulting from a cotransfected β-galactosidase expression vector. The results represent the mean values of 6 independent experiments; error bars indicate the standard deviation. A western blot illustrating the expression of αB-crystallin is shown in Figure S1.

Pseudophosphorylated αB-crystallin interacts with Gemin3

Pseudophosphorylated αB-crystallin does not contain a canonical nuclear localization signal and likely enters the nucleus via an alternative route by binding to a specific adaptor complex. In a yeast two-hybrid system we found that wild-type αB-crystallin is able to interact with the C-terminal 246 residues of Gemin3 (data not shown). Gemin3 is a subunit of the SMN complex (322) and we have previously shown that αB-STD, but not the non-phosphorylatable αB-STA, can interact with the SMN protein, another

subunit of the same complex (311). The SMN complex facilitates the assembly of snRNPs and their import into the nucleus (315), to allow partial accumulation in nuclear speckles. Since αB-STD also localizes in these speckles, we hypothesized that the interaction with this complex facilitates the nuclear accumulation of αB-STD (311). To confirm the interaction of αB-crystallin with Gemin3, a co-immunoprecipitation experiment was performed, using lysates of HeLa cells cotransfected with different αB-crystallin expression constructs. The wild-type and mutant αB-crystallin were efficiently precipitated with anti-αB-crystallin antibody (Figure 3 lower panel).
Gemin3 co-immunoprecipitated with wild-type αB-crystallin (Figure 3 upper panel), which confirms the interaction observed in the two-hybrid system. The efficiency of the coprecipitation of Gemin3 with αB-STA was similar as that observed for the wild-type αB-crystallin, but appeared to be much higher with αB-STD. These results show that αB-crystallin is able to interact with Gemin3 and suggest that the affinity of this interaction is increased by the phosphorylation of αB-crystallin.

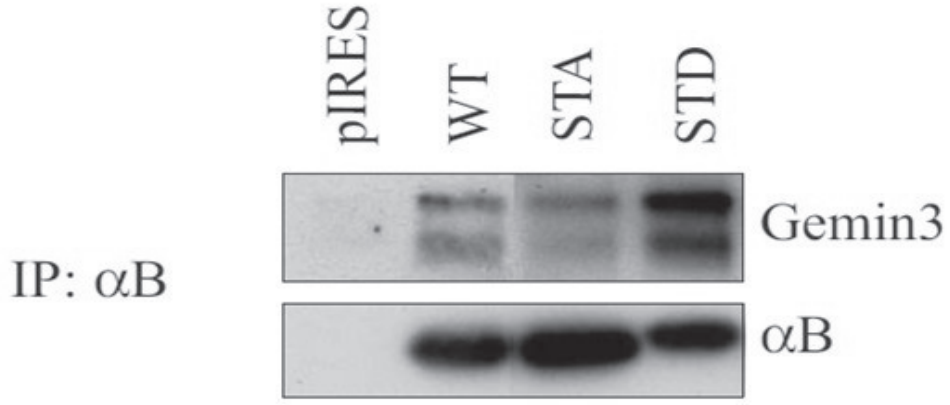

Figure 3. Co-immunoprecipitation of Gemin3 with αB-crystallin. Extracts of HeLa cells, transfected with pIRES as a control or pIRES constructs coding for wild-type (WT), non-phosphorylatable αB-crystallin (αB-STA) or pseudophosphorylated αB-crystallin (αB-STD) were subjected to immunoprecipitation with a monoclonal antibody against αB-crystallin. The immunoprecipitates were analyzed by immunoblotting using a mouse monoclonal antibody against Gemin3 and rabbit polyclonal antibodies to αB-crystallin. Note that Gemin3 shows two bands, of which the lower band is likely a degradation product.

Nuclear localization of pseudophosphorylated αB-crystallin is facilitated by Gemin3 and Gemin2

To investigate whether nuclear speckle localization of αB-STD is Gemin3-dependent, stably transfected HeLa αB-STD cells were used with doxycyclin-inducible expression of αB-STD. The expression of αB-STD was induced 24 hours after transfection with siRNAs directed against Gemin3. αB-crystallin was visualized by immunostaining and the number of cells containing αB-crystallin-positive nuclear speckles was determined. As can be seen in figure 4b and 4c, 84% and 85% of cells that were treated with unrelated control siRNAs (Luciferase and POP1) showed nuclear speckle staining. This was comparable to cells that were not transfected with siRNA, indicating that siRNA treatment did not influence the presence of αB-STD in the nuclei (results not shown). Two distinct siRNAs (Gemin3.1 and Gemin3.2) resulted in down-regulation of Gemin3 expression, as demonstrated by western blotting (Fig. 4a). Knockdown of Gemin3 with these two siRNAs resulted in a significant reduction of cells containing αB-STD positive speckles (Figure 4b and 4c, 35% and 61%, respectively). To confirm the involvement of the SMN complex in αB-STD import (323), also Gemin2 expression was down-regulated with two different siRNAs (Figure 4a). Gemin2 depletion also resulted in decreased numbers of cells containing αB-STD positive speckles (Figure 4b and 4c, 52% and 56% respectively). These results strongly suggest that the SMN complex is involved in nuclear speckle localization of pseudophosphorylated αB-crystallin.

Nuclear import of pseudophosphorylated αB-crystallin is facilitated by the SMN complex

To obtain additional evidence for the involvement of complete SMN complex in nuclear import of αB-STD, an *in vitro* nuclear import system with digitonin-permeabilized HeLa cells was used (324). Digitonin permeabilizes the cell membrane, whilst the nuclear membrane remains intact, allowing to reconstitute nuclear import by reticulocyte lysate containing ATP and GTP. First, we tested whether fluorescently labeled recombinant αB-STD was indeed imported into the nucleus in this system. The results showed that αB-STD was not only imported into the nucleus, but was also targeted to nuclear speckles (Fig. 5A), which was confirmed by the colocalization with the nuclear speckle marker SC35 (data not shown). Thus, the *in vitro* localization of αB-STD is similar to that observed in transiently transfected cell lines (61). The *in vitro* nuclear import of αB-STD is an active process, as shown by the inhibition of import at 4°C (Figure 5a). In contrast to αB-STD, fluorescently labeled wild-type and non-phosphorylatable αB-crystallin (αB-STA) only showed background staining in the

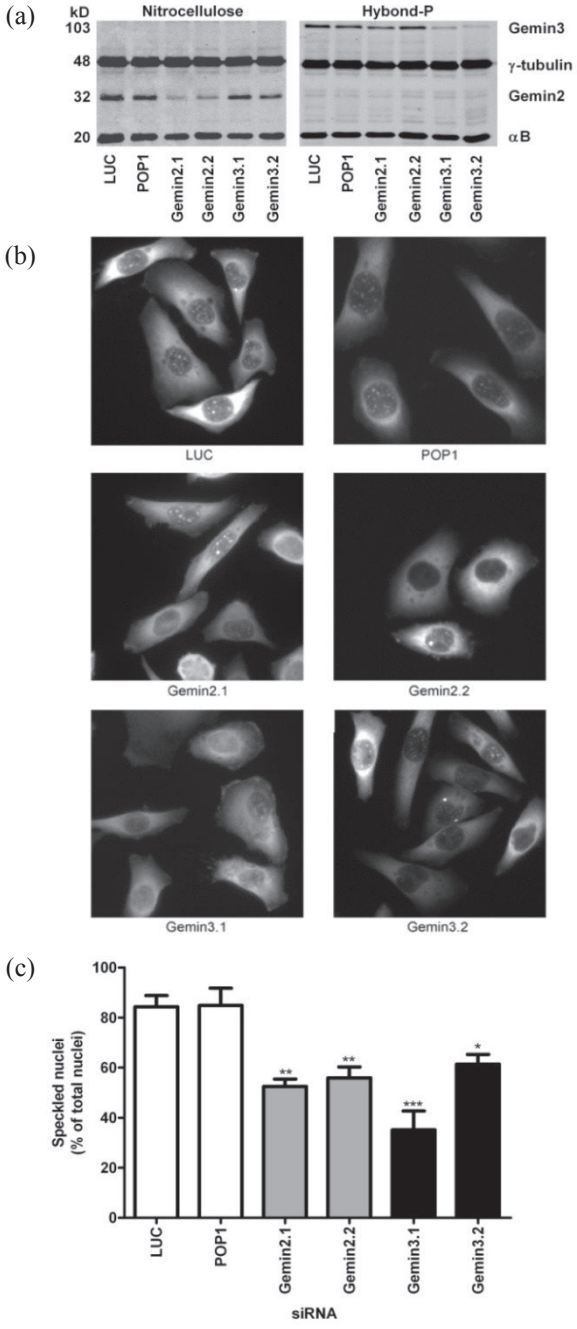

Figure 4. The effect of knockdown of Gemin3 and Gemin2 on the nuclear import of pseudophosphorylated αB-STD. Doxycyclin-inducible T-REx™-HeLa-αB-STD cells were treated with two different Gemin3 siRNAs, two different Gemin2 siRNAs and two negative control siRNAs (LUC and POP1). After 24 hours 1 μg/μl doxycyclin was added to induce αB-STD expression and 16 hours later the cells were analyzed. (A) Knockdown of Gemin3 and Gemin2 was assessed by western blotting analysis. αB-crystallin and γ-tubulin were used as loading controls (**a**). T-REx™-HeLa-αB-STD cells treated with the different siRNAs were stained for αB-crystallin (**b**). The percentages of the siRNA-treated cells containing αB-crystallin-positive speckles in the nucleus were determined and are shown in the graph (**c**). Statistical analysis was performed using One-way ANOVA and Tukey's Multiple Comparison Test. *** $P<0.001$, ** $0.001<P<0.01$, * $0.01<P<0.05$.

nucleus, indicating that these proteins were not imported into the nucleus, which agrees with previous *in situ* results (61). To test whether import of pseudophosphorylated αB-crystallin depends on the SMN complex we immunodepleted reticulocyte lysates from this complex using antibodies directed to SMN and Gemin3. As can be seen in Figure 5c, the Gemin3- and SMN-depleted lysates indeed contained strongly reduced levels of Gemin3 and SMN. Importantly, Gemin3 depletion resulted in efficient co-depletion of SMN, and vice versa, consistent with the removal of the complete SMN complex by this procedure. The SMN-depleted lysates resulted in a significant reduction of the accumulation of αB-STD in nuclear speckles (Figure 5b). To confirm that these effects were due to depletion of the SMN complex, purified SMN complex was added to the SMN-depleted reticulocyte lysate. The addition of the SMN complex indeed rescued the import and speckle localization of αB-STD (Figure 5b). These results show that nuclear import of pseudophosphorylated αB-crystallin is facilitated by the SMN complex.

DISCUSSION

Differential phosphorylation of αB-crystallin is required for nuclear localization (311) and occurs depending on cell cycle and cellular status (56;57). Nuclear speckle accumulation of αB-crystallin can be enhanced by mimicking phosphorylation at three phosphorylation sites (311). Here we show that upon heat shock, the pseudophosphorylated αB-crystallin does not reside in nuclear speckles, but is distributed over the nucleoplasm and re-accumulates in the speckles after release from stress. This is in concurrence with findings of Van den IJssel and coworkers, who showed that the speckle-localized endogenous αB-crystallin in U373 cells significantly diminished after heat shock (309). Nucleoplasmic αB-crystallin is able to protect nuclear proteins, as shown by the ability of pseudophosphorylated αB-crystallin to enhance the refolding of heat-shock-denatured nuclear luciferase. These results suggest that nuclear speckle-localized αB-crystallin, besides acting as a molecular chaperone for nuclear speckle proteins under non-stressed conditions, serves as a depot to allow a rapid increase of αB-crystallin in the nucleoplasm to respond to heat stress. Nuclear αB-crystallin has been shown to help to prevent methylglyoxal-induced apoptosis in retinal pigment epithelial cells, indicating that nuclear αB-crystallin also has a protective role under other stress conditions (325).

αB-crystallin does not play an active role in the refolding of partially unfolded proteins, though it has been proposed to keep substrate proteins in a folding-competent state,

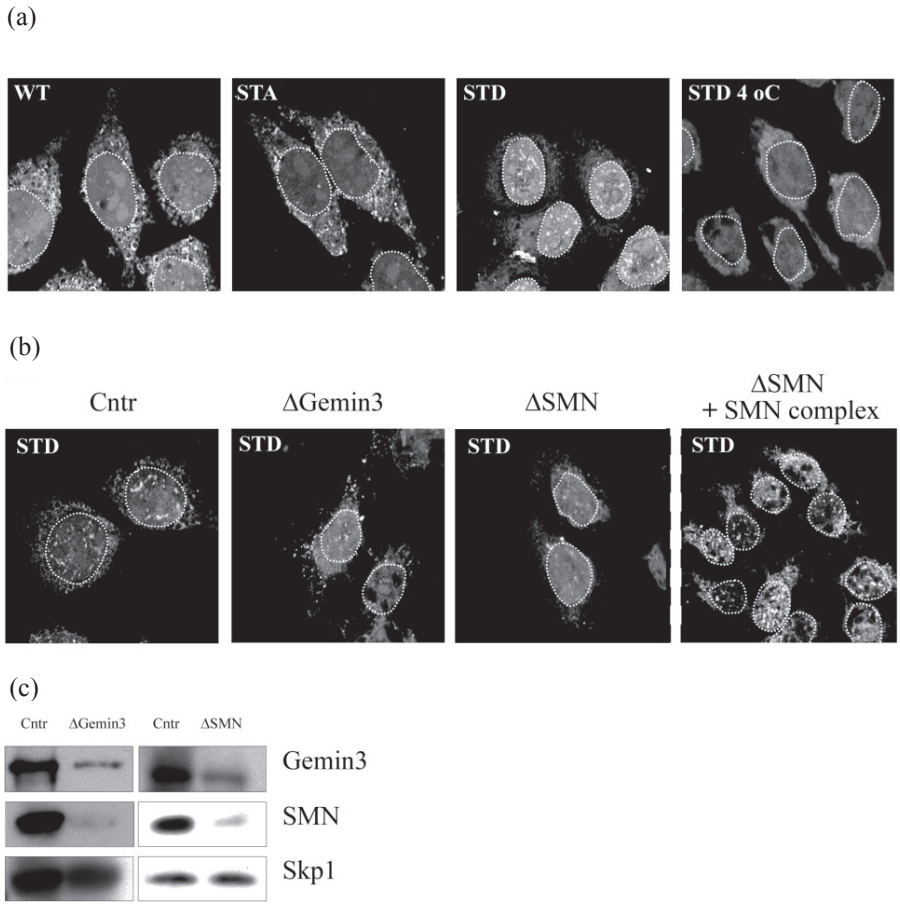

Figure 5. ***In vitro*** **nuclear import of pseudophosphorylated αB-crystallin is dependent on the SMN complex.** *In vitro* nuclear import assays were conducted by incubating digitonin-permeabilized HeLa cells for 1 hour at room temperature with reticulocyte lysates containing ATP and GTP. Import reactions were performed with FITC-labeled recombinant wild-type αB-crystallin (WT), non-phosphorylatable αB-crystallin (αB-STA) and pseudophosphorylated αB-crystallin (αB-STD). As a negative control the import assay with αB-STD was conducted at 4°C (STD 4°C) (**a**). Import reactions of αB-STD with rabbit reticulocyte lysates immunodepleted with anti-Gemin3 antibodies (ΔGemin3), anti-SMN antibodies (ΔSMN) and control-depleted (Cntr). The impaired import of αB-STD with SMN-depleted reticulocyte lysate could be rescued by addition of purified SMN complex (ΔSMN+ SMN complex) (**b**). The immunodepleted reticulocyte lysates were analyzed by western blot to assess depletion. Skp1 was used as a loading control (**c**). Dotted circles indicate the position of the nuclei.

thereby facilitating ATP-dependent refolding by other molecular chaperones, such as Hsp70 (78). During heat stress, importin β-mediated nucleocytoplasmic trafficking is strongly reduced, thereby preventing the active import of cytoplasmic proteins into the nucleus. In contrast to most cytoplasmic proteins, nuclear import of Hsp70 is upregulated during heat shock (326), which is mediated by a novel nuclear import carrier, named Hikeshi (327;328). The nuclear Hsp70 might subsequently act in concert with αB-crystallin to restore heat shock-induced damage inside the nucleus.

αB-crystallin forms polydisperse complexes containing 10 to 40 subunits. Pseudophosphorylation reduces the size of the oligomeric complex of αB-crystallin (60;307;329), but these complexes are still too large to allow passive diffusion into the nucleus, as shown by the lack of nuclear import of αB-STD at 4°C (Figure 5a). Because of the absence of a recognizable nuclear localization signal sequence (312), the nuclear import of αB-crystallin is expected to be mediated by an alternative import carrier. A clue for such a carrier came from yeast-two-hybrid experiments, which demonstrated that αB-crystallin interacts with the C-terminal 246 residues of Gemin3. Although the non-phosphorylated αB-crystallin can interact with Gemin3, in co-immunoprecipitation experiments, Gemin3 was more efficiently pulled down by pseudophosphorylated αB-crystallin, suggesting that hyperphosphorylation increases the affinity for Gemin3. Pseudophosphorylation reduces the interaction between the αB-crystallin subunits (329), which might facilitate the binding to Gemin3. Consistent with the involvement of Gemin3, as a subunit of the SMN complex, in subcellular transport processes (323), Gemin3 appeared to mediate nuclear import of pseudophosphorylated αB-crystallin. This activity of Gemin3 is probably related to its association with the SMN complex, as demonstrated by additional experiments in which the levels of Gemin2 and SMN were reduced. These data strongly suggest that the SMN complex is responsible for nuclear import of αB-STD. SMN is able to directly interact with importin β, as shown in a GST-pulldown assay (330), which might facilitate the interaction with the nuclear pore complex to stimulate the nuclear import of the complex (331). Since SMN colocalizes with phosphorylated αB-crystallin in the nuclear speckles (311), it is likely that this complex is also involved in the accumulation of nuclear αB-crystallin in speckles.

Besides αB-crystallin, the C-terminus of Gemin3 is also able to interact with another member of the small heat shock protein family, HspB8 (332). However, so far no evidence for the accumulation of HspB8 in nuclear speckles has been obtained (312).

Two other small heat shock proteins have been described to localize to nuclear speckles, HspB1 and HspB7. V5-tagged HspB7 constitutively localizes to nuclear speckles, indicating that posttranslational modifications are not involved or are

constitutively present. The nuclear speckle localization signal is situated in the N-terminus of HspB7, but it is not known whether this part is able to interact with Gemin3. Speckle-localized HspB7 does not enhance refolding of heat-denatured nuclear firefly luciferase, suggesting that the association with the nuclear speckles is not related to protein refolding (312).

The accumulation of HspB1 in nuclear speckles depends on more than one signal. Upon stress HspB1 is phosphorylated by the mitogen-activated protein kinase (MAPK) pathway. Phosphorylation of HspB1 has been shown to be necessary for recruitment to speckles, but by itself is not sufficient to support nuclear import (333). Therefore, the phosphorylation of HspB1 may have a similar function as the Ser-45 phosphorylation of αB-crystallin (311). Heat stress induces entrance of HspB1 into the nucleus, which suggests the involvement of a heat shock activated nuclear import factor. αB-STD is able to recruit endogenous HspB1 to nuclear speckles without an additional heat shock (unpublished data), indicating that αB-crystallin is capable to stimulate nuclear import of HspB1. Since heat stress stimulates nuclear accumulation of αB-crystallin (334), it is possible that αB-crystallin in part is responsible for the heat shock-induced nuclear accumulation of HspB1. Nuclear HspB1 has been shown to contribute to increased chaperone capacity in the nucleus under stress conditions, which, similar to the activity of αB-crystallin, seems to be localized outside the nuclear speckles (79).

In summary, our data suggest that phosphorylated αB-crystallin present in nuclear speckles of unstressed cells temporarily moves to the nucleoplasm upon heat shock, providing a rapid increase in chaperone capacity to bind unfolded proteins. The import of phosphorylated αB-crystallin into the nucleus is facilitated by the SMN complex via the interaction with Gemin3. Further investigations are needed to shed more light on the functional activities of αB-crystallin and other small heat-shock proteins in the nucleus, both under normal and under stress conditions.

SUPPLEMENTARY FIGURES

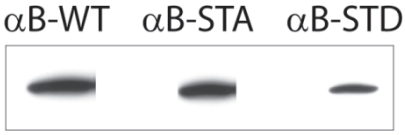

Figure S1. αB-crystallin expression. Expression of wild-type αB-crystallin (WT), non-phosphorylatable αB-crystallin (αB-STA) or pseudophosphorylated αB-crystallin (αB-STD) in transiently transfected HeLa cells. αB-crystallin expression was analyzed by immunoblotting using a monoclonal antibody.

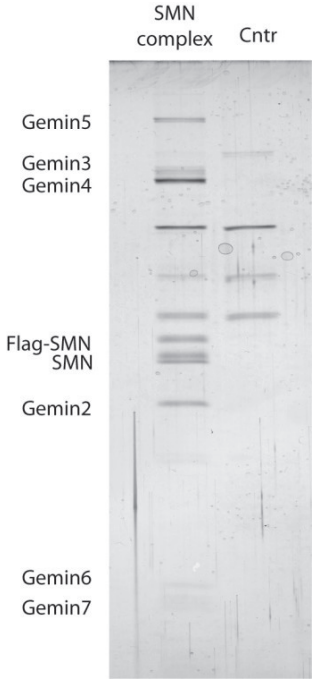

Figure S2. Composition of purified SMN complex. The purified SMN complex was separated by SDS-polyacrylamide gel electrophoresis, followed by silver staining. The SMN complex was purified form HeLa cells stably expressing Flag-tagged SMN protein using anti-FLAG-tag antibodies. The complex was eluted with an excess of Flag-tag peptide. The control lane (Cntr) contains proteins isolated in parallel by the same procedure from control HeLa cells.

CHAPTER 7
GENERAL DISCUSSION

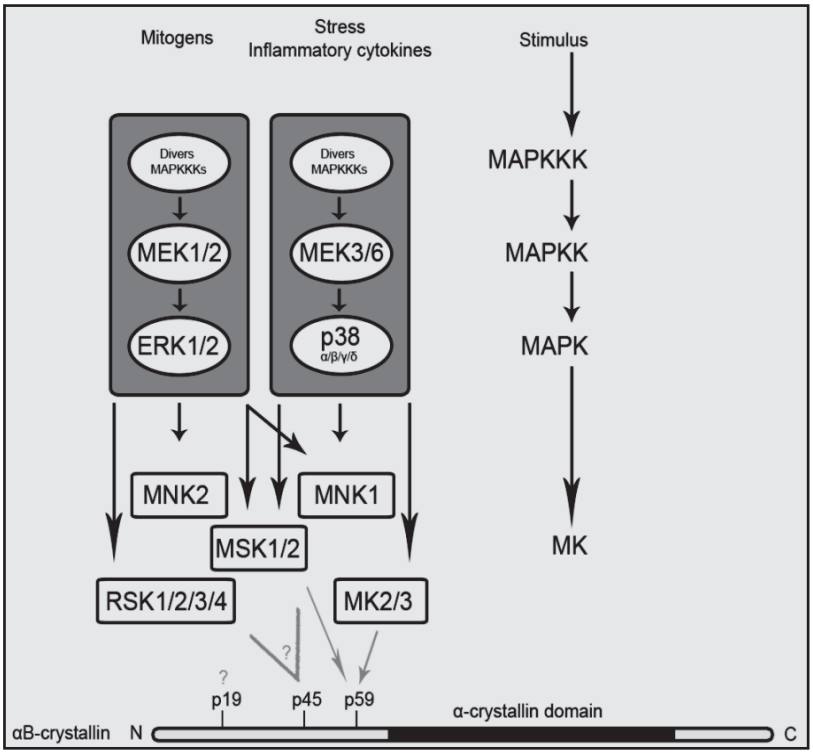

As described in *Chapter 1* αB-crystallin can exert the 'classical' sHSP chaperoning function during cellular stress. Unfolding proteins are captured by large oligomeric complexes formed by homomeric interactions between αB-crystallin subunits and by heteromeric interactions with other sHSPs, thereby preventing further unfolding and stimulating recovery. Also non-protein recovery related functions are described for this protein, like interaction with the apoptosis-inducing proteins to influence their activity and cytoskeletal proteins to stimulate proper formation of cytoskeletal structures. Moreover, αB-crystallin is implicated in various diseases, including several solid tumors, like hepatocellular carcinoma (240), breast cancer (126;222), renal cell carcinoma (335;336) and several brain tumor types (337-339). Increased expression of αB-crystallin in these cancers is often correlated with poor clinical outcome. The predictive value of αB-crystallin upregulation in HNSCC for disease survival rates, however, was subject to debate (220;221). To improve the understanding of the predictive value we analyzed the αB-crystallin expression levels in a HNSCC cohort of which 38 biopsies were available. Our results show that high αB-crystallin expression levels correlate with a shorter disease-free survival (DFS) (*Chapter 3*).

7.1 αB-CRYSTALLIN EXPRESSION IS CORRELATED WITH METASTASIS FORMATION

To get a better understanding of the mechanisms leading to shorter DFS upon αB-crystallin expression, we looked into two major factors that determine DFS: metastasis formation and local-regional recurrence. Local-regional recurrence refers to a recurrence of a tumor localized in the area of the primary tumor site and/or the lymph nodes. For a cell to become tumorigenic, evasion of apoptosis is essential (*Chapter 2*). As αB-crystallin can interact with apoptotic proteins (*Chapter 1*), high αB-crystallin expression could lead to enhanced cell survival after radiation or chemotherapy, thereby leading to tumor regrowth and thus local-regional failure. Remarkably, we did not find any correlation with local-regional recurrence, showing that interaction with apoptotic proteins probably is not the mode of action leading to worse prognosis of the HNSCC patients in this cohort.

Our data indicated, however, that high αB-crystallin expression correlates with metastasis formation (*Chapter 3)*. One of the steps necessary for cancers to metastasize, is enhanced cell invasion and migration (*Chapter 2)*. As described in *Chapter 3*, HNSCC UT-SCC-15 cell migration is reduced upon αB-crystallin knockdown. Furthermore, the motility of HeLa cells was faster upon overexpression of αB-crystallin and slower upon use of αB-crystallin siRNA (Figure 1). These data show

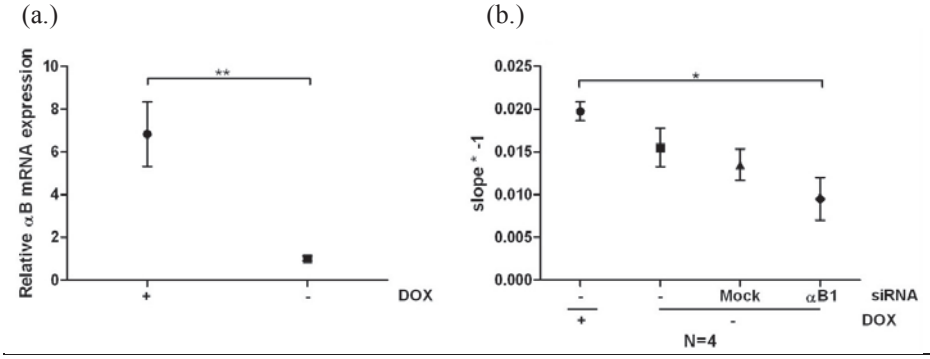

Figure 1. Cell motility of T-REx™-HeLa-pcDNA4-αB-crystallin wild type cell. Doxycyclin (DOX)-induced expression of αB-crystallin in the T-REx™-HeLa-pcDNA4-αB-crystallin wild type cell line resulted in a 7-fold increase of of αB-crystallin mRNA (unpaired t-test $p < 0.05$) (**a**). Cell motility (gap closure) assay (for details see *Chapter 3*). Doxycyclin treated cells showed a tendency of faster gap closure, which was not significant compared to untreated or luciferase-siRNA (Mock) treated controls (**b**). A significant difference in gap closure rate was observed between DOX treated cells and cells in which αB-crystallin was knocked-down by siRNA transfection ($p < 0.05$ using One-way ANOVA and Tukey's Multiple Comparison Test).

that αB-crystallin expression can have an effect on cell motility. As this is a very complex multifactorial process, the mechanism of action of αB-crystallin in this process remains to be elucidated.

Cell migration is dependent on cytoskeletal structures (340). Cell movement is initiated at the leading edge of a cell, where protrusions are formed composed of a branched filamentous (F)-actin filament network, known as lamellipodia. At the termini of these filaments filopodia are formed, which are antennae-like structures containing tight bundles of F-actin. During cellular extension, focal adhesions are formed; flat structures, which contact the surface. αB-crystallin is able to interact with actin filaments and other cytoskeletal structures (*Chapter 1*) (62), which are important for maintaining the integrity of the filaments, especially under stressful circumstances (*Chapter 1*). We hypothesized that αB-crystallin functionally interacts with the cytoskeletal network of filopodia during cell migration. Previously, it was found that inmigrating porcine lens epithelial cells a fraction of αB-crystallinis localized to the leading edges of the cell membrane or in the lamellipodia (62), indicating that αB-crystallin indeed can have a function in cell motility. We investigated whether αB-crystallin affects filopodia formation in HNSCC and other cell lines, by analyzing their quantity and shape upon overexpression or knock-down of αB-crystallin. No effect was

observed. These data suggest that the effect of αB-crystallin is not mediated via filopodia formation or is very subtle, thereby making it difficult to visualize.

7.2 VEGF SECRETION IS INFLUENCED BY αB-CRYSTALLIN EXPRESSION

As described in *Chapter 1*, αB-crystallin can be phosphorylated at S45 by mitogen-activated protein kinases (MAPK) ERK1/2, via an unknown mitogen activated protein kinase-activated protein kinase (MK), and at S59 by MK2, which is specifically targeted by the MAPK p38 pathway (Figure 2). Interestingly, Aggeli and coworkers reported that upon oxidative stress, αB-crystallin can be phosphorylated at S59 by MSK1 as well (Figure 2) (341), which means that ERK1/2 may also lead to αB-crystallin phosphorylation on S59, via MSK1 (Figure 2) (226;342) and could therefore alter functioning of αB-crystallin, related to phosphorylation of either S45 or S59.
By using two mouse models of intraocular disease, oxygen-induced retinopathy and laser-induced choroidal neovascularization, Kase and coworkers found that under hypoxic conditions, phosphorylation of αB-crystallin at S59 is upregulated and also chaperone activity was increased (226;227). Immunoprecipitation studies showed that αB-crystallin can bind to VEGF. Moreover, it was shown that αB-crystallin and VEGF are colocalized in the endoplasmic reticulum (ER) under chemical hypoxia. The localization of αB-crystallin in the ER has only been reported in lens epithelial cells, thus the significance of this finding in other types of cells is currently unknown. In the ER, proteins can be properly refolded and eventually secreted via the Golgi system (226;227). A more efficient rescue of unfolded VEGF in a tumorigenic context could lead to enhanced tumor vascularisation and metastatic potential (*Chapter 2)* (229;230;343-345). In *Chapter 3* we show that αB-crystallin knockdown reduced VEGF secretion in HNSCC cells. Furthermore, upon overexpression of wild type αB-crystallin in stably transffected TREx HeLa cells, VEGF secretion was found to be upregulated under normoxic as well as hypoxic culturing conditions (Figure 3). In the T-REx™-HeLa-pcDNA4-αB-Crystallin wild type cell line, VEGF secretion was increased compared to the negative control T-REx-HeLa-pcDNA4 cell line, also in the absence of doxycyclin (DOX) treatment. This can be explained by leakage expression of αB-Crystallin, which is not visible on western blot. Quantitative RT-PCR using HEK293 cells containing the same control and αB-crystallin constructs show αB-crystallin expression levels that are elevated in cells containing the αB-crystallin construct not treated with DOX, compared to cells with the control construct. These levels, however, were not as high as when αB-crystallin expression was induced with

DOX (personal communication).
As VEGF secretion is linked to tumor progression (*Chapter 2*), this indicates that αB-crystallin expression might influence VEGF secretion in a tumorigenic context, but it is unknown if this accomplished via increased chaperoning of VEGF in the ER. Therefore, it would be interesting to determine if αB-crystallin and VEGF colocalize in the endoplasmic reticulum (ER) of HNSCC cell lines as well.
A common phenomenon in HNSCC and triple negative/basal-like breast cancer is EGFR overexpression, which leads to enhanced EGFR signaling, and this predicts poor

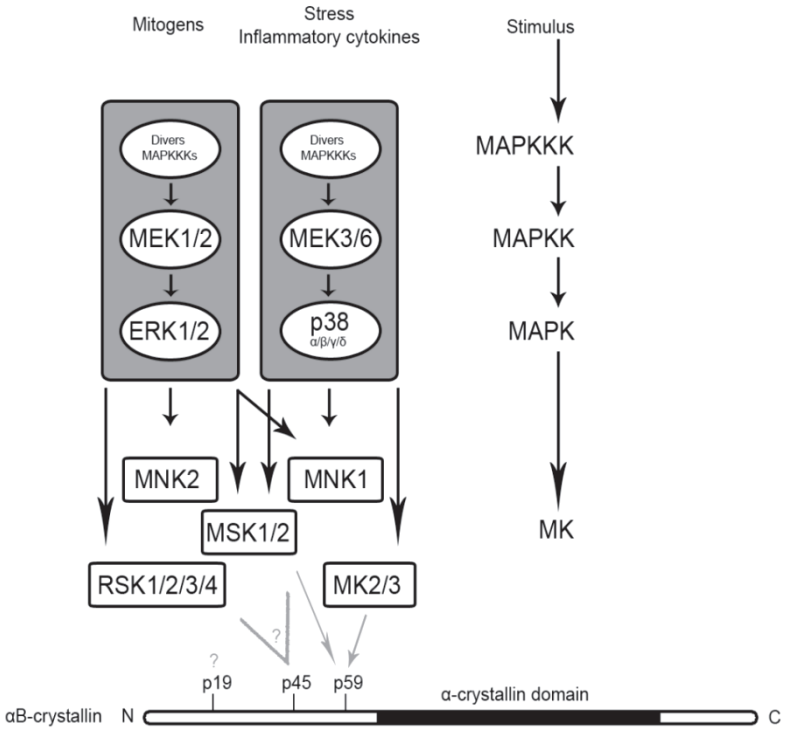

Figure 2. Regulation of αB-crystallin phosphoryl-ation by ERK1/2 and p38. As described in *Chapter 1*, αB-crystallin can be phosphorylated at serine 45 by ERK1/2 and at serine 59 by MK2, which is specifically targeted by the p38 pathway and MSK1. The kinase responsible for phosphorylation at serine 19 is unknown. Which MK is targeted by the ERK1/2 pathway and ultimately is involved in the phosphorylation of serine 45 is unknown. Many MKs can be cross-activated by the ERK1/2 as well as the p38 pathway. Figure adapted from ref. (342).

prognosis for cancer patients *(Chapter 2)*. Interestingly, EGFR activation, via activation of the ERK1/2 kinase pathway, also leads to enhanced VEGF secretion (346;347). As ERK1/2 can have an influence on αB-crystallin functioning, via phosphorylation of S45 and/or S59, and αB-crystallin phosphorylated at S59 can lead to increased VEGF secretion, we propose a model that αB-crystallin expression, under hypoxic conditions and in combination with EGFR activation, leads to significantly elevated levels of VEGF signaling (Figure 4).
Drug therapies are being developed, that target EGFR as well as neutralize VEGF using a single IgG molecule (210). The blocking of multiple pathways reduces the chance of tumor survival via escape pathways (348). αB-crystallin might be a valuable additional target for treatment in view of its roles in (hypoxic) cancer cell survival and VEGF secretion (*Chapter 4*). Recently, Chen and co-workers developed a potent small molecular inhibitor, NCI-41356, which can block the interaction between αB-crystallin and VEGF. In *in vivo* human breast cancer xenograft models, this molecule significantly inhibits tumor growth and vasculature development. This shows that, in accordance with our results, αB-crystallin influences VEGF in a tumorigenic context (349). In aged and cataract eye lenses, a proteolytic βA1/A3-crystallin peptide fragment is present (SDAYHIERLMSFRPIC), which can interact with regions in the α-crystallin domain and C-terminus of αB-crystallin and can interfere with αB-crystallin functioning (350). As cell penetrating peptides already have been proposed as anti-cancer drugs (351-353), the identified αB-crystallin-binding peptide could be modified into a cell penetrating peptide and could be used to target αB-crystallin protein itself. In contrast to the small molecular inhibitor, the peptide may interfere with more αB-crystallin-related functions and may therefore have a stronger inhibitory effect on cancer cell survival. Ultimately, the use of αB-crystallin-targeting treatments alongside existing treatments might lead to better outcome for the patients.

7.3 αB-CRYSTALLIN IS UPREGULATED BY ROS-STRESS

As a member of the chaperone protein family, αB-crystallin expression can be induced upon certain types of stress (*Chapter 1*). We showed in HNSCC biopsies, that more αB-crystallin protein is present in hypoxic tumor areas compared to normoxic areas (*Chapter 4*). To explain this phenomenon, we tested whether αB-crystallin expression is induced upon hypoxic incubation of HNSCC cells (*Chapter 4*). Surprisingly, αB-crystallin mRNA was downregulated in hypoxic HNSCC cells as opposed to VEGF mRNA, which, as reported before, was upregulated (283). Only when the hypoxic

period was followed by reoxygenation, αB-crystallin mRNA was upregulated. *In vivo* studies have demonstrated that periods of reoxygenation are associated with transiently increased levels of ROS (199;200). As described in *Chapter 2*, intermittent hypoxia, cyclic periods of hypoxia and normoxia in tumor cells, might lead to the presence of ROS in hypoxic tumor areas. ROS formation is also observed in necrotic tumor areas, which are often present in the core of hypoxic areas (181; 202). To investigate whether αB-crystallin might be upregulated in hypoxic areas due to ROS, we either increased ROS levels in HNSCC cell lines or reduced ROS levels by incubating with the ROS-scavenger N-acetylcysteine and determined αB-crystallin mRNA expression levels. The results showed that αB-crystallin expression levels are indeed upregulated upon ROS-formation, strongly suggesting that ROS plays a role in elevated αB-crystallin expression in hypoxic areas of HNSCC (*Chapter 4*). The mechanism by which αB-crystallin expression is induced under circumstances of hypoxia and ROS is not yet known. We have investigated a series of factors that might be involved, including heat shock factor 1 (HSF1), lens epithelial derived growth factor (LEDGF), NF-E2-related factor 2 (NRF2) and ETS-1, in HNSCC cells by quantitative RT-PCR, but the data was inconclusive. The tumor microenvironment is characterized, amongst other conditions, by hypoxia and low-glucose concentrations (354). In *Chapter 4* we show that αB-crystallin knockdown leads to decreased cell survival under hypoxic conditions as well

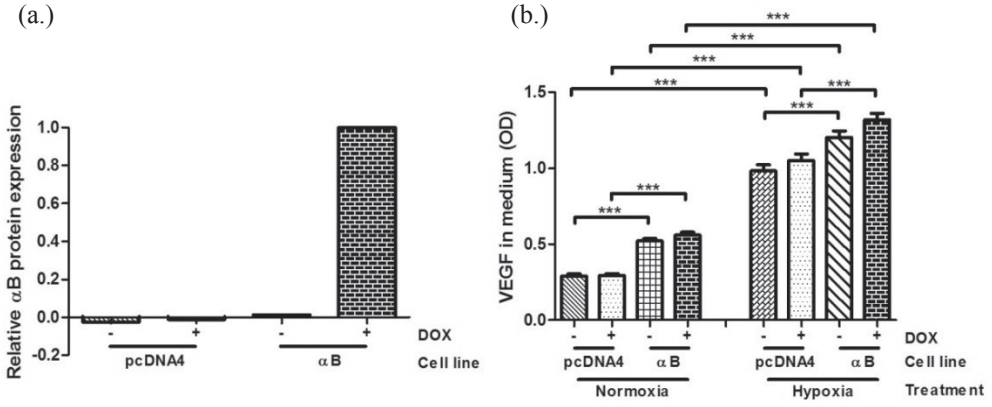

Figure 3. Influence of αB-crystallin overexpression on VEGF secretion. The doxycycline-inducible T-REx™-HeLa-pcDNA4-αB-Crystallin wild type cell line and T-REx™-HeLa-pcDNA4 control cell line were treated with doxycyclin. The protein expression levels were assessed by western blotting (**a**). VEGF secretion levels were determined by ELISA (**b**). Statistical analysis was performed using One-way ANOVA and Tukey's Multiple Comparison Test. *** $P < 0.001$, * $0.01 < P < 0.05$; a.u: absorbance units

as under low glucose conditions. The susceptibility of these cells for glucose stress, especially when combined with hypoxia, could be due to the Warburg affect. Most cancer cells produce energy primarily by glycolysis followed by lactic acid fermentation in the cytosol. In normal cells, energy is produced by a low rate of glycolysis followed by oxidation of pyruvate in mitochondria (355;356). Recently, Liu and coworkers reported that the bidirectional gene pair HspB2/αB-crystallin (described in *Chapter 1*) is a novel direct target of p53 (described in *Chapter 2*). Knockdown of HspB2 as well as αB-crystallin leads to increased glucose concentration and decreased lactate levels in the culture medium and to an increase of intracellular ROS (357). Possibly, the ROS-induced upregulation of αB-crystallin expression is part of a feedback loop which may contribute to the reduction of ROS levels. 'Side-effects' of ROS-induced αB-crystallin upregulation are enhanced glucose metabolism and (hypoxic) cell survival. As hypoxia is linked to metastasis formation via HIF-1-upregulation of angiogenesis-inducing genes, like VEGF (*Chapter 2*), this could ultimately lead to increased metastasis potential (*Chapter 3*).

7.4 αB-CRYSTALLIN AS A BIOMARKER AND TARGET FOR TREATMENT FOR TRIPLE-NEGATIVE/BASAL-LIKE CANCERS

Triple-negative/basal-like breast cancer remains a complicated disease to treat. A study by Dent at al. shows that women with a triple-negative breast cancer are more likely to die during follow-up than women with other types of breast cancers (42% versus 28%). Median time to death was 4.2 years versus 6 years. These women also experienced higher rates of distant recurrence (34% versus 20%) and these occurred sooner after diagnosis (2.6 versus 5.0 years) (358). A better understanding of the heterogeneity in gene expression of triple-negative/basal-like breast cancer is desired as this may help the development of patient subgroup-specific therapies (359).
Tsang et al. showed that αB-crystallin could be a useful biomarker for triple negative and basal breast cancers (292) and Moyano et al. found that overexpression of αB-crystallin in MCF-10A mammary epithelial cells led to malignant progression and upregulated expression of ERK1/2 and phospho-ERK1/2 (pERK1/2), AKT and phospho-AKT (pAKT). In *Chapter 5* we show that αB-crystallin expression is correlated with triple negative and basal-like markers. Recently, this was found as well by Koletsa and coworkers. Analysis of 940 tumors showed that in their tumor microarray (TMA) αB-crystallin was expressed more frequently in triple-negative breast carcinomas (45% vs. 15%) and its expression correlated with basal cytokeratin protein expression (360). In our breast cancer TMA, we also found a correlation

between αB-crystallin expression with pERK1/2 expression. However, when triple negative breast cell lines are depleted of αB-crystallin, this does not affect pERK1/2. Therefore, it is not clear yet whether αB-crystallin-induced malignant progression is modulated via the ERK1/2 pathway (293).

An ideal biomarker for clinical use has a sensitivity and specificity of more than 90% (361). Basal-like marker smooth muscle actin (SMA) has a specificity of 70% and a sensitivity of 100% and basal-like marker cytokeratin (CK)5/6 shows 76% specificity and 33% sensitivity. In our cohort, the specificity and sensitivity of αB-crystallin as a biomarker for triple negativity is 72% and 55%, respectively, which is similar to CK5/6. Although not ideal, αB-crystallin might be useful as an additional biomarker in a clinical setting. In addition, as explained above for HNSCC, αB-crystallin might be an interesting additional target for therapy, especially since estrogen receptor (ER), progesterone receptor (PR) and epidermal growth factor receptor 2 (HER2)-targeted therapy does not work for triple negative breast cancer (*Chapter 2*).

Basal-like and triple-negative breast cancers are regarded similar in literature, as the majority of triple negative cancers are of basal-like phenotype and the majority of tumors expressing 'basal' markers are triple negative (*Chapter 2*) (362).

An indication that elevated αB-crystallin expression might be specifically correlated with the basal-like subgroup of triple negative breast cancers, was obtained by analyzing the αB-crystallin expression in four triple-negative cell lines, MDA-MB231, MDA-MB436, MDA-MB468 and HCC1937. Using gene expression profiling, Lehmann and coworkers showed that MDA-MB231 and MDA-MB436 are of the mesenchymal-like subtype and MDA-MB468 and HCC1937 are basal-like (363). αB-crystallin protein expression was only detectable in MDA-MB468 and HCC1937, substantiating the possibility that αB-crystallin represents a specific marker for the basal-like breast cancer and not for triple negativity *per se*. Interestingly, the pattern of metastatic spread of tumors with a basal-like phenotype seems to be different from that of non-basal-like cancers: they less frequently metastasize to axillary nodes and bones and they favor a hematogenous spread, leading to distant metastasis formation (364-367). In our HNSCC cohort, we did also find that αB-crystallin was correlated with distant metastasis formation and not with loco-regional recurrence. Hypothetically, the presence of αB-crystallin might have a role in the preference of distant metastatic spread of basal-like breast cancer. More support for the association of αB-crystallin expression with basal-like breast cancer might be obtained by analyzing whether αB-crystallin also correlates with other basal/myoepithelial markers in breast cancer tissues, like CD10, maspin, calponin, p63 or p75 (368;369). Whether the basal/myoepithelial-like cancers originate from myoepithelial cells, already expressing

these markers, or are derived from a pluripotent stem cell, ultimately expressing these markers during cancer progression, is still under discussion (289;370-373). More knowledge about the development basal-like and other types of breast cancer and about the differences, e.g. in the metastatic spread, may ultimately lead to improvement of the treatment.

7.5 αB-CRYSTALLIN CAN FUNCTION AS A NUCLEAR CHAPERONE

In HNSCC biopsies stained with αB-crystallin antibodies, some nuclear αB-crystallin staining was observed (unpublished results). In the last experimental chapter of this thesis (*Chapter 6*), we describe how αB-crystallin can be transported into the nucleus via interaction with Gemin3, a component of the SMN complex. The SMN complex is well-known for its function in the assembly of spliceosomal small nuclear ribonucleoproteins (snRNPs), consisting of small nuclear RNAs (snRNAs) U1, U2, U5, andU4/U6, the Sm proteins (B/B', D1, D2,D3, E, F, and G), and a number of U snRNP-specific proteins. The snRNAs are exported from the nucleus to the cytoplasm via interaction with CRM1 (374), where the SMN complex directly recognizes both the Sm proteins and snRNAs and facilitates their assembly into snRNPs. The snRNP import factor snurportin 1 binds the snRNPs, facilitating importin β-mediated nuclear import (375;376). In the nucleus, the snRNPs assemble into spliceosomes, together with many other proteins and are responsible for the removal of introns from pre-mRNA (377).

Narayanan *et al.* showed that snurportin 1 interacts with (cytoplasmic) SMN and Gemin3, which are both components of the SMN complex (330), and that this facilitates the nuclear uptake of snRNPs (315). In non-stressed cells, a fraction of phosphorylated αB-crystallin is present in nuclear speckles, which contain, besides SC35 and other splicing factors (61;310) also snRNPs (378). Since phosphorylated αB-crystallin can also interact with the SMN complex (311), we hypothesized that the nuclear import of αB-crystallin might be facilitated by this complex. In *Chapter 6* we show that αB-crystallin directly interacts with Gemin3 in a yeast two-hybrid system.

Knockdown of Gemin3 strongly reduced the accumulation of αB-STD, a mutant that mimics the phosphorylation αB-crystallin, in nuclear speckles. Furthermore, depletion of SMN inhibited nuclear import of fluorescently labeled recombinant αB-STD, which could be restored by the supplementation with the purified SMN complex. These results indicate that the SMN-complex facilitates the accumulation of phosphorylated αB-crystallin in nuclear speckles. Via its interaction with Gemin3 αB-crystallin may influence the functions of the SMN complex. As described by Cauchi, components of

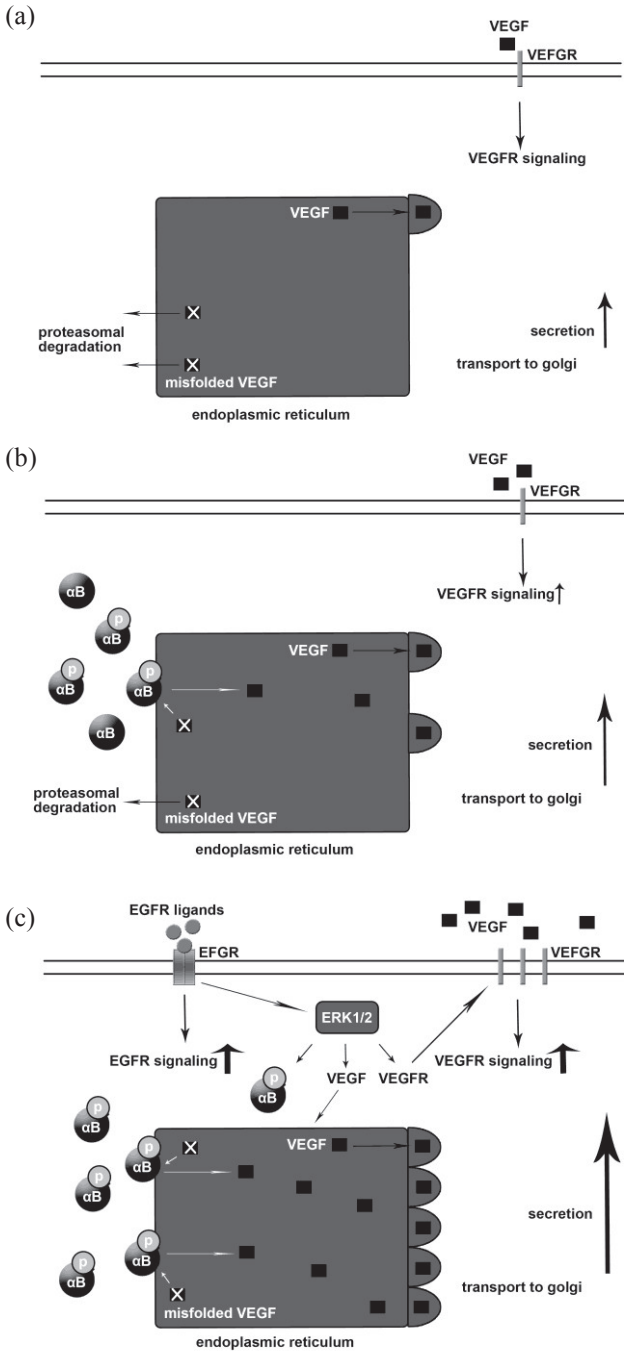
(a)
VEGF
VEFGR
VEGFR signaling
VEGF
proteasomal degradation
misfolded VEGF
secretion
transport to golgi
endoplasmic reticulum
(b)
VEGF
VEFGR
VEGFR signaling
αB
VEGF
proteasomal degradation
misfolded VEGF
secretion
transport to golgi
endoplasmic reticulum
(c)
EGFR ligands
EFGR
VEGF
VEFGR
ERK1/2
EGFR signaling
VEGF
VEGFR
VEGFR signaling
αB
VEGF
misfolded VEGF
secretion
transport to golgi
endoplasmic reticulum

Figure 4. The influence of αB-crystallin expression and phosphorylation under hypoxia and in tumors expressing EGFR. Under hypoxic circumstances, VEGF expression is upregulated by binding of HIF1 to the VEGF promoter. Correctly folded VEGF is transported to the Golgi-apparatus and secreted, where it can induce autocrine (and paracrine) signaling, when binding to the VEGF receptor (VEGFR). Misfolded protein will be degraded by the proteasome (**a**). If αB-crystallin is present in a tumor, this protein can bind the misfolded VEGF, preventing breakdown, and direct endoplasmic VEGF to the reticulum (ER), where it is correctly refolded and eventually secreted via the Golgi apparatus leading to enhanced signaling (**b**). In case a tumor expresses EGFR (which can occur in combination with hypoxia), ERK1/2 becomes activated and the expression of VEGF and VEGFR is induced. Moreover, if αB-crystallin is present, it can become hyperphosphorylated at S59 by ERK1/2, leading to rescue of more VEGF and thus even more VEGF can be secreted than under hypoxic conditions alone. Moreover, as VEGFR is upregulated as well, VEGFR signaling is enhanced massively. Therefore, a combination of EGFR expression, αB-crystallin expression and hypoxia could result in enhanced tumor progression (**c**). This figure is based on illustrations in the following references (227;346;347).

the SMN complex are not only involved in snRNPs biosynthesis (379). Gemin3 can perform important cellular functions independent of the SMN complex. Gemin3 is present in mRNP and miRNP complexes containing AGO2, which are responsible for gene silencing. Gemin3 can also interact with SF-1, a nuclear receptor essential for the development of gonads, the adrenal gland and the ventromedialhypothalamic nucleus, leading to repression of the transcriptional activity of SF-1. Also interaction with METS has been described, which is a repressor of Ets target genes, involved in Ras-dependent proliferation. The interaction with Gemin3 is essential for the anti-proliferative effects of METS. αB-crystallin might affect these different activities of Gemin3 by affecting the interaction with the other Gemin3 interacting proteins.

The function of αB-crystallin in the nuclear speckles is currently unknown. In *Chapter 6*, we show that upon heat-shock, αB-crystallin speckle localization is lost and this protein is localized diffusely throughout the nucleus. Moreover, αB-crystallin can perform the classical chaperoning function, as shown by the refolding of nuclear luciferase after heat stress. αB-crystallin may also have more specific functions in the nucleus, as it has been shown that by inhibiting the activation of nuclear caspases, nuclear αB-crystallin has anti-apoptotic activity in retinal pigment epithelial cells (113;325). αB-crystallin also colocalizes with nuclear lamin A/C (334;380). The intra-nuclear lamina network has an important function, since it is involved in the regulation of many processes, such as gene regulation, DNA replication, chromatin organization, nuclear architecture and nuclear assembly (381-383). Therefore, it is not surprising that

altered lamin expression has also been observed in various cancers, frequently correlating with tumorigenic potential and malignant transformation (384;385). A functional role of αB-crystallin in the nuclear lamin network has not been demonstrated so far. We hypothesize that increase accumulation of αB-crystallin in the nucleus might drive cancer formation by improving lamin-functioning.

7.6 CONCLUDING REMARKS

It is evident that αB-crystallin is a very versatile protein, exerting functions in the cytoplasm as well as in the nucleus. It is also clear that this protein can assist in tumor formation and development of metastasis. This thesis provides suggestions in which direction we have to look for the cellular processes in which αB-crystallin is involved, i.e. enhancing cell motility and VEGF expression and helping in hypoxic cell survival, ultimately leading to worse prognosis for (HNSCC) patients. The exact molecular mechanisms of the action of αB-crystallin in these processes remain to be elucidated. Therefore, it is important to investigate the involvement of αB-crystallin in more detail. A better understanding of these processes may reveal whether αB-crystallin is indeed a feasible target for anti-cancer treatments.

REFERENCE LIST

(1) Mörner CT. (1894) *Untersuchung der Proteinsubstanzen in den sichtbrechenden Medien de Auges.* Hoppe-Seyler's Z Physiol.Chemie , 16.

(2) van der Ouderaa F.J., de Jong W.W., Groenendijk G.W., Bloemendal H. (1974) *Sequence of the first 68 residues of the alpha B2 chain of bovine alpha-crystallin*. Biochem Biophys Res Commun 57: 112.

(3) van der Ouderaa F.J., de Jong W.W., Bloemendal H. (1973) *The amino-acid sequence of the alphaA2 chain of bovine alpha-crystallin*. Eur J Biochem 39: 207.

(4) Ingolia T.D., Craig E.A. (1982) *Four small Drosophila heat shock proteins are related to each other and to mammalian alpha-crystallin*. Proc Natl Acad Sci U S A 79: 2360.

(5) Horwitz J. (1992) *Alpha-crystallin can function as a molecular chaperone*. Proc Natl Acad Sci U S A 89: 10449.

(6) Pasta S.Y., Raman B., Ramakrishna T., Rao C. (2004) *The IXI/V motif in the C-terminal extension of alpha-crystallins: alternative interactions and oligomeric assemblies*. Mol Vis 10: 655.

(7) Pasta S.Y., Raman B., Ramakrishna T., Rao C. (2003) *Role of the conserved SRLFDQFFG region of alpha-crystallin, a small heat shock protein. Effect on oligomeric size, subunit exchange, and chaperone-like activity*. J Biol Chem 278: 51159.

(8) Iwaki A., Nagano T., Nakagawa M., Iwaki T., Fukumaki Y. (1997) *Identification and characterization of the gene encoding a new member of the alpha-crystallin/small hsp family, closely linked to the alphaB-crystallin gene in a head-to-head manner*. Genomics 45: 386.

(9) Elicker K.S., Hutson L.D. (2007) *Genome-wide analysis and expression profiling of the small heat shock proteins in zebrafish*. Gene 403: 60.

(10) Franck E., Madsen O., van Rheede T., Ricard G., Huynen M.A., de Jong W.W. (2004) *Evolutionary diversity of vertebrate small heat shock proteins*. J Mol Evol 59: 792.

(11) Thompson J.D., Higgins D.G., Gibson T.J. (1994) *CLUSTAL W: improving the sensitivity of progressive multiple sequence alignment through sequence weighting, position-specific gap penalties and weight matrix choice*. Nucleic Acids Res 22: 4673.

(12) Nicholas K.B. Nicholas H.B., Deerfield DW, editors (1997) *GeneDoc: Analysis and Visualization of Genetic Variation*. EMBNEW.NEWS 14.

(13) Jehle S., van Rossum B., Stout J.R., Noguchi S.M., Falber K., Rehbein K., et al. (2009) *alphaB-crystallin: a hybrid solid-state/solution-state NMR investigation reveals structural aspects of the heterogeneous oligomer*. J Mol Biol 385: 1481.

(14) van de Schootbrugge C., Boelens W.C. (2010). *Introduction to Small Heat Shock Proteins*. In: Simon S, Arrigo AP, editors. Small Stress Proteins and Human Diseases. Nova Science Publishers.

(15) Guindon S., Gascuel O. (2003) *A simple, fast, and accurate algorithm to estimate large phylogenies by maximum likelihood*. Syst Biol 52: 696.

(16) Gusev N.B., Bogatcheva N.V., Marston S.B. (2002) *Structure and properties of small heat shock proteins (sHsp) and their interaction with cytoskeleton proteins*. Biochemistry (Mosc) 67: 511.

(17) Mymrikov E.V., Seit-Nebi A.S., Gusev N.B. (2011) *Heterooligomeric complexes of human small heat shock proteins*. Cell Stress Chaperones.

(18) van den Oetelaar P.J., van Someren P.F., Thomson J.A., Siezen R.J., Hoenders H.J. (1990) *A dynamic quaternary structure of bovine alpha-crystallin as indicated from intermolecular exchange of subunits*. Biochemistry 29: 3488.

(19) Bova M.P., Ding L.L., Horwitz J., Fung B.K. (1997) *Subunit exchange of alphaA-*

crystallin. J Biol Chem 272: 29511.
(20) Delbecq S.P., Jehle S., Klevit R. (2012) *Binding determinants of the small heat shock protein, alphaB-crystallin: recognition of the 'IxI' motif*. EMBO J 31: 4587.
(21) Sudnitsyna M.V., Mymrikov E.V., Seit-Nebi A.S., Gusev N.B. (2012) *The role of intrinsically disordered regions in the structure and functioning of small heat shock proteins*. Curr Protein Pept Sci 13: 76.
(22) de Jong W.W., Caspers G.J., Leunissen J.A. (1998) *Genealogy of the alpha-crystallin--small heat-shock protein superfamily*. Int J Biol Macromol 22: 151.
(23) Koteiche H.A., Mchaourab H.S. (1999) *Folding pattern of the alpha-crystallin domain in alphaA-crystallin determined by site-directed spin labeling*. J Mol Biol 294: 561.
(24) Morris A.M., Treweek T.M., Aquilina J.A., Carver J.A., Walker M.J. (2008) *Glutamic acid residues in the C-terminal extension of small heat shock protein 25 are critical for structural and functional integrity*. FEBS J 275: 5885.
(25) van Montfort R.L., Basha E., Friedrich K.L., Slingsby C., Vierling E. (2001) *Crystal structure and assembly of a eukaryotic small heat shock protein*. Nat Struct Biol 8: 1025.
(26) Li Y., Schmitz K.R., Salerno J.C., Koretz J.F. (2007) *The role of the conserved COOH-terminal triad in alphaA-crystallin aggregation and functionality*. Mol Vis 13: 1758.
(27) Saji H., Iizuka R., Yoshida T., Abe T., Kidokoro S., Ishii N., et al. (2008) *Role of the IXI/V motif in oligomer assembly and function of StHsp14.0, a small heat shock protein from the acidothermophilic archaeon, Sulfolobus tokodaii strain 7*. Proteins 71: 771.
(28) Jehle S., Vollmar B.S., Bardiaux B., Dove K.K., Rajagopal P., Gonen T., et al. (2011) *N-terminal domain of alphaB-crystallin provides a conformational switch for multimerization and structural heterogeneity*. Proc Natl Acad Sci U S A 108: 6409.
(29) Aquilina J.A., Benesch J.L., Bateman O.A., Slingsby C., Robinson C.V. (2003) *Polydispersity of a mammalian chaperone: mass spectrometry reveals the population of oligomers in alphaB-crystallin*. Proc Natl Acad Sci U S A 100: 10611.
(30) Delbecq S.P., Klevit R.E. (2013) *One size does not fit all: The oligomeric states of alphaB crystallin*. FEBS Lett 587: 1073.
(31) Braun N., Zacharias M., Peschek J., Kastenmuller A., Zou J., Hanzlik M., et al. (2011) *Multiple molecular architectures of the eye lens chaperone alphaB-crystallin elucidated by a triple hybrid approach*. Proc Natl Acad Sci U S A 108: 20491.
(32) Dillmann W.H. (1999) *Small heat shock proteins and protection against injury*. Ann N Y Acad Sci 874: 66.
(33) Tallot P., Grongnet J.F., David J.C. (2003) *Dual perinatal and developmental expression of the small heat shock proteins [FC12]aB-crystallin and Hsp27 in different tissues of the developing piglet*. Biol Neonate 83: 281.
(34) Ciocca D.R., Oesterreich S., Chamness G.C., McGuire W.L., Fuqua S.A. (1993) *Biological and clinical implications of heat shock protein 27,000 (Hsp27): a review*. J Natl Cancer Inst 85: 1558.
(35) Efthymiou C.A., Mocanu M.M., de Belleroche J., Wells D.J., Latchmann D.S., Yellon D.M. (2004) *Heat shock protein 27 protects the heart against myocardial infarction*. Basic Res Cardiol 99: 392.
(36) Lutsch G., Vetter R., Offhauss U., Wieske M., Grone H.J., Klemenz R., et al. (1997) *Abundance and location of the small heat shock proteins HSP25 and alphaB-crystallin in rat and human heart*. Circulation 96: 3466.
(37) Verschuure P., Tatard C., Boelens W.C., Grongnet J.F., David J.C. (2003) *Expression of small heat shock proteins HspB2, HspB8, Hsp20 and cvHsp in different tissues of the perinatal developing pig*. Eur J Cell Biol 82: 523.
(38) van de Klundert F.A., Gijsen M.L., van den IJssel P.R., Snoeckx L.H., de Jong W.W. (1998) *alpha B-crystallin and hsp25 in neonatal cardiac cells--differences in cellular*

localization under stress conditions. Eur J Cell Biol 75: 38.
(39) Srinivasan A.N., Nagineni C.N., Bhat S.P. (1992) *alpha A-crystallin is expressed in non-ocular tissues*. J Biol Chem 267: 23337.
(40) Egwuagu C.E., Chepelinsky A.B. (1997) *Extralenticular expression of the alpha A-crystallin promoter/gamma interferon transgene*. Exp Eye Res 64: 491.
(41) Dubin R.A., Wawrousek E.F., Piatigorsky J. (1989) *Expression of the murine alpha B-crystallin gene is not restricted to the lens*. Mol Cell Biol 9: 1083.
(42) Bhat S.P., Nagineni C.N. (1989) *alpha B subunit of lens-specific protein alpha-crystallin is present in other ocular and non-ocular tissues*. Biochem Biophys Res Commun 158: 319.
(43) Swamynathan S.K., Piatigorsky J. (2007) *Regulation of the mouse alphaB-crystallin and MKBP/HspB2 promoter activities by shared and gene specific intergenic elements: the importance of context dependency*. Int J Dev Biol 51: 689.
(44) Doerwald L., van Rheede T., Dirks R.P., Madsen O., Rexwinkel R., van Genesen S.T., et al. (2004) *Sequence and functional conservation of the intergenic region between the head-to-head genes encoding the small heat shock proteins alphaB-crystallin and HspB2 in the mammalian lineage*. J Mol Evol 59: 674.
(45) de T.A., Le M.A., Mezger V. (2012) *Transcriptional regulation of small HSP-HSF1 and beyond*. Int J Biochem Cell Biol 44: 1593.
(46) Taylor R.P., Benjamin I.J. (2005) *Small heat shock proteins: a new classification scheme in mammals*. J Mol Cell Cardiol 38: 433.
(47) Golenhofen N., Ness W., Wawrousek E.F., Drenckhahn D. (2002) *Expression and induction of the stress protein alpha-B-crystallin in vascular endothelial cells*. Histochem Cell Biol 117: 203.
(48) Yu A.L., Fuchshofer R., Birke M., Priglinger S.G., Eibl K.H., Kampik A., et al. (2007) *Hypoxia/reoxygenation and TGF-beta increase alphaB-crystallin expression in human optic nerve head astrocytes*. Exp Eye Res 84: 694.
(49) Omar R., Pappolla M. (1993) *Oxygen free radicals as inducers of heat shock protein synthesis in cultured human neuroblastoma cells: relevance to neurodegenerative disease*. Eur Arch Psychiatry Clin Neurosci 242: 262.
(50) Hawse J.R., Cumming J.R., Oppermann B., Sheets N.L., Reddy V.N., Kantorow M. (2003) *Activation of metallothioneins and alpha-crystallin/sHSPs in human lens epithelial cells by specific metals and the metal content of aging clear human lenses*. Invest Ophthalmol Vis Sci 44: 672.
(51) Boluyt M.O., Brevick J.L., Rogers D.S., Randall M.J., Scalia A.F., Li Z.B. (2006) *Changes in the rat heart proteome induced by exercise training: Increased abundance of heat shock protein hsp20*. Proteomics 6: 3154.
(52) Vissing K., Bayer M.L., Overgaard K., Schjerling P., Raastad T. (2008) *Heat shock protein translocation and expression response is attenuated in response to repeated eccentric exercise*. Acta Physiol (Oxf).
(53) Wilhelmus M.M., Otte-Holler I., Wesseling P., de Waal R.M., Boelens W.C., Verbeek M.M. (2006) *Specific association of small heat shock proteins with the pathological hallmarks of Alzheimer's disease brains*. Neuropathol Appl Neurobiol 32: 119.
(54) Arrigo A.P., Simon S., Gibert B., Kretz-Remy C., Nivon M., Czekalla A., et al. (2007) *Hsp27 (HspB1) and alphaB-crystallin (HspB5) as therapeutic targets*. FEBS Lett 581: 3665.
(55) Golenhofen N., Ness W., Koob R., Htun P., Schaper W., Drenckhahn D. (1998) *Ischemia-induced phosphorylation and translocation of stress protein alpha B-crystallin to Z lines of myocardium*. Am J Physiol 274: H1457-H1464.
(56) Ito H., Okamoto K., Nakayama H., Isobe T., Kato K. (1997) *Phosphorylation of alphaB-*

crystallin in response to various types of stress. J Biol Chem 272: 29934.
(57) Kato K., Ito H., Kamei K., Inaguma Y., Iwamoto I., Saga S. (1998) *Phosphorylation of alphaB-crystallin in mitotic cells and identification of enzymatic activities responsible for phosphorylation*. J Biol Chem 273: 28346.
(58) Ito H., Kamei K., Iwamoto I., Inaguma Y., Nohara D., Kato K. (2001) *Phosphorylation-induced change of the oligomerization state of alpha B-crystallin*. J Biol Chem 276: 5346.
(59) Kato K., Hasegawa K., Goto S., Inaguma Y. (1994) *Dissociation as a result of phosphorylation of an aggregated form of the small stress protein, hsp27*. J Biol Chem 269: 11274.
(60) Ahmad M.F., Raman B., Ramakrishna T., Rao C. (2008) *Effect of phosphorylation on alpha B-crystallin: differences in stability, subunit exchange and chaperone activity of homo and mixed oligomers of alpha B-crystallin and its phosphorylation-mimicking mutant*. J Mol Biol 375: 1040.
(61) den Engelsman J., Bennink E.J., Doerwald L., Onnekink C., Wunderink L., Andley U.P., et al. (2004) *Mimicking phosphorylation of the small heat-shock protein alphaB-crystallin recruits the F-box protein FBX4 to nuclear SC35 speckles*. Eur J Biochem 271: 4195.
(62) Maddala R., Rao V.P. (2005) *alpha-Crystallin localizes to the leading edges of migrating lens epithelial cells*. Exp Cell Res 306: 203.
(63) Launay N., Goudeau B., Kato K., Vicart P., Lilienbaum A. (2006) *Cell signaling pathways to alphaB-crystallin following stresses of the cytoskeleton*. Exp Cell Res 312: 3570.
(64) Gupta R., Srivastava O.P. (2004) *Deamidation affects structural and functional properties of human alphaA-crystallin and its oligomerization with alphaB-crystallin*. J Biol Chem 279: 44258.
(65) Kamei A., Iwase H., Masuda K. (1997) *Cleavage of amino acid residue(s) from the N-terminal region of alpha A- and alpha B-crystallins in human crystalline lens during aging*. Biochem Biophys Res Commun 231: 373.
(66) Takeuchi N., Ouchida A., Kamei A. (2004) *C-terminal truncation of alpha-crystallin in hereditary cataractous rat lens*. Biol Pharm Bull 27: 308.
(67) Chen S.J., Sun T.X., Akhtar N.J., Liang J.J. (2001) *Oxidation of human lens recombinant alphaA-crystallin and cysteine-deficient mutants*. J Mol Biol 305: 969.
(68) Blakytny R., Carver J.A., Harding J.J., Kilby G.W., Sheil M.M. (1997) *A spectroscopic study of glycated bovine alpha-crystallin: investigation of flexibility of the C-terminal extension, chaperone activity and evidence for diglycation*. Biochim Biophys Acta 1343: 299.
(69) Nagaraj R.H., Oya-Ito T., Padayatti P.S., Kumar R., Mehta S., West K., et al. (2003) *Enhancement of chaperone function of alpha-crystallin by methylglyoxal modification*. Biochemistry 42: 10746.
(70) Satish K.M., Mrudula T., Mitra N., Bhanuprakash R.G. (2004) *Enhanced degradation and decreased stability of eye lens alpha-crystallin upon methylglyoxal modification*. Exp Eye Res 79: 577.
(71) Seidler N.W., Yeargans G.S., Morgan T.G. (2004) *Carnosine disaggregates glycated alpha-crystallin: an in vitro study*. Arch Biochem Biophys 427: 110.
(72) Fujii N., Matsumoto S., Hiroki K., Takemoto L. (2001) *Inversion and isomerization of Asp-58 residue in human alphaA-crystallin from normal aged lenses and cataractous lenses*. Biochim Biophys Acta 1549: 179.
(73) Stromer T., Ehrnsperger M., Gaestel M., Buchner J. (2003) *Analysis of the interaction of small heat shock proteins with unfolding proteins*. J Biol Chem 278: 18015.

(74) Quinlan R.A., Brenner M., Goldman J.E., Messing A. (2007) *GFAP and its role in Alexander disease*. Exp Cell Res 313: 2077.
(75) Outeiro T.F., Klucken J., Strathearn K.E., Liu F., Nguyen P., Rochet J.C., et al. (2006) *Small heat shock proteins protect against alpha-synuclein-induced toxicity and aggregation*. Biochem Biophys Res Commun 351: 631.
(76) Sharma M.C., Goebel H.H. (2005) *Protein aggregate myopathies*. Neurol India 53: 273.
(77) Haslbeck M., Franzmann T., Weinfurtner D., Buchner J. (2005) *Some like it hot: the structure and function of small heat-shock proteins*. Nat Struct Mol Biol 12: 842.
(78) Lee G.J., Vierling E. (2000) *A small heat shock protein cooperates with heat shock protein 70 systems to reactivate a heat-denatured protein*. Plant Physiol 122: 189.
(79) Bryantsev A.L., Kurchashova S.Y., Golyshev S.A., Polyakov V.Y., Wunderink H.F., Kanon B., et al. (2007) *Regulation of stress-induced intracellular sorting and chaperone function of Hsp27 (HspB1) in mammalian cells*. Biochem J 407: 407.
(80) Matuszewska M., Kuczynska-Wisnik D., Laskowska E., Liberek K. (2005) *The small heat shock protein IbpA of Escherichia coli cooperates with IbpB in stabilization of thermally aggregated proteins in a disaggregation competent state*. J Biol Chem 280: 12292.
(81) Mogk A., Deuerling E., Vorderwulbecke S., Vierling E., Bukau B. (2003) *Small heat shock proteins, ClpB and the DnaK system form a functional triade in reversing protein aggregation*. Mol Microbiol 50: 585.
(82) Haslbeck M., Miess A., Stromer T., Walter S., Buchner J. (2005) *Disassembling protein aggregates in the yeast cytosol. The cooperation of Hsp26 with Ssa1 and Hsp104*. J Biol Chem 280: 23861.
(83) Cashikar A.G., Duennwald M., Lindquist S.L. (2005) *A chaperone pathway in protein disaggregation. Hsp26 alters the nature of protein aggregates to facilitate reactivation by Hsp104*. J Biol Chem 280: 23869.
(84) Arrigo A.P. (2013) *Human small heat shock proteins: Protein interactomes of homo- and hetero-oligomeric complexes: An update*. FEBS Lett.
(85) Zantema A., Verlaan-De Vries M., Maasdam D., Bol S., van der E.A. (1992) *Heat shock protein 27 and alpha B-crystallin can form a complex, which dissociates by heat shock*. J Biol Chem 267: 12936.
(86) Kato K., Goto S., Inaguma Y., Hasegawa K., Morishita R., Asano T. (1994) *Purification and characterization of a 20-kDa protein that is highly homologous to alpha B crystallin*. J Biol Chem 269: 15302.
(87) Sugiyama Y., Suzuki A., Kishikawa M., Akutsu R., Hirose T., Waye M.M., et al. (2000) *Muscle develops a specific form of small heat shock protein complex composed of MKBP/HSPB2 and HSPB3 during myogenic differentiation*. J Biol Chem 275: 1095.
(88) Sun X., Welsh M.J., Benndorf R. (2006) *Conformational changes resulting from pseudophosphorylation of mammalian small heat shock proteins--a two-hybrid study*. Cell Stress Chaperones 11: 61.
(89) Lelj-Garolla B., Mauk A.G. (2006) *Self-association and chaperone activity of Hsp27 are thermally activated*. J Biol Chem 281: 8169.
(90) Bukach O.V., Glukhova A.E., Seit-Nebi A.S., Gusev N.B. (2008) *Heterooligomeric complexes formed by human small heat shock proteins HspB1 (Hsp27) and HspB6 (Hsp20)*. Biochim Biophys Acta.
(91) Charette S.J., Lavoie J.N., Lambert H., Landry J. (2000) *Inhibition of Daxx-mediated apoptosis by heat shock protein 27*. Mol Cell Biol 20: 7602.
(92) Fu L., Liang J.J. (2002) *Detection of protein-protein interactions among lens crystallins in a mammalian two-hybrid system assay*. J Biol Chem 277: 4255.
(93) Pipkin W., Johnson J.A., Creazzo T.L., Burch J., Komalavilas P., Brophy C. (2003)

Localization, macromolecular associations, and function of the small heat shock-related protein HSP20 in rat heart. Circulation 107: 469.
(94) Fontaine J.M., Sun X., Benndorf R., Welsh M.J. (2005) *Interactions of HSP22 (HSPB8) with HSP20, alphaB-crystallin, and HSPB3*. Biochem Biophys Res Commun 337: 1006.
(95) Sun X., Fontaine J.M., Rest J.S., Shelden E.A., Welsh M.J., Benndorf R. (2004) *Interaction of human HSP22 (HSPB8) with other small heat shock proteins*. J Biol Chem 279: 2394.
(96) Irobi J., Van Impe K., Seeman P., Jordanova A., Dierick I., Verpoorten N., et al. (2004) *Hot-spot residue in small heat-shock protein 22 causes distal motor neuropathy*. Nature Genetics 36: 597.
(97) Kato K., Shinohara H., Goto S., Inaguma Y., Morishita R., Asano T. (1992) *Copurification of small heat shock protein with alpha B crystallin from human skeletal muscle*. J Biol Chem 267: 7718.
(98) Benndorf R., Sun X., Gilmont R.R., Biederman K.J., Molloy M.P., Goodmurphy C.W., et al. (2001) *HSP22, a new member of the small heat shock protein superfamily, interacts with mimic of phosphorylated HSP27 ((3D)HSP27)*. J Biol Chem 276: 26753.
(99) Mounier N., Arrigo A.P. (2002) *Actin cytoskeleton and small heat shock proteins: how do they interact?* Cell Stress Chaperones 7: 167.
(100) Brown D.D., Christine K.S., Showell C., Conlon F.L. (2007) *Small heat shock protein Hsp27 is required for proper heart tube formation*. Genesis 45: 667.
(101) Perng M.D., Cairns L., van den I.J., Prescott A., Hutcheson A.M., Quinlan R.A. (1999) *Intermediate filament interactions can be altered by HSP27 and alphaB-crystallin*. J Cell Sci 112 (Pt 13): 2099.
(102) Bennardini F., Wrzosek A., Chiesi M. (1992) *Alpha B-crystallin in cardiac tissue. Association with actin and desmin filaments*. Circ Res 71: 288.
(103) Nicholl I.D., Quinlan R.A. (1994) *Chaperone activity of alpha-crystallins modulates intermediate filament assembly*. EMBO J 13: 945.
(104) Bova M.P., Yaron O., Huang Q., Ding L., Haley D.A., Stewart P.L., et al. (1999) *Mutation R120G in alphaB-crystallin, which is linked to a desmin-related myopathy, results in an irregular structure and defective chaperone-like function*. Proc Natl Acad Sci U S A 96: 6137.
(105) Vicart P., Caron A., Guicheney P., Li Z., Prevost M.C., Faure A., et al. (1998) *A missense mutation in the alphaB-crystallin chaperone gene causes a desmin-related myopathy*. Nat Genet 20: 92.
(106) Hagemann T.L., Boelens W.C., Wawrousek E.F., Messing A. (2009) *Suppression of GFAP toxicity by {alpha}B-crystallin in mouse models of Alexander disease*. Hum Mol Genet.
(107) Arai H., Atomi Y. (1997) *Chaperone activity of alpha B-crystallin suppresses tubulin aggregation through complex formation*. Cell Struct Funct 22: 539.
(108) Kato K., Ito H., Inaguma Y., Okamoto K., Saga S. (1996) *Synthesis and accumulation of alphaB crystallin in C6 glioma cells is induced by agents that promote the disassembly of microtubules*. J Biol Chem 271: 26989.
(109) Xi J.H., Bai F., McGaha R., Andley U.P. (2006) *Alpha-crystallin expression affects microtubule assembly and prevents their aggregation*. FASEB J 20: 846.
(110) Houck S.A., Clark J.I. (2010) *Dynamic subunit exchange and the regulation of microtubule assembly by the stress response protein human alphaB crystallin*. PLoS One 5: e11795.
(111) Mao Y.W., Liu J.P., Xiang H., Li D.W. (2004) *Human alphaA- and alphaB-crystallins bind to Bax and Bcl-X(S) to sequester their translocation during staurosporine-induced apoptosis*. Cell Death Differ 11: 512.

(112) Kamradt M.C., Chen F., Cryns V.L. (2001) *The small heat shock protein alpha B-crystallin negatively regulates cytochrome c- and caspase-8-dependent activation of caspase-3 by inhibiting its autoproteolytic maturation*. J Biol Chem 276: 16059.
(113) Stegh A.H., Kesari S., Mahoney J.E., Jenq H.T., Forloney K.L., Protopopov A., et al. (2008) *Bcl2L12-mediated inhibition of effector caspase-3 and caspase-7 via distinct mechanisms in glioblastoma*. Proc Natl Acad Sci U S A 105: 10703.
(114) Li R., Reiser G. (2011) *Phosphorylation of Ser45 and Ser59 of alphaB-crystallin and p38/extracellular regulated kinase activity determine alphaB-crystallin-mediated protection of rat brain astrocytes from C2-ceramide- and staurosporine-induced cell death*. J Neurochem 118: 354.
(115) den Engelsman J., Keijsers V., de Jong W.W., Boelens W.C. (2003) *The small heat-shock protein alpha B-crystallin promotes FBX4-dependent ubiquitination*. J Biol Chem 278: 4699.
(116) Lin D.I., Barbash O., Kumar K.G., Weber J.D., Harper J.W., Klein-Szanto A.J., et al. (2006) *Phosphorylation-dependent ubiquitination of cyclin D1 by the SCF(FBX4-alphaB crystallin) complex*. Mol Cell 24: 355.
(117) Boelens W.C., Croes Y., de Jong W.W. (2001) *Interaction between alphaB-crystallin and the human 20S proteasomal subunit C8/alpha7*. Biochim Biophys Acta 1544: 311.
(118) Dehle F.C., Ecroyd H., Musgrave I.F., Carver J.A. (2010) *alphaB-Crystallin inhibits the cell toxicity associated with amyloid fibril formation by kappa-casein and the amyloid-beta peptide*. Cell Stress Chaperones 15: 1013.
(119) Shammas S.L., Waudby C.A., Wang S., Buell A.K., Knowles T.P., Ecroyd H., et al. (2011) *Binding of the molecular chaperone alphaB-crystallin to Abeta amyloid fibrils inhibits fibril elongation*. Biophys J 101: 1681.
(120) Vos M.J., Zijlstra M.P., Kanon B., van Waarde-Verhagen M.A., Brunt E.R., Oosterveld-Hut H.M., et al. (2010) *HSPB7 is the most potent polyQ aggregation suppressor within the HSPB family of molecular chaperones*. Hum Mol Genet 19: 4677.
(121) Bruinsma I.B., Bruggink K.A., Kinast K., Versleijen A.A., Segers-Nolten I.M., Subramaniam V., et al. (2011) *Inhibition of alpha-synuclein aggregation by small heat shock proteins*. Proteins 79: 2956.
(122) Sun Y., MacRae T.H. (2005) *Small heat shock proteins: molecular structure and chaperone function*. Cell Mol Life Sci 62: 2460.
(123) Perng M.D., Wen S.F., van den I.J., Prescott A.R., Quinlan R.A. (2004) *Desmin aggregate formation by R120G alphaB-crystallin is caused by altered filament interactions and is dependent upon network status in cells*. Mol Biol Cell 15: 2335.
(124) Sanbe A., Osinska H., Villa C., Gulick J., Klevitsky R., Glabe C.G., et al. (2005) *Reversal of amyloid-induced heart disease in desmin-related cardiomyopathy*. Proc Natl Acad Sci U S A 102: 13592.
(125) Sacconi S., Feasson L., Antoine J.C., Pecheux C., Bernard R., Cobo A.M., et al. (2011) *A novel CRYAB mutation resulting in multisystemic disease*. Neuromuscul Disord.
(126) Moyano J.V., Evans J.R., Chen F., Lu M., Werner M.E., Yehiely F., et al. (2006) *AlphaB-crystallin is a novel oncoprotein that predicts poor clinical outcome in breast cancer*. J Clin Invest 116: 261.
(127) Oesterreich S., Weng C.N., Qiu M., Hilsenbeck S.G., Osborne C.K., Fuqua S.A. (1993) *The small heat shock protein hsp27 is correlated with growth and drug resistance in human breast cancer cell lines*. Cancer Res 53: 4443.
(128) Rocchi P., So A., Kojima S., Signaevsky M., Beraldi E., Fazli L., et al. (2004) *Heat shock protein 27 increases after androgen ablation and plays a cytoprotective role in hormone-refractory prostate cancer*. Cancer Res 64: 6595.
(129) Oesterreich S., Schunck H., Benndorf R., Bielka H. (1991) *Cisplatin induces the small*

heat shock protein hsp25 and thermotolerance in Ehrlich ascites tumor cells. Biochem Biophys Res Commun 180: 243.
(130) Geiger T.R., Peeper D.S. (2009) *Metastasis mechanisms*. Biochim Biophys Acta 1796: 293.
(131) Folkman J., Shing Y. (1992) *Angiogenesis*. J Biol Chem 267: 10931.
(132) Hudson T.J., Anderson W., Artez A., Barker A.D., Bell C., Bernabe R.R., et al. (2010) *International network of cancer genome projects*. Nature 464: 993.
(133) Stratton M.R., Campbell P.J., Futreal P.A. (2009) *The cancer genome*. Nature 458: 719.
(134) Cairns R.A., Harris I.S., Mak T.W. (2011) *Regulation of cancer cell metabolism*. Nat Rev Cancer 11: 85.
(135) Parsons D.W., Jones S., Zhang X., Lin J.C., Leary R.J., Angenendt P., et al. (2008) *An integrated genomic analysis of human glioblastoma multiforme*. Science 321: 1807.
(136) Hanahan D., Weinberg R.A. (2000) *The hallmarks of cancer*. Cell 100: 57.
(137) Hanahan D., Folkman J. (1996) *Patterns and emerging mechanisms of the angiogenic switch during tumorigenesis*. Cell 86: 353.
(138) Hanahan D., Weinberg R.A. (2011) *Hallmarks of cancer: the next generation*. Cell 144: 646.
(139) Spandidos D.A. (2007) *Oncogenes and tumor suppressor genes as paradigms in oncogenesis*. J BUON 12 Suppl 1: S9.
(140) Munger K. (2002) *Disruption of oncogene/tumor suppressor networks during human carcinogenesis*. Cancer Invest 20: 71.
(141) Chinnam M., Goodrich D.W. (2011) *RB1, development, and cancer*. Curr Top Dev Biol 94: 129.
(142) Ozaki T., Nakagawara A. (2011) *p53: the attractive tumor suppressor in the cancer research field*. J Biomed Biotechnol 2011: 603925.
(143) Gutierrez C., Schiff R. (2011) *HER2: biology, detection, and clinical implications*. Arch Pathol Lab Med 135: 55.
(144) Musgrove E.A., Caldon C.E., Barraclough J., Stone A., Sutherland R.L. (2011) *Cyclin D as a therapeutic target in cancer*. Nat Rev Cancer 11: 558.
(145) Clapp R.W., Jacobs M.M., Loechler E.L. (2008) *Environmental and occupational causes of cancer: new evidence 2005-2007*. Rev Environ Health 23: 1.
(146) Clapp R.W., Howe G.K., Jacobs M.M. (2007) *Environmental and occupational causes of cancer: a call to act on what we know*. Biomed Pharmacother 61: 631.
(147) Calabrese P., Tavare S., Shibata D. (2004) *Pretumor progression: clonal evolution of human stem cell populations*. Am J Pathol 164: 1337.
(148) Oliveira P.A., Colaco A., Chaves R., Guedes-Pinto H., De-La-Cruz P.L., Lopes C. (2007) *Chemical carcinogenesis*. An Acad Bras Cienc 79: 593.
(149) Kamangar F., Dores G.M., Anderson W.F. (2006) *Patterns of cancer incidence, mortality, and prevalence across five continents: defining priorities to reduce cancer disparities in different geographic regions of the world*. J Clin Oncol 24: 2137.
(150) Parkin D.M., Bray F., Ferlay J., Pisani P. (2005) *Global cancer statistics, 2002*. CA Cancer J Clin 55: 74.
(151) Rothenberg S.M., Ellisen L.W. (2012) *The molecular pathogenesis of head and neck squamous cell carcinoma*. J Clin Invest 122: 1951.
(152) Brandsma J.L., Abramson A.L. (1989) *Association of papillomavirus with cancers of the head and neck*. Arch Otolaryngol Head Neck Surg 115: 621.
(153) Scully C. (1993) *Oncogenes, tumor suppressors and viruses in oral squamous carcinoma*. J Oral Pathol Med 22: 337.
(154) Lund V.J., Howard D.J. (1990) *Head and neck cancer in the young: a prognostic conundrum?* J Laryngol Otol 104: 544.

(155) Derynck R. (1992) *The physiology of transforming growth factor-alpha*. Adv Cancer Res 58: 27.
(156) Todd R., Chou M.Y., Matossian K., Gallagher G.T., Donoff R.B., Wong D.T. (1991) *Cellular sources of transforming growth factor-alpha in human oral cancer*. J Dent Res 70: 917.
(157) Wong D.T., Todd R., Tsuji T., Donoff R.B. (1996) *Molecular biology of human oral cancer*. Crit Rev Oral Biol Med 7: 319.
(158) Downward J., Yarden Y., Mayes E., Scrace G., Totty N., Stockwell P., et al. (1984) *Close similarity of epidermal growth factor receptor and v-erb-B oncogene protein sequences*. Nature 307: 521.
(159) Ullrich A., Coussens L., Hayflick J.S., Dull T.J., Gray A., Tam A.W., et al. (1984) *Human epidermal growth factor receptor cDNA sequence and aberrant expression of the amplified gene in A431 epidermoid carcinoma cells*. Nature 309: 418.
(160) Wells A., Bishop J.M., Helmeste D. (1988) *Amplified gene for the epidermal growth factor receptor in a human glioblastoma cell line encodes an enzymatically inactive protein*. Mol Cell Biol 8: 4561.
(161) Di M.E., Pierce J.H., Fleming T.P., Kraus M.H., Molloy C.J., Aaronson S.A., et al. (1989) *Autocrine interaction between TGF alpha and the EGF-receptor: quantitative requirements for induction of the malignant phenotype*. Oncogene 4: 831.
(162) Di Fiore P.P., Pierce J.H., Fleming T.P., Hazan R., Ullrich A., King C.R., et al. (1987) *Overexpression of the human EGF receptor confers an EGF-dependent transformed phenotype to NIH 3T3 cells*. Cell 51: 1063.
(163) Liao Y.M., Kim C., Yen Y. (2011) *Mammalian target of rapamycin and head and neck squamous cell carcinoma*. Head Neck Oncol 3: 22.
(164) Reis-Filho J.S., Pusztai L. (2011) *Gene expression profiling in breast cancer: classification, prognostication, and prediction*. Lancet 378: 1812.
(165) Turaga K., Acs G., Laronga C. (2010) *Gene expression profiling in breast cancer*. Cancer Control 17: 177.
(166) Rastelli F., Biancanelli S., Falzetta A., Martignetti A., Casi C., Bascioni R., et al. (2010) *Triple-negative breast cancer: current state of the art*. Tumori 96: 875.
(167) Osborne C., Wilson P., Tripathy D. (2004) *Oncogenes and tumor suppressor genes in breast cancer: potential diagnostic and therapeutic applications*. Oncologist 9: 361.
(168) Leong A.S., Zhuang Z. (2011) *The changing role of pathology in breast cancer diagnosis and treatment*. Pathobiology 78: 99.
(169) Eckhardt B.L., Francis P.A., Parker B.S., Anderson R.L. (2012) *Strategies for the discovery and development of therapies for metastatic breast cancer*. Nat Rev Drug Discov 11: 479.
(170) Kong D., Li Y., Wang Z., Sarkar F.H. (2011) *Cancer Stem Cells and Epithelial-to-Mesenchymal Transition (EMT)-Phenotypic Cells: Are They Cousins or Twins?* Cancers (Basel) 3: 716.
(171) Thiery J.P. (2002) *Epithelial-mesenchymal transitions in tumour progression*. Nat Rev Cancer 2: 442.
(172) Geiger T.R., Peeper D.S. (2005) *The neurotrophic receptor TrkB in anoikis resistance and metastasis: a perspective*. Cancer Res 65: 7033.
(173) Zhu Z., Sanchez-Sweatman O., Huang X., Wiltrout R., Khokha R., Zhao Q., et al. (2001) *Anoikis and metastatic potential of cloudman S91 melanoma cells*. Cancer Res 61: 1707.
(174) Dvorak H.F. (1986) *Tumors: wounds that do not heal. Similarities between tumor stroma generation and wound healing*. N Engl J Med 315: 1650.
(175) Kim M., Gans J.D., Nogueira C., Wang A., Paik J.H., Feng B., et al. (2006) *Comparative oncogenomics identifies NEDD9 as a melanoma metastasis gene*. Cell 125: 1269.

(176) Sanz-Moreno V., Gadea G., Ahn J., Paterson H., Marra P., Pinner S., et al. (2008) *Rac activation and inactivation control plasticity of tumor cell movement*. Cell 135: 510.
(177) Guo W., Giancotti F.G. (2004) *Integrin signalling during tumour progression*. Nat Rev Mol Cell Biol 5: 816.
(178) Bergers G., Benjamin L.E. (2003) *Tumorigenesis and the angiogenic switch*. Nat Rev Cancer 3: 401.
(179) Kalluri R. (2003) *Basement membranes: structure, assembly and role in tumour angiogenesis*. Nat Rev Cancer 3: 422.
(180) Roskoski R., Jr. (2007) *Vascular endothelial growth factor (VEGF) signaling in tumor progression*. Crit Rev Oncol Hematol 62: 179.
(181) Harris A.L. (2002) *Hypoxia--a key regulatory factor in tumour growth*. Nat Rev Cancer 2: 38.
(182) Lu X., Kang Y. (2010) *Hypoxia and hypoxia-inducible factors: master regulators of metastasis*. Clin Cancer Res 16: 5928.
(183) Semenza G.L. (2003) *Targeting HIF-1 for cancer therapy*. Nat Rev Cancer 3: 721.
(184) Bussink J., van der Kogel A.J., Kaanders J.H. (2008) *Patterns and levels of hypoxia in head and neck squamous cell carcinomas and their relationship to patient outcome: in regard to Evans et al. (Int J Radiat Oncol Biol Phys 2007;69:1024-1031)*. Int J Radiat Oncol Biol Phys 70: 1616.
(185) Rademakers S.E., Span P.N., Kaanders J.H., Sweep F.C., van der Kogel A.J., Bussink J. (2008) *Molecular aspects of tumour hypoxia*. Mol Oncol 2: 41.
(186) Harrison L.B., Chadha M., Hill R.J., Hu K., Shasha D. (2002) *Impact of tumor hypoxia and anemia on radiation therapy outcomes*. Oncologist 7: 492.
(187) Chaudary N., Hill R.P. (2009) *Increased expression of metastasis-related genes in hypoxic cells sorted from cervical and lymph nodal xenograft tumors*. Lab Invest 89: 587.
(188) Raghunand N., Gatenby R.A., Gillies R.J. (2003) *Microenvironmental and cellular consequences of altered blood flow in tumours*. Br J Radiol 76 Spec No 1: S11-S22.
(189) Ahn G.O., Brown M. (2007) *Targeting tumors with hypoxia-activated cytotoxins*. Front Biosci 12: 3483.
(190) Semenza G.L. (2009) *Regulation of cancer cell metabolism by hypoxia-inducible factor 1*. Semin Cancer Biol 19: 12.
(191) Bristow R.G., Hill R.P. (2008) *Hypoxia and metabolism. Hypoxia, DNA repair and genetic instability*. Nat Rev Cancer 8: 180.
(192) Lunt S.J., Chaudary N., Hill R.P. (2009) *The tumor microenvironment and metastatic disease*. Clin Exp Metastasis 26: 19.
(193) Tatum J.L., Kelloff G.J., Gillies R.J., Arbeit J.M., Brown J.M., Chao K.S., et al. (2006) *Hypoxia: importance in tumor biology, noninvasive measurement by imaging, and value of its measurement in the management of cancer therapy*. Int J Radiat Biol 82: 699.
(194) Liu Y., Song X., Wang X., Wei L., Liu X., Yuan S., et al. (2010) *Effect of chronic intermittent hypoxia on biological behavior and hypoxia-associated gene expression in lung cancer cells*. J Cell Biochem 111: 554.
(195) Jain R.K. (2009) *A new target for tumor therapy*. N Engl J Med 360: 2669.
(196) Fukumura D., Duda D.G., Munn L.L., Jain R.K. (2010) *Tumor microvasculature and microenvironment: novel insights through intravital imaging in pre-clinical models*. Microcirculation 17: 206.
(197) Mazzone M., Dettori D., Leite de O.R., Loges S., Schmidt T., Jonckx B., et al. (2009) *Heterozygous deficiency of PHD2 restores tumor oxygenation and inhibits metastasis via endothelial normalization*. Cell 136: 839.
(198) Toffoli S., Michiels C. (2008) *Intermittent hypoxia is a key regulator of cancer cell and endothelial cell interplay in tumours*. FEBS J 275: 2991.

(199) Zhu X., Zuo L., Cardounel A.J., Zweier J.L., He G. (2007) *Characterization of in vivo tissue redox status, oxygenation, and formation of reactive oxygen species in postischemic myocardium*. Antioxid Redox Signal 9: 447.
(200) Prabhakar N.R., Kumar G.K., Nanduri J., Semenza G.L. (2007) *ROS signaling in systemic and cellular responses to chronic intermittent hypoxia*. Antioxid Redox Signal 9: 1397.
(201) Sandin A., Dagnell M., Gonon A., Pernow J., Stangl V., Aspenstrom P., et al. (2011) *Hypoxia followed by re-oxygenation induces oxidation of tyrosine phosphatases*. Cell Signal 23: 820.
(202) Morgan M.J., Kim Y.S., Liu Z.G. (2008) *TNFalpha and reactive oxygen species in necrotic cell death*. Cell Res 18: 343.
(203) Hussain S.P., Hofseth L.J., Harris C.C. (2003) *Radical causes of cancer*. Nat Rev Cancer 3: 276.
(204) Wu W.S. (2006) *The signaling mechanism of ROS in tumor progression*. Cancer Metastasis Rev 25: 695.
(205) Masuda S. (2012) *Breast cancer pathology: the impact of molecular taxonomy on morphological taxonomy*. Pathol Int 62: 295.
(206) Elston C.W. (1984) *The assessment of histological differentiation in breast cancer*. Aust N Z J Surg 54: 11.
(207) Boscolo-Rizzo P., Maronato F., Marchiori C., Gava A., Da Mosto M.C. (2008) *Long-term quality of life after total laryngectomy and postoperative radiotherapy versus concurrent chemoradiotherapy for laryngeal preservation*. Laryngoscope 118: 300.
(208) Vergeer M.R., Doornaert P.A., Rietveld D.H., Leemans C.R., Slotman B.J., Langendijk J.A. (2009) *Intensity-modulated radiotherapy reduces radiation-induced morbidity and improves health-related quality of life: results of a nonrandomized prospective study using a standardized follow-up program*. Int J Radiat Oncol Biol Phys 74: 1.
(209) Ross G.M. (1999) *Induction of cell death by radiotherapy*. Endocr Relat Cancer 6: 41.
(210) Zhang N., Erjala K., Kulmala J., Qiu X., Sundvall M., Elenius K., et al. (2009) *Concurrent cetuximab, cisplatin, and radiation for squamous cell carcinoma of the head and neck in vitro*. Radiother Oncol 92: 388.
(211) Borek C. (2004) *Antioxidants and radiation therapy*. J Nutr 134: 3207S.
(212) Fang Y.Z., Yang S., Wu G. (2002) *Free radicals, antioxidants, and nutrition*. Nutrition 18: 872.
(213) Kaanders J.H., Bussink J., van der Kogel A.J. (2004) *Clinical studies of hypoxia modification in radiotherapy*. Semin Radiat Oncol 14: 233.
(214) Bache M., Kappler M., Said H.M., Staab A., Vordermark D. (2008) *Detection and specific targeting of hypoxic regions within solid tumors: current preclinical and clinical strategies*. Curr Med Chem 15: 322.
(215) Vincenzi B., Zoccoli A., Pantano F., Venditti O., Galluzzo S. (2010) *Cetuximab: from bench to bedside*. Curr Cancer Drug Targets 10: 80.
(216) Mehra R., Cohen R.B., Burtness B.A. (2008) *The role of cetuximab for the treatment of squamous cell carcinoma of the head and neck*. Clin Adv Hematol Oncol 6: 742.
(217) Goerner M., Seiwert T.Y., Sudhoff H. (2010) *Molecular targeted therapies in head and neck cancer--an update of recent developments-*. Head Neck Oncol 2: 8.
(218) Seiwert T.Y., Cohen E.E. (2008) *Targeting angiogenesis in head and neck cancer*. Semin Oncol 35: 274.
(219) Steelman L.S., Chappell W.H., Abrams S.L., Kempf R.C., Long J., Laidler P., et al. (2011) *Roles of the Raf/MEK/ERK and PI3K/PTEN/Akt/mTOR pathways in controlling growth and sensitivity to therapy-implications for cancer and aging*. Aging (Albany NY) 3: 192.

(220) Chin D., Boyle G.M., Williams R.M., Ferguson K., Pandeya N., Pedley J., et al. (2005) *Alpha B-crystallin, a new independent marker for poor prognosis in head and neck cancer*. Laryngoscope 115: 1239.
(221) Boslooper K., King-Yin L.A., Gao J., Weinstein S., Johnson N. (2008) *The clinicopathological roles of alpha-B-crystallin and p53 expression in patients with head and neck squamous cell carcinoma*. Pathology 40: 500.
(222) Sitterding S.M., Wiseman W.R., Schiller C.L., Luan C., Chen F., Moyano J.V., et al. (2008) *AlphaB-crystallin: a novel marker of invasive basal-like and metaplastic breast carcinomas*. Ann Diagn Pathol 12: 33.
(223) Kim H.S., Lee Y., Lim Y.A., Kang H.J., Kim L.S. (2011) *alphaB-Crystallin is a Novel Oncoprotein Associated with Poor Prognosis in Breast Cancer*. J Breast Cancer 14: 14.
(224) Gruvberger-Saal S.K., Parsons R. (2006) *Is the small heat shock protein alphaB-crystallin an oncogene?* J Clin Invest 116: 30.
(225) Ghosh J.G., Shenoy A.K., Jr., Clark J.I. (2007) *Interactions between important regulatory proteins and human alphaB crystallin*. Biochemistry 46: 6308.
(226) Kase S., He S., Sonoda S., Kitamura M., Spee C., Wawrousek E., et al. (2010) *alphaB-crystallin regulation of angiogenesis by modulation of VEGF*. Blood 115: 3398.
(227) Kerr B.A., Byzova T.V. (2010) *alphaB-crystallin: a novel VEGF chaperone*. Blood 115: 3181.
(228) Martiny-Baron G., Marme D. (1995) *VEGF-mediated tumour angiogenesis: a new target for cancer therapy*. Curr Opin Biotechnol 6: 675.
(229) Hu Z., Fan C., Livasy C., He X., Oh D.S., Ewend M.G., et al. (2009) *A compact VEGF signature associated with distant metastases and poor outcomes*. BMC Med 7: 9.
(230) Bremnes R.M., Camps C., Sirera R. (2006) *Angiogenesis in non-small cell lung cancer: the prognostic impact of neoangiogenesis and the cytokines VEGF and bFGF in tumours and blood*. Lung Cancer 51: 143.
(231) Leemans C.R., Braakhuis B.J., Brakenhoff R.H. (2011) *The molecular biology of head and neck cancer*. Nat Rev Cancer 11: 9.
(232) Hoogsteen I.J., Marres H.A., Wijffels K.I., Rijken P.F., Peters J.P., van den Hoogen F.J., et al. (2005) *Colocalization of carbonic anhydrase 9 expression and cell proliferation in human head and neck squamous cell carcinoma*. Clin Cancer Res 11: 97.
(233) Troost E.G., Bussink J., Slootweg P.J., Peeters W.J., Merkx M.A., van der Kogel A.J., et al. (2010) *Histopathologic validation of 3'-deoxy-3'-18F-fluorothymidine PET in squamous cell carcinoma of the oral cavity*. J Nucl Med 51: 713.
(234) Rijken P.F., Bernsen H.J., Peters J.P., Hodgkiss R.J., Raleigh J.A., van der Kogel A.J. (2000) *Spatial relationship between hypoxia and the (perfused) vascular network in a human glioma xenograft: a quantitative multi-parameter analysis*. Int J Radiat Oncol Biol Phys 48: 571.
(235) Yaromina A., Zips D., Thames H.D., Eicheler W., Krause M., Rosner A., et al. (2006) *Pimonidazole labelling and response to fractionated irradiation of five human squamous cell carcinoma (hSCC) lines in nude mice: the need for a multivariate approach in biomarker studies*. Radiother Oncol 81: 122.
(236) Span P.N., Grebenchtchikov N., Geurts-Moespot J., Westphal J.R., Lucassen A.M., Sweep C.G. (2000) *EORTC Receptor and Biomarker Study Group Report: a sandwich enzyme-linked immunosorbent assay for vascular endothelial growth factor in blood and tumor tissue extracts*. Int J Biol Markers 15: 184.
(237) Zusterzeel P.L., Span P.N., Dijksterhuis M.G., Thomas C.M., Sweep F.C., Massuger L.F. (2009) *Serum vascular endothelial growth factor: a prognostic factor in cervical cancer*. J Cancer Res Clin Oncol 135: 283.
(238) Geback T., Schulz M.M., Koumoutsakos P., Detmar M. (2009) *TScratch: a novel and*

simple software tool for automated analysis of monolayer wound healing assays. Biotechniques 46: 265.
(239) Goplen D., Bougnaud S., Rajcevic U., Boe S.O., Skaftnesmo K.O., Voges J., et al. (2010) *alphaB-crystallin is elevated in highly infiltrative apoptosis-resistant glioblastoma cells*. Am J Pathol 177: 1618.
(240) Tang Q., Liu Y.F., Zhu X.J., Li Y.H., Zhu J., Zhang J.P., et al. (2009) *Expression and prognostic significance of the alpha B-crystallin gene in human hepatocellular carcinoma*. Hum Pathol 40: 300.
(241) Cicek M., Samant R.S., Kinter M., Welch D.R., Casey G. (2004) *Identification of metastasis-associated proteins through protein analysis of metastatic MDA-MB-435 and metastasis-suppressed BRMS1 transfected-MDA-MB-435 cells*. Clin Exp Metastasis 21: 149.
(242) Ivanov O., Chen F., Wiley E.L., Keswani A., Diaz L.K., Memmel H.C., et al. (2008) *alphaB-crystallin is a novel predictor of resistance to neoadjuvant chemotherapy in breast cancer*. Breast Cancer Res Treat 111: 411.
(243) Hicklin D.J., Ellis L.M. (2005) *Role of the vascular endothelial growth factor pathway in tumor growth and angiogenesis*. J Clin Oncol 23: 1011.
(244) Christopoulos A., Ahn S.M., Klein J.D., Kim S. (2010) *Biology of vascular endothelial growth factor and its receptors in head and neck cancer: Beyond angiogenesis*. Head Neck.
(245) Dimberg A., Rylova S., Dieterich L.C., Olsson A.K., Schiller P., Wikner C., et al. (2008) *alphaB-crystallin promotes tumor angiogenesis by increasing vascular survival during tube morphogenesis*. Blood 111: 2015.
(246) Ruan Q., Han S., Jiang W.W., Boulton M.E., Chen Z.J., Law B.K., et al. (2011) *{alpha}B-crystallin, a effecter of unfolded protein response, confers anti-VEGF resistance to breast cancer via maintenance of intracrine VEGF in endothelial cells*. Mol Cancer Res.
(247) Naresh K.N., Nerurkar A.Y., Borges A.M. (2001) *Angiogenesis is redundant for tumour growth in lymph node metastases*. Histopathology 38: 466.
(248) Kyzas P.A., Stefanou D., Batistatou A., Agnantis N.J. (2005) *Prognostic significance of VEGF immunohistochemical expression and tumor angiogenesis in head and neck squamous cell carcinoma*. J Cancer Res Clin Oncol 131: 624.
(249) Endo K., Shirai A., Furukawa M., Yoshizaki T. (2006) *Prognostic value of cell motility activation factors in patients with tongue squamous cell carcinoma*. Hum Pathol 37: 1111.
(250) Ho P.Y., Chueh S.C., Chiou S.H., Wang S.M., Lin W.C., Lee I.L., et al. (2012) *alphaB-Crystallin in clear cell renal cell carcinoma: Tumor progression and prognostic significance*. Urol Oncol.
(251) Benke E.M., Ji Y., Patel V., Wang H., Miyazaki H., Yeudall W.A. (2010) *VEGF-C contributes to head and neck squamous cell carcinoma growth and motility*. Oral Oncol 46: e19-e24.
(252) Lucas J.T., Jr., Salimath B.P., Slomiany M.G., Rosenzweig S.A. (2010) *Regulation of invasive behavior by vascular endothelial growth factor is HEF1-dependent*. Oncogene 29: 4449.
(253) Singh B.N., Rao K.S., Ramakrishna T., Rangaraj N., Rao C. (2007) *Association of alphaB-crystallin, a small heat shock protein, with actin: role in modulating actin filament dynamics in vivo*. J Mol Biol 366: 756.
(254) Brizel D.M., Sibley G.S., Prosnitz L.R., Scher R.L., Dewhirst M.W. (1997) *Tumor hypoxia adversely affects the prognosis of carcinoma of the head and neck*. Int J Radiat Oncol Biol Phys 38: 285.

(255) Ralph S.J., Rodriguez-Enriquez S., Neuzil J., Saavedra E., Moreno-Sanchez R. (2010) *The causes of cancer revisited: "mitochondrial malignancy" and ROS-induced oncogenic transformation - why mitochondria are targets for cancer therapy*. Mol Aspects Med 31: 145.
(256) Cooke M.S., Evans M.D., Dizdaroglu M., Lunec J. (2003) *Oxidative DNA damage: mechanisms, mutation, and disease*. FASEB J 17: 1195.
(257) Parcellier A., Schmitt E., Brunet M., Hammann A., Solary E., Garrido C. (2005) *Small heat shock proteins HSP27 and alphaB-crystallin: cytoprotective and oncogenic functions*. Antioxid Redox Signal 7: 404.
(258) Kamradt M.C., Chen F., Sam S., Cryns V.L. (2002) *The small heat shock protein alpha B-crystallin negatively regulates apoptosis during myogenic differentiation by inhibiting caspase-3 activation*. J Biol Chem 277: 38731.
(259) Tallot P., Grongnet J.F., David J.C. (2003) *Dual perinatal and developmental expression of the small heat shock proteins [FC12]aB-crystallin and Hsp27 in different tissues of the developing piglet*. Biol Neonate 83: 281.
(260) Mao Y., Zhang D.W., Lin H., Xiong L., Liu Y., Li Q.D., et al. (2012) *Alpha B-crystallin is a new prognostic marker for laryngeal squamous cell carcinoma*. J Exp Clin Cancer Res 31: 101.
(261) van de Schootbrugge C., Bussink J., Span P.N., Sweep F.C., Grenman R., Stegeman H., et al. (2013) *alphaB-crystallin stimulates VEGF secretion and tumor cell migration and correlates with enhanced distant metastasis in head and neck squamous cell carcinoma*. BMC Cancer 13: 128.
(262) Chelouche-Lev D., Kluger H.M., Berger A.J., Rimm D.L., Price J.E. (2004) *alphaB-crystallin as a marker of lymph node involvement in breast carcinoma*. Cancer 100: 2543.
(263) Nefti O., Grongnet J.F., David J.C. (2005) *Overexpression of alphaB crystallin in the gastrointestinal tract of the newborn piglet after hypoxia*. Shock 24: 455.
(264) Louapre P., Grongnet J.F., Tanguay R.M., David J.C. (2005) *Effects of hypoxia on stress proteins in the piglet heart at birth*. Cell Stress Chaperones 10: 17.
(265) Wessel G.M., McClay D.R. (1986) *Two embryonic, tissue-specific molecules identified by a double-label immunofluorescence technique for monoclonal antibodies*. J Histochem Cytochem 34: 703.
(266) Rademakers S.E., Lok J., van der Kogel A.J., Bussink J., Kaanders J.H. (2011) *Metabolic markers in relation to hypoxia; staining patterns and colocalization of pimonidazole, HIF-1alpha, CAIX, LDH-5, GLUT-1, MCT1 and MCT4*. BMC Cancer 11: 167.
(267) Li C., Jackson R.M. (2002) *Reactive species mechanisms of cellular hypoxia-reoxygenation injury*. Am J Physiol Cell Physiol 282: C227-C241.
(268) Onozuka H., Tsuchihara K., Esumi H. (2011) *Hypoglycemic/hypoxic condition in vitro mimicking the tumor microenvironment markedly reduced the efficacy of anticancer drugs*. Cancer Sci 102: 975.
(269) Malhotra R., Brosius F.C., III. (1999) *Glucose uptake and glycolysis reduce hypoxia-induced apoptosis in cultured neonatal rat cardiac myocytes*. J Biol Chem 274: 12567.
(270) Sandulache V.C., Ow T.J., Pickering C.R., Frederick M.J., Zhou G., Fokt I., et al. (2011) *Glucose, not glutamine, is the dominant energy source required for proliferation and survival of head and neck squamous carcinoma cells*. Cancer 117: 2926.
(271) Meijer T.W., Kaanders J.H., Span P.N., Bussink J. (2012) *Targeting hypoxia, HIF-1, and tumor glucose metabolism to improve radiotherapy efficacy*. Clin Cancer Res 18: 5585.
(272) Perez-Perri J.I., Acevedo J.M., Wappner P. (2011) *Epigenetics: new questions on the response to hypoxia*. Int J Mol Sci 12: 4705.
(273) Johnson A.B., Denko N., Barton M.C. (2008) *Hypoxia induces a novel signature of*

chromatin modifications and global repression of transcription. Mutat Res 640: 174.
(274) Imura T., Shimohama S., Sato M., Nishikawa H., Madono K., Akaike A., et al. (1999) *Differential expression of small heat shock proteins in reactive astrocytes after focal ischemia: possible role of beta-adrenergic receptor*. J Neurosci 19: 9768.
(275) Li T., Mo X., Jiang Z., He W., Lu W., Zhang H., et al. (2012) *Study of alphaB-crystallin expression in Gerbil BCAO model of transient global cerebral ischemia*. Oxid Med Cell Longev 2012: 945071.
(276) Bertuzzi A., Fasano A., Gandolfi A., Sinisgalli C. (2010) *Necrotic core in EMT6/Ro tumour spheroids: Is it caused by an ATP deficit?* J Theor Biol 262: 142.
(277) Takahashi E. (2008) *Anoxic cell core can promote necrotic cell death in cardiomyocytes at physiological extracellular PO2*. Am J Physiol Heart Circ Physiol 294: H2507-H2515.
(278) Naranjo-Suarez S., Carlson B.A., Tsuji P.A., Yoo M.H., Gladyshev V.N., Hatfield D.L. (2012) *HIF-independent regulation of thioredoxin reductase 1 contributes to the high levels of reactive oxygen species induced by hypoxia*. PLoS One 7: e30470.
(279) Bennewith K.L., Raleigh J.A., Durand R.E. (2002) *Orally administered pimonidazole to label hypoxic tumor cells*. Cancer Res 62: 6827.
(280) Bennewith K.L., Durand R.E. (2004) *Quantifying transient hypoxia in human tumor xenografts by flow cytometry*. Cancer Res 64: 6183.
(281) Yaung J., Jin M., Barron E., Spee C., Wawrousek E.F., Kannan R., et al. (2007) *alpha-Crystallin distribution in retinal pigment epithelium and effect of gene knockouts on sensitivity to oxidative stress*. Mol Vis 13: 566.
(282) Vaupel P. (2004) *Tumor microenvironmental physiology and its implications for radiation oncology*. Semin Radiat Oncol 14: 198.
(283) Jung J.E., Lee H.G., Cho I.H., Chung D.H., Yoon S.H., Yang Y.M., et al. (2005) *STAT3 is a potential modulator of HIF-1-mediated VEGF expression in human renal carcinoma cells*. FASEB J 19: 1296.
(284) Rofstad E.K., Gaustad J.V., Egeland T.A., Mathiesen B., Galappathi K. (2010) *Tumors exposed to acute cyclic hypoxic stress show enhanced angiogenesis, perfusion and metastatic dissemination*. Int J Cancer 127: 1535.
(285) Chaudary N., Hill R.P. (2007) *Hypoxia and metastasis*. Clin Cancer Res 13: 1947.
(286) Volkmann J., Reuning U., Rudelius M., Hafner N., Schuster T., AB V.R., et al. (2012) *High expression of crystallin alphaB represents an independent molecular marker for unfavourable ovarian cancer patient outcome and impairs T*. Int J Cancer.
(287) Toft D.J., Cryns V.L. (2011) *Minireview: Basal-like breast cancer: from molecular profiles to targeted therapies*. Mol Endocrinol 25: 199.
(288) Chacon R.D., Costanzo M.V. (2010) *Triple-negative breast cancer*. Breast Cancer Res 12 Suppl 2: S3.
(289) Da S.L., Clarke C., Lakhani S.R. (2007) *Demystifying basal-like breast carcinomas*. J Clin Pathol 60: 1328.
(290) Kobayashi S. (2008) *Basal-like subtype of breast cancer: a review of its unique characteristics and their clinical significance*. Breast Cancer 15: 153.
(291) Podo F., Buydens L.M., Degani H., Hilhorst R., Klipp E., Gribbestad I.S., et al. (2010) *Triple-negative breast cancer: present challenges and new perspectives*. Mol Oncol 4: 209.
(292) Tsang J.Y., Lai M.W., Wong K.H., Chan S.K., Lam C.C., Tsang A.K., et al. (2012) *alphaB-crystallin is a useful marker for triple negative and basal breast cancers*. Histopathology 61: 378.
(293) Jechlinger M., Grunert S., Beug H. (2002) *Mechanisms in epithelial plasticity and metastasis: insights from 3D cultures and expression profiling*. J Mammary Gland Biol Neoplasia 7: 415.

(294) Oh H.Y., Lee E.J., Yoon S., Chung B.H., Cho K.S., Hong S.J. (2007) *Cholesterol level of lipid raft microdomains regulates apoptotic cell death in prostate cancer cells through EGFR-mediated Akt and ERK signal transduction*. Prostate 67: 1061.
(295) Kashyap A.S., Hollier B.G., Manton K.J., Satyamoorthy K., Leavesley D.I., Upton Z. (2011) *Insulin-like growth factor-I:vitronectin complex-induced changes in gene expression effect breast cell survival and migration*. Endocrinology 152: 1388.
(296) Nagelkerke A., van Kuijk S.J., Sweep F.C., Nagtegaal I.D., Hoogerbrugge N., Martens J.W., et al. (2011) *Constitutive expression of gamma-H2AX has prognostic relevance in triple negative breast cancer*. Radiother Oncol 101: 39.
(297) Wennemers M., Bussink J., Grebenchtchikov N., Sweep F.C., Span P.N. (2011) *TRIB3 protein denotes a good prognosis in breast cancer patients and is associated with hypoxia sensitivity*. Radiother Oncol 101: 198.
(298) Hudis C.A., Gianni L. (2011) *Triple-negative breast cancer: an unmet medical need*. Oncologist 16 Suppl 1: 1.
(299) Allen L.F., Sebolt-Leopold J., Meyer M.B. (2003) *CI-1040 (PD184352), a targeted signal transduction inhibitor of MEK (MAPKK)*. Semin Oncol 30: 105.
(300) Umemura S., Yoshida S., Ohta Y., Naito K., Osamura R.Y., Tokuda Y. (2007) *Increased phosphorylation of Akt in triple-negative breast cancers*. Cancer Sci 98: 1889.
(301) Chrestensen C.A., Shuman J.K., Eschenroeder A., Worthington M., Gram H., Sturgill T.W. (2007) *MNK1 and MNK2 regulation in HER2-overexpressing breast cancer lines*. J Biol Chem 282: 4243.
(302) Alvarez R.H., Valero V., Hortobagyi G.N. (2010) *Emerging targeted therapies for breast cancer*. J Clin Oncol 28: 3366.
(303) Morrison L.E., Hoover H.E., Thuerauf D.J., Glembotski C.C. (2003) *Mimicking phosphorylation of alphaB-crystallin on serine-59 is necessary and sufficient to provide maximal protection of cardiac myocytes from apoptosis*. Circ Res 92: 203.
(304) Inaguma Y., Hasegawa K., Goto S., Ito H., Kato K. (1995) *Induction of the synthesis of hsp27 and alpha B crystallin in tissues of heat-stressed rats and its suppression by ethanol or an alpha 1-adrenergic antagonist*. J Biochem 117: 1238.
(305) Acunzo J., Katsogiannou M., Rocchi P. (2012) *Small heat shock proteins HSP27 (HspB1), alphaB-crystallin (HspB5) and HSP22 (HspB8) as regulators of cell death*. Int J Biochem Cell Biol.
(306) Wettstein G., Bellaye P.S., Micheau O., Bonniaud P. (2012) *Small heat shock proteins and the cytoskeleton: an essential interplay for cell integrity?* Int J Biochem Cell Biol 44: 1680.
(307) Ecroyd H., Meehan S., Horwitz J., Aquilina J.A., Benesch J.L., Robinson C.V., et al. (2007) *Mimicking phosphorylation of alphaB-crystallin affects its chaperone activity*. Biochem J 401: 129.
(308) Koteiche H.A., Mchaourab H.S. (2003) *Mechanism of chaperone function in small heat-shock proteins. Phosphorylation-induced activation of two-mode binding in alphaB-crystallin*. J Biol Chem 278: 10361.
(309) van den IJssel P., Wheelock R., Prescott A., Russell P., Quinlan R.A. (2003) *Nuclear speckle localisation of the small heat shock protein alpha B-crystallin and its inhibition by the R120G cardiomyopathy-linked mutation*. Exp Cell Res 287: 249.
(310) van Rijk A.E., Stege G.J., Bennink E.J., May A., Bloemendal H. (2003) *Nuclear staining for the small heat shock protein alphaB-crystallin colocalizes with splicing factor SC35*. Eur J Cell Biol 82: 361.
(311) den Engelsman J., Gerrits D., de Jong W.W., Robbins J., Kato K., Boelens W.C. (2005) *Nuclear import of {alpha}B-crystallin is phosphorylation-dependent and hampered by hyperphosphorylation of the myopathy-related mutant R120G*. J Biol Chem 280: 37139.

(312) Vos M.J., Kanon B., Kampinga H.H. (2009) *HSPB7 is a SC35 speckle resident small heat shock protein*. Biochim Biophys Acta 1793: 1343.
(313) Spector D.L., Lamond A.I. (2011) *Nuclear speckles*. Cold Spring Harb Perspect Biol 3.
(314) Fischer U., Liu Q., Dreyfuss G. (1997) *The SMN-SIP1 complex has an essential role in spliceosomal snRNP biogenesis*. Cell 90: 1023.
(315) Narayanan U., Achsel T., Luhrmann R., Matera A.G. (2004) *Coupled in vitro import of U snRNPs and SMN, the spinal muscular atrophy protein*. Mol Cell 16: 223.
(316) Otter S., Grimmler M., Neuenkirchen N., Chari A., Sickmann A., Fischer U. (2007) *A comprehensive interaction map of the human survival of motor neuron (SMN) complex*. J Biol Chem 282: 5825.
(317) Nollen E.A., Salomons F.A., Brunsting J.F., Want J.J., Sibon O.C., Kampinga H.H. (2001) *Dynamic changes in the localization of thermally unfolded nuclear proteins associated with chaperone-dependent protection*. Proc Natl Acad Sci U S A 98: 12038.
(318) Heldens L., Dirks R.P., Hensen S.M., Onnekink C., van Genesen S.T., Rustenburg F., et al. (2010) *Co-chaperones are limiting in a depleted chaperone network*. Cell Mol Life Sci 67: 4035.
(319) Adam S.A., Marr R.S., Gerace L. (1990) *Nuclear protein import in permeabilized mammalian cells requires soluble cytoplasmic factors*. J Cell Biol 111: 807.
(320) Pellizzoni L., Yong J., Dreyfuss G. (2002) *Essential role for the SMN complex in the specificity of snRNP assembly*. Science 298: 1775.
(321) Mattijssen S., Hinson E.R., Onnekink C., Hermanns P., Zabel B., Cresswell P., et al. (2011) *Viperin mRNA is a novel target for the human RNase MRP/RNase P endoribonuclease*. Cell Mol Life Sci 68: 2469.
(322) Charroux B., Pellizzoni L., Perkinson R.A., Shevchenko A., Mann M., Dreyfuss G. (1999) *Gemin3: A novel DEAD box protein that interacts with SMN, the spinal muscular atrophy gene product, and is a component of gems*. J Cell Biol 147: 1181.
(323) Todd A.G., Morse R., Shaw D.J., McGinley S., Stebbings H., Young P.J. (2010) *SMN, Gemin2 and Gemin3 associate with beta-actin mRNA in the cytoplasm of neuronal cells in vitro*. J Mol Biol 401: 681.
(324) Dingwall C., Palacios I. (1998) *In vitro systems for the reconstitution of snRNP and protein nuclear import*. Methods Cell Biol 53: 517.
(325) Jeong W.J., Rho J.H., Yoon Y.G., Yoo S.H., Jeong N.Y., Ryu W.Y., et al. (2012) *Cytoplasmic and Nuclear Anti-Apoptotic Roles of alphaB-Crystallin in Retinal Pigment Epithelial Cells*. PLoS One 7: e45754.
(326) Lamian V., Small G.M., Feldherr C.M. (1996) *Evidence for the existence of a novel mechanism for the nuclear import of Hsc70*. Exp Cell Res 228: 84.
(327) Kodiha M., Chu A., Matusiewicz N., Stochaj U. (2004) *Multiple mechanisms promote the inhibition of classical nuclear import upon exposure to severe oxidative stress*. Cell Death Differ 11: 862.
(328) Kose S., Furuta M., Imamoto N. (2012) *Hikeshi, a nuclear import carrier for Hsp70s, protects cells from heat shock-induced nuclear damage*. Cell 149: 578.
(329) Aquilina J.A., Benesch J.L., Ding L.L., Yaron O., Horwitz J., Robinson C.V. (2004) *Phosphorylation of alphaB-crystallin alters chaperone function through loss of dimeric substructure*. J Biol Chem 279: 28675.
(330) Narayanan U., Ospina J.K., Frey M.R., Hebert M.D., Matera A.G. (2002) *SMN, the spinal muscular atrophy protein, forms a pre-import snRNP complex with snurportin1 and importin beta*. Hum Mol Genet 11: 1785.
(331) Hamada M., Haeger A., Jeganathan K.B., van Ree J.H., Malureanu L., Walde S., et al. (2011) *Ran-dependent docking of importin-beta to RanBP2/Nup358 filaments is essential for protein import and cell viability*. J Cell Biol 194: 597.

(332) Sun X., Fontaine J.M., Hoppe A.D., Carra S., DeGuzman C., Martin J.L., et al. (2010) *Abnormal interaction of motor neuropathy-associated mutant HspB8 (Hsp22) forms with the RNA helicase Ddx20 (gemin3)*. Cell Stress Chaperones 15: 567.
(333) Bryantsev A.L., Chechenova M.B., Shelden E.A. (2007) *Recruitment of phosphorylated small heat shock protein Hsp27 to nuclear speckles without stress*. Exp Cell Res 313: 195.
(334) Adhikari A.S., Sridhar R.K., Rangaraj N., Parnaik V.K., Mohan R.C. (2004) *Heat stress-induced localization of small heat shock proteins in mouse myoblasts: intranuclear lamin A/C speckles as target for alphaB-crystallin and Hsp25*. Exp Cell Res 299: 393.
(335) Shi T., Dong F., Liou L.S., Duan Z.H., Novick A.C., DiDonato J.A. (2004) *Differential protein profiling in renal-cell carcinoma*. Mol Carcinog 40: 47.
(336) Holcakova J., Hernychova L., Bouchal P., Brozkova K., Zaloudik J., Valik D., et al. (2008) *Identification of alphaB-crystallin, a biomarker of renal cell carcinoma by SELDI-TOF MS*. Int J Biol Markers 23: 48.
(337) Aoyama A., Steiger R.H., Frohli E., Schafer R., von D.A., Wiestler O.D., et al. (1993) *Expression of alpha B-crystallin in human brain tumors*. Int J Cancer 55: 760.
(338) Iwaki T., Iwaki A., Miyazono M., Goldman J.E. (1991) *Preferential expression of alpha B-crystallin in astrocytic elements of neuroectodermal tumors*. Cancer 68: 2230.
(339) Odreman F., Vindigni M., Gonzales M.L., Niccolini B., Candiano G., Zanotti B., et al. (2005) *Proteomic studies on low- and high-grade human brain astrocytomas*. J Proteome Res 4: 698.
(340) Mattila P.K., Lappalainen P. (2008) *Filopodia: molecular architecture and cellular functions*. Nat Rev Mol Cell Biol 9: 446.
(341) Aggeli I.K., Beis I., Gaitanaki C. (2008) *Oxidative stress and calpain inhibition induce alpha B-crystallin phosphorylation via p38-MAPK and calcium signalling pathways in H9c2 cells*. Cell Signal 20: 1292.
(342) Roux P.P., Blenis J. (2004) *ERK and p38 MAPK-activated protein kinases: a family of protein kinases with diverse biological functions*. Microbiol Mol Biol Rev 68: 320.
(343) Aldridge S.E., Lennard T.W., Williams J.R., Birch M.A. (2005) *Vascular endothelial growth factor acts as an osteolytic factor in breast cancer metastases to bone*. Br J Cancer 92: 1531.
(344) Konecny G.E., Meng Y.G., Untch M., Wang H.J., Bauerfeind I., Epstein M., et al. (2004) *Association between HER-2/neu and vascular endothelial growth factor expression predicts clinical outcome in primary breast cancer patients*. Clin Cancer Res 10: 1706.
(345) Gasparini G., Toi M., Gion M., Verderio P., Dittadi R., Hanatani M., et al. (1997) *Prognostic significance of vascular endothelial growth factor protein in node-negative breast carcinoma*. J Natl Cancer Inst 89: 139.
(346) Larsen A.K., Ouaret D., El O.K., Petitprez A. (2011) *Targeting EGFR and VEGF(R) pathway cross-talk in tumor survival and angiogenesis*. Pharmacol Ther 131: 80.
(347) Lichtenberger B.M., Tan P.K., Niederleithner H., Ferrara N., Petzelbauer P., Sibilia M. (2010) *Autocrine VEGF signaling synergizes with EGFR in tumor cells to promote epithelial cancer development*. Cell 140: 268.
(348) Ciardiello F., Troiani T., Bianco R., Orditura M., Morgillo F., Martinelli E., et al. (2006) *Interaction between the epidermal growth factor receptor (EGFR) and the vascular endothelial growth factor (VEGF) pathways: a rational approach for multi-target anticancer therapy*. Ann Oncol 17 Suppl 7: vii109-vii114.
(349) Chen Z., Ruan Q., Han S., Xi L., Jiang W., Jiang H., et al. (2014) *Discovery of structure-based small molecular inhibitor of alphaB-crystallin against basal-like/triple-negative breast cancer development in vitro and in vivo*. Breast Cancer Res Treat 145: 45.
(350) Rao G., Santhoshkumar P., Sharma K.K. (2008) *Anti-chaperone betaA3/A1(102-117)*

peptide interacting sites in human alphaB-crystallin. Mol Vis 14: 666.
(351) Li Z.J., Cho C.H. (2012) *Peptides as targeting probes against tumor vasculature for diagnosis and drug delivery*. J Transl Med 10 Suppl 1: S1.
(352) Macewan S.R., Chilkoti A. (2012) *Harnessing the power of cell-penetrating peptides: activatable carriers for targeting systemic delivery of cancer therapeutics and imaging agents*. Wiley Interdiscip Rev Nanomed Nanobiotechnol.
(353) Moktan S., Raucher D. (2012) *Anticancer activity of proapoptotic peptides is highly improved by thermal targeting using elastin-like polypeptides*. Int J Pept Res Ther 18: 227.
(354) Lee Y.J., Moon M.S., Kwon S.J., Rhee J.G. (2005) *Hypoxia and low glucose differentially augments TRAIL-induced apoptotic death*. Mol Cell Biochem 270: 89.
(355) Gatenby R.A., Gillies R.J. (2004) *Why do cancers have high aerobic glycolysis?* Nat Rev Cancer 4: 891.
(356) Alfarouk K.O., Muddathir A.K., Shayoub M.E. (2011) *Tumor acidity as evolutionary spite*. Cancers (Basel) 3: 408.
(357) Liu S., Yan B., Lai W., Chen L., Xiao D., Xi S., et al. (2014) *As a novel p53 direct target, bidirectional gene HspB2/alphaB-crystallin regulates the ROS level and Warburg effect*. Biochim Biophys Acta 1839: 592.
(358) Dent R., Trudeau M., Pritchard K.I., Hanna W.M., Kahn H.K., Sawka C.A., et al. (2007) *Triple-negative breast cancer: clinical features and patterns of recurrence*. Clin Cancer Res 13: 4429.
(359) Shastry M., Yardley D.A. (2013) *Updates in the treatment of basal/triple-negative breast cancer*. Curr Opin Obstet Gynecol 25: 40.
(360) Koletsa T., Stavridi F., Bobos M., Kostopoulos I., Kotoula V., Eleftheraki A.G., et al. (2014) *alphaB-crystallin is a marker of aggressive breast cancer behavior but does not independently predict for patient outcome: a combined analysis of two randomized studies*. BMC Clin Pathol 14: 28.
(361) Brower V. (2011) *Biomarkers: Portents of malignancy*. Nature 471: S19-S21.
(362) Badve S., Dabbs D.J., Schnitt S.J., Baehner F.L., Decker T., Eusebi V., et al. (2011) *Basal-like and triple-negative breast cancers: a critical review with an emphasis on the implications for pathologists and oncologists*. Mod Pathol 24: 157.
(363) Lehmann B.D., Bauer J.A., Chen X., Sanders M.E., Chakravarthy A.B., Shyr Y., et al. (2011) *Identification of human triple-negative breast cancer subtypes and preclinical models for selection of targeted therapies*. J Clin Invest 121: 2750.
(364) Fulford L.G., Reis-Filho J.S., Ryder K., Jones C., Gillett C.E., Hanby A., et al. (2007) *Basal-like grade III invasive ductal carcinoma of the breast: patterns of metastasis and long-term survival*. Breast Cancer Res 9: R4.
(365) Rodriguez-Pinilla S.M., Sarrio D., Honrado E., Hardisson D., Calero F., Benitez J., et al. (2006) *Prognostic significance of basal-like phenotype and fascin expression in node-negative invasive breast carcinomas*. Clin Cancer Res 12: 1533.
(366) Tsuda H., Takarabe T., Hasegawa F., Fukutomi T., Hirohashi S. (2000) *Large, central acellular zones indicating myoepithelial tumor differentiation in high-grade invasive ductal carcinomas as markers of predisposition to lung and brain metastases*. Am J Surg Pathol 24: 197.
(367) Hicks D.G., Short S.M., Prescott N.L., Tarr S.M., Coleman K.A., Yoder B.J., et al. (2006) *Breast cancers with brain metastases are more likely to be estrogen receptor negative, express the basal cytokeratin CK5/6, and overexpress HER2 or EGFR*. Am J Surg Pathol 30: 1097.
(368) Dewar R., Fadare O., Gilmore H., Gown A.M. (2011) *Best practices in diagnostic immunohistochemistry: myoepithelial markers in breast pathology*. Arch Pathol Lab Med

135: 422.
(369) Sopel M. (2010) *The myoepithelial cell: its role in normal mammary glands and breast cancer*. Folia Morphol (Warsz) 69: 1.
(370) Leibl S., Gogg-Kammerer M., Sommersacher A., Denk H., Moinfar F. (2005) *Metaplastic breast carcinomas: are they of myoepithelial differentiation?: immunohistochemical profile of the sarcomatoid subtype using novel myoepithelial markers*. Am J Surg Pathol 29: 347.
(371) Gusterson B. (2009) *Do 'basal-like' breast cancers really exist?* Nat Rev Cancer 9: 128.
(372) Boecker W., Buerger H. (2003) *Evidence of progenitor cells of glandular and myoepithelial cell lineages in the human adult female breast epithelium: a new progenitor (adult stem) cell concept*. Cell Prolif 36 Suppl 1: 73.
(373) Petersen O.W., Polyak K. (2010) *Stem cells in the human breast*. Cold Spring Harb Perspect Biol 2: a003160.
(374) Fornerod M., Ohno M., Yoshida M., Mattaj I.W. (1997) *CRM1 is an export receptor for leucine-rich nuclear export signals*. Cell 90: 1051.
(375) Strasser A., Dickmanns A., Schmidt U., Penka E., Urlaub H., Sekine M., et al. (2004) *Purification, crystallization and preliminary crystallographic data of the m3G cap-binding domain of human snRNP import factor snurportin 1*. Acta Crystallogr D Biol Crystallogr 60: 1628.
(376) Mitrousis G., Olia A.S., Walker-Kopp N., Cingolani G. (2008) *Molecular basis for the recognition of snurportin 1 by importin beta*. J Biol Chem 283: 7877.
(377) Kolb S.J., Battle D.J., Dreyfuss G. (2007) *Molecular functions of the SMN complex*. J Child Neurol 22: 990.
(378) Morimoto M., Boerkoel C.F. (2013) *The Role of Nuclear Bodies in Gene Expression and Disease*. Biology (Basel) 2: 976.
(379) Cauchi R.J. (2010) *SMN and Gemins: 'we are family' ... or are we?: insights into the partnership between Gemins and the spinal muscular atrophy disease protein SMN*. Bioessays 32: 1077.
(380) Dechat T., Pfleghaar K., Sengupta K., Shimi T., Shumaker D.K., Solimando L., et al. (2008) *Nuclear lamins: major factors in the structural organization and function of the nucleus and chromatin*. Genes Dev 22: 832.
(381) Gruenbaum Y., Margalit A., Goldman R.D., Shumaker D.K., Wilson K.L. (2005) *The nuclear lamina comes of age*. Nat Rev Mol Cell Biol 6: 21.
(382) Gonzalez-Suarez I., Redwood A.B., Gonzalo S. (2009) *Loss of A-type lamins and genomic instability*. Cell Cycle 8: 3860.
(383) Warren D.T., Shanahan C.M. (2011) *Defective DNA-damage repair induced by nuclear lamina dysfunction is a key mediator of smooth muscle cell aging*. Biochem Soc Trans 39: 1780.
(384) Ho C.Y., Lammerding J. (2012) *Lamins at a glance*. J Cell Sci 125: 2087.
(385) Foster C.R., Przyborski S.A., Wilson R.G., Hutchison C.J. (2010) *Lamins as cancer biomarkers*. Biochem Soc Trans 38: 297.

SUMMARY

αB-Crystallin, also known as HSPB5, is a member of the small heat shock family. In human, this family consists of 10 different members (HSPB1-10). Already in 1894 it was discovered that αB-crystallin is highly expressed in the eye lens of mammals. Later, it turned out that this protein is present in almost every tissue, especially in heart and muscle. Over the years, the function of this protein has been clarified. Cells contain many different proteins, which can be seen as 'the machines of the cell' that help the cells to perform their function. They can only work when they are folded in the correct way and may lose their proper folding when the cell is exposed to stress. Misfolded proteins are dangerous to the cell and are therefore trapped by chaperone proteins, which can refold these proteins or help them to be degraded via the ubiquitin-proteasome-system. When this system malfunctions, the misfolded proteins can accumulate and aggregate, leading to a dysfunctional cell. Eventually, this can lead to diseases such as Parkinson's, Huntington's and Alzheimer's disease.

αB-Crystallin expression is increased in cells that are exposed to several kinds of stress, like heat stress, osmotic stress, hypoxia/reoxygenation stress, oxidative stress and stress caused by exposure to heavy metals (***Chapter 1***). The elevated expression levels are beneficial as αB-crystallin, alone or together with other HSPBs, is capable of binding (partly) unfolded proteins. These proteins can then be refolded by other chaperone proteins (for example HSP40 and HSP70), which prevents the breakdown of these proteins (***Chapter 1***). In this way, cells may function normally again as soon as the stress is over. Because αB-crystallin is beneficial for a cell, it is also connected to the pathogenesis of cancer. A tumor is formed when cells exhibit uncontrolled cell division and do not want to die in a proper way. Tumors can be benign or malignant. Characteristics of benign tumors are their low grow rates, their inability to invade other tissues and their lack of spreading to other parts of the body. Malignant tumors have the propensity to grow fast and invade surrounding tissues causing damage. The first tumor that forms is called the primary tumor. Tumors that later appear in other parts of the body are called secondary tumors or metastases (***Chapter 2***). In ***Chapter 3*** we investigated whether and how αB-crystallin is involved in the development of head and neck squamous cell carcinoma (HNSCC). Previously, two studies were published about the presence of αB-crystallin in HNSCC and in both studies semi-quantitative methods were applied. One study showed that the presence of αB-crystallin could predict shorter survival of HNSCC patients, compared to patients with little or no αB-crystallin in their tumors. In the other study the amount of αB-crystallin did not affect the prognosis of the patient. To obtain more certainty about the role of αB-crystallin, a

quantitative method was used to determine whether or not the amount of αB-crystallin correlated with a worse prognosis for the patient. During a period of 10 years patients were followed to investigate whether the primary tumor recurred, tumors were formed nearby the primary tumor or metastases were formed. We found that patients with high levels of αB-crystallin in their tumor biopsies had a shorter life-span as they had a higher chance of metastasis formation. In ***Chapter 2*** the steps necessary for metastasis formation are explained, including cell migration through blood vessels from one part of the body to another. To facilitate this, important steps are increased cell motility and the formation of blood vessels (under influence of the VEGF protein). Previous research showed that αB-crystallin was present in the region of migrating pig epithelial lens cells and that it was necessary for cell migration. αB-Crystallin could therefore have an influence on cell motility. It had been shown before that more blood vessels were formed in damaged retina of mice when αB-crystallin was present in the cells, which was dependent on VEGF. To investigate this further, we determined if a decrease of the amount of αB-crystallin protein would influence the capacity of HNSCC cells to migrate or secrete VEGF. It was shown that the cells moved slower and secreted less VEGF when there was less αB-crystallin present. In other cells (HeLa cells) we increased the amount of αB-crystallin and these cells moved faster and secreted more VEGF. Thus, in case of a tumor, the presence of αB-crystallin might be associated with faster moving cells, which secrete more VEGF. This could contribute to metastasis formation.

Most solid tumors contain areas that are not well oxygenated (termed hypoxia), as described in ***Chapter 2***. This is due to a lack of or poorly developed blood vessels in the tumors. A shortage of oxygen is stressful for the cell. As the expression of αB-crystallin can be upregulated due to several kinds of stress, we analyzed the presence of αB-crystallin in hypoxic areas in HNSCC biopsies using two fluorescent dyes, one indicative for αB-crystallin and one for hypoxia, in ***Chapter 4***. As high proportions of the two dyes overlapped, we determined the influence of hypoxia on the expression of αB-crystallin mRNA and protein in HNSCC cells. We found that the amount of αB-crystallin decreased instead of increased. As explained in ***Chapter 2*** it is possible that sometimes blood flow stops and resumes in the poorly constructed blood vessels. This phenomenon is called hypoxia/reoxygenation. As a result of the sudden flow of oxygen, reactive oxygen species (ROS) can be formed. In ***Chapter 4*** experiments are described in which we first exposed HNSCC cells to hypoxia and then reoxygenated the cells. The amount of αB-crystallin mRNA and protein decreased upon hypoxia and increased again upon reoxygenation. To determine whether the increase is due to ROS, HNSCC cells were exposed to higher levels of ROS by adding H_2O_2 or lower levels by

adding a reagent that captures ROS. The amount of αB-crystallin mRNA was increased under influence of ROS and decreased when ROS was captured. When ROS was captured during the reoxygenation phase, the amount of αB-crystallin mRNA increased to a lesser extent. This means that αB-crystallin expression during the reoxygenation phase indeed can be upregulated by ROS. Next, we showed that αB-crystallin can help cells to survive hypoxia. It was already known that tumors with a high amount of hypoxic cells are prone to form metastases (***Chapter 2***). As αB-crystallin can help to retain cells in the hypoxic regions, αB-crystallin could also contribute to the formation of metastases in this way.

Another common type of cancer is breast cancer, which represents a very diverse group of tumors (***Chapter 2***). By studying the genes that are expressed in the breast tumor, a broad distinction can be made: tumors that show an expression pattern similar to normal breast cells, luminal A, luminal B, enriched for HER2 and the expression of basal-like genes (***Chapter 2***). These biomarkers are used to diagnose in an early stage or to improve treatment. Another subdivision that is used is based on the expression of certain types of receptors in the cells: the estrogen receptor (ER), the progesterone receptor (PR) and the HER2 receptor (***Chapter 2***). There are breast tumors that do not express any receptor, these are called 'triple-negative'. The triple-negative tumors often show a basal-like gene expression pattern and patients often have a worse prognosis. As described above, the presence of αB-crystallin also is an indication for a worse prognosis. In ***Chapter 5*** we determined if the expression of αB-crystallin correlates with the expression of genes which are linked to the development of tumors (pERK1/2, pAKT, pmTOR, EGFR and IGF-1R). It was studied as well if αB-crystallin correlates with triple-negativity and the expression of basal-like genes (CK5/6 and SMA). For this purpose we used tissue microarrays (TMA), which allow analyzing different biopsies simultaneously. αB-Crystallin indeed correlated with both triple-negativity and the expression of basal-like genes. This could mean that patients with a high amount of αB-crystallin in their tumor biopsies would not benefit from medication directed against the ER, PR and/or the HER2-receptor, as chances are high that these receptors are not present in those tumors. For these patients another therapy could be considered. As the cells do contain αB-crystallin, the therapy could be directed against this protein. Recently, a peptide was developed, that can disrupt the interaction between αB-crystallin and VEGF (***Chapter 7***). This peptide slowed down tumor growth and the development of blood vessels. Possibly, this approach could be applied in the treatment of (breast) cancer.

The function of proteins can be altered by amendments in the proteins, called post-translation modifications. The function of the αB-crystallin protein can be amended by

adding a phosphate group at three different positions in the protein, serine 19, 45 and 59 (***Chapter 1***). When serine 59 becomes phosphorylated, αB-crystallin is transported from the cytoplasm to the nucleus. Phosphorylation of serine 45 results in the accumulation of αB-crystallin in certain nuclear structures, called speckles. How αB-crystallin is translocated to the nucleus and what the function is in the speckles was not known. In ***Chapter 6***, we first analyzed how αB-crystallin ends up in the nucleus. Using a technique called 'yeast two-hybrid screening', we found that αB-crystallin, of which the phosphorylation of the three serine residues was mimicked (αB-STD), can bind a protein called Gemin3. This protein is part of the so-called SMN complex. This complex was already known to be involved in nuclear import of proteins. A decrease of the amount of Gemin2 (another protein in the SMN complex) and Gemin3 resulted in less αB-STD speckles in the nucleus. To obtain information about the function of the speckles, we studied what the result of cell stress was on the distribution of αB-crystallin in the nucleus. We overexpressed αB-STD in HeLa cells and heated the cells for 45 minutes at 45^{o}C (heat-shock) after which the cells were returned to 37^{o}C. Directly and 6 hours after heat shock, αB-STD was diffusely distributed throughout the nucleus. After 24 hours, αB-STD was present in the speckles again. To determine whether nuclear αB-crystallin has chaperone activity, another protein (luciferase) was overexpressed in the nucleus. After heat-shock, the function of this protein was restored faster when αB-STD was present. These results suggest that phosphorylated αB-crystallin is stored in the speckles until it is needed. Under the influence of stress it is released from the speckles and can bind poorly-folded proteins. This way nuclear αB-crystallin helps these proteins to become re-folded and functional again.

It is clear that αB-crystallin is a very versatile protein that can function in the cytoplasm as well as the nucleus. It is also clear that this protein can contribute to metastasis formation of (HNSCC) tumors. In this thesis, cellular processes are described that can be involved: increase of cell motility, increase of VEGF secretion and helping cell survival after hypoxia. The molecular mechanisms still have to be elucidated. It is therefore important that the contribution of αB-crystallin in these processes will be studied further.

SAMENVATTING

αB-Crystalline, ook wel HSPB5 genoemd, behoort tot de familie van kleine *'heat-shock*' eiwitten. Bij de mens bestaat deze familie uit 10 verschillende leden (HSPB1-10). Al in 1894 is ontdekt dat αB-crystalline veel voorkomt in de ooglens van zoogdieren. Later is gebleken dat αB-crystalline in bijna elk weefsel aanwezig is, met name in het hart en in spieren. De functie van dit eiwit werd in de loop der jaren opgehelderd. Cellen bevatten zeer veel verschillende eiwitten, die de 'machines van de cel' worden genoemd en ervoor zorgen dat de cel kan functioneren. Ze kunnen hun werk slechts doen als ze op de juiste manier gevouwen zijn. Ze kunnen echter hun structuur verliezen wanneer de cel blootgesteld wordt aan stress. Slecht gevouwen eiwitten zijn gevaarlijk voor de cel en worden daarom opgevangen door zogeheten chaperonne eiwitten, die proberen de eiwitten te hervouwen of af te laten breken door middel van het zogenaamde ubiquitine-proteasoom-systeem. Als dit niet goed gebeurt kunnen de slecht gevouwen eiwitten zich gaan ophopen en samenklonteren, waardoor de cel niet meer normaal functioneert. Uiteindelijk kunnen hierdoor ziektes ontstaan, zoals de ziekte van Parkinson, Huntington en Alzheimer.
αB-Crystalline komt verhoogd tot expressie in cellen die blootgesteld zijn aan verschillende soorten stress, zoals hittestress, osmotische stress, hypoxie/reoxygenering stress, oxidatieve stress en stress veroorzaakt door de blootstelling aan zware metalen (***Hoofdstuk 1***). De verhoogde aanwezigheid bij stress is gunstig, omdat αB-crystalline, alleen of in samenwerking met andere HSPBs, in staat is om (deels) ontvouwen eiwitten te binden. Hierna kunnen deze eiwitten door andere chaperonne eiwitten (bijvoorbeeld HSP40 en HSP70) weer teruggevouwen worden in de juiste structuur en hoeven dus niet te worden afgebroken (***Hoofdstuk 1***). De cel is op deze manier na blootstelling aan stress zo snel als mogelijk weer in staat normaal te functioneren. Omdat de aanwezigheid van αB-crystalline gunstig is voor de cel wordt dit ook in verband gebracht met het ontstaan van verschillende soorten kanker. Kanker ontstaat wanneer de celdeling op hol slaat en cellen niet op de reguliere manier doodgaan. Tumoren kunnen goedaardig en kwaadaardig zijn. Kenmerken van goedaardige tumoren zijn dat ze langzaam groeien, ze geen andere weefsels binnendringen en zich niet verder verspreiden in het lichaam. Kwaadaardige tumoren hebben de neiging om heel snel te groeien. Ze dringen ook de nabijgelegen weefsels en organen binnen, waardoor deze beschadigd raken. De tumor die zich het eerst ontwikkelt, heet de primaire tumor. Tumoren die zich later ontwikkelen in andere delen van het lichaam (uitzaaien) heten secundaire tumoren of metastasen (***Hoofdstuk 2***). In ***Hoofdstuk 3*** van dit proefschrift hebben we gekeken of en hoe het eiwit αB-crystalline een rol kan

spelen bij de ontwikkeling van kwaadaardige hoofd-/halskanker (in het Engels *head and neck squamous cell carcinoma* genoemd, afgekort HNSCC). Over het voorkomen van αB-crystalline in HNSCC tumoren zijn al twee studies gepubliceerd, waarbij gebruik is gemaakt van semi-kwantitatieve analysemethoden. Een van deze studies liet zien dat de aanwezigheid van αB-crystalline zou kunnen voorspellen dat patiënten met HNSCC korter leven dan patiënten met weinig of geen αB-crystalline in hun tumoren. In de andere studie werd het verband tussen prognose en de hoeveelheid aB-crystalline niet gevonden. Om meer duidelijkheid te krijgen over de rol van αB-crystalline is in ***Hoofdstuk 3*** op een kwantitatieve manier geanalyseerd of de hoeveelheid αB-crystalline in een primair tumorbiopt correleerde met een slechtere prognose voor de patiënt. Er is bij patiënten met HNSCC gedurende een periode van 10 jaar onderzocht of de primaire tumor terugkeerde, of er tumoren in de buurt van de primaire tumor werden gevormd, of dat er metastasen gevormd werden. Het bleek dat patiënten met veel αB-crystalline in het primaire tumorbiopt korter leefden, omdat ze een grotere kans hadden om metastasen te ontwikkelen. In ***Hoofdstuk 2*** wordt uitgelegd welke stappen er nodig zijn voor de vorming van metastasen, waaronder celmigratie door bloedvaten van de ene plek naar de andere plek in het lichaam. Onder andere verhoogde celmotiliteit (vermogen tot beweging van een cel) en de aanmaak van bloedvaten (onder invloed van onder andere het VEGF eiwit) zijn hiervoor belangrijk. Uit eerder onderzoek is gebleken dat αB-crystalline aanwezig was op plekken in migrerende varkenslens epitheelcellen die nodig zijn voor de celmigratie. αB-Crystalline zou dus invloed kunnen hebben op celmotiliteit. Verder is er reeds een onderzoek uitgevoerd dat liet zien dat er meer nieuwe bloedvatvorming in beschadigde retina van muizen plaatsvond wanneer er αB-crystalline in deze cellen aanwezig was. Deze bloedvatvorming was afhankelijk van VEGF. Om dit verder te onderzoeken is door ons geanalyseerd of een verlaging van de hoeveelheid αB-crystalline zowel invloed had op het vermogen van HNSCC cellen om te migreren als op het vermogen om VEGF uit te scheiden. De cellen bleken langzamer te bewegen en minder VEGF uit te scheiden wanneer er minder αB-crystalline aanwezig was. In andere cellen (HeLa cellen) is de hoeveelheid αB-crystalline juist verhoogd. Deze cellen bleken sneller te bewegen en meer VEGF uit te scheiden. In het geval van een tumor zou de aanwezigheid van veel αB-crystalline dus ook sneller bewegende cellen en een hogere VEGF productie kunnen betekenen, wat een bijdrage zou kunnen leveren aan de vorming van metastasen.

Zoals beschreven in ***Hoofdstuk 2***, zijn er in de meeste solide tumoren plekken aanwezig met weinig zuurstof (hypoxie genoemd). Dit komt doordat er te weinig of slecht gevormde bloedvaten in de tumoren aanwezig zijn. Een tekort aan zuurstof is

stressvol voor de cel en de expressie van αB-crystalline kan verhoogd worden door verschillende soorten stress. Daarom hebben in ***Hoofdstuk 4*** in HNSCC biopten de aanwezigheid van αB-crystalline in hypoxische gebieden geanalyseerd middels het aankleuren van hypoxie en αB-crystalline met verschillende fluorescerende stoffen. Omdat er in hoge mate overlap werd gevonden, hebben we vervolgens bestudeerd welke invloed hypoxie heeft op de hoeveelheid αB-crystalline mRNA en αB-crystalline eiwit in HNSCC cellen. Het bleek dat hypoxie de hoeveelheid αB-crystalline juist verlaagt in plaats van verhoogt. Zoals uitgelegd in ***Hoofdstuk 2*** kan het mogelijk zijn dat er toch af en toe bloed stroomt door de vaak slecht aangelegde bloedvaten in tumoren. Dit wordt hypoxie/reoxygenatie genoemd. Door de plotselinge toevoer van zuurstof kunnen reactieve zuurstofdeeltjes (*reactive oxygen species*, ROS genoemd) ontstaan. In ***Hoofdstuk 4*** worden experimenten beschreven, waarin HNSCC cellen hypoxisch zijn gemaakt en daarna weer zuurstof aan de cellen is toegevoegd. De hoeveelheid αB-crystalline mRNA en eiwit bleek omlaag te gaan bij hypoxie en juist weer omhoog bij reoxygenatie. Om na te gaan of ROS de oorzaak is van deze verhoging, werden HNSCC cellen blootgesteld aan hogere hoeveelheden ROS door het toevoegen van H_2O_2 of aan een verlaging van de hoeveelheid door het toevoegen van een stofje wat ROS wegvangt. De hoeveelheid αB-crystalline mRNA in de cel bleek omhoog te gaan onder invloed van ROS en omlaag bij het wegvangen van ROS. Als ROS werd weggevangen tijdens de reoxygenatiefase ging de hoeveelheid αB-crystalline mRNA minder omhoog. Dit wil zeggen dat αB-crystalline expressie tijdens reoxygenatie dus inderdaad gereguleerd kan worden door ROS. Daarna hebben we aangetoond dat αB-crystalline cellen die last hebben van hypoxie kan helpen overleven. Het was reeds bekend dat tumoren met veel hypoxische cellen vaker metastaseren (***Hoofdstuk 2***). Omdat αB-crystalline cellen in hypoxische regio's kan helpen overleven, zou αB-crystalline dus ook kunnen bijdragen aan de ontwikkeling van metastasen.

Een andere veelvoorkomende kanker is borstkanker, die uit een heel diverse groep van tumoren bestaat (***Hoofdstuk 2***). Door na te gaan welke genen tot expressie komen in borsttumoren, kan er een brede onderverdeling worden gemaakt: tumoren die een expressiepatroon laten zien zoals normaal in de borst, luminaal A en B, verrijkt voor HER2 en expressie van '*basal-like*' genen (***Hoofdstuk 2***). Deze biomarkers worden gebruikt om in een zo vroeg mogelijk stadium een diagnose te kunnen stellen en ook voor het verbeteren van de behandeling. Een andere manier voor de onderverdeling van borsttumoren is het aantonen van bepaalde receptoren (signaalontvangers) in de tumorcellen: de oestrogeenreceptor (ER), de progesteronreceptor (PR) en de HER2-receptor (***Hoofdstuk 2***). Er zijn borsttumoren waarbij alle drie de receptoren niet tot

expressie komen. Deze tumoren worden 'triple-negatief' genoemd. De triple-negatieve tumoren laten vaak het *basal-like* genexpressiepatroon zien en patiënten met dit type tumor hebben een slechtere prognose. Omdat, zoals hierboven beschreven, de aanwezigheid van αB-crystalline ook een indicatie is voor een slechtere prognose, is in ***Hoofdstuk 5*** bepaald of de expressie van αB-crystalline correleerde met de expressie van genen die in verband worden gebracht met het ontstaan van tumoren (pERK1/2, pAKT, pmTOR, EGFR en IGF-1R). Hierbij is ook geanalyseerd of αB-crystalline correleerde met 'triple-negativiteit' en met de expressie van *basal-like* genen (CK5/6 en SMA). Dit is gedaan met *tissue microarrays* (TMA), waarbij vele verschillende biopten tegelijkertijd aangekleurd en bestudeerd kunnen worden. αB-Crystalline expressie bleek inderdaad gecorreleerd met 'triple-negativiteit' en met de expressie van de *basal-like* genen. Dit zou kunnen betekenen dat patiënten met veel αB-crystalline in hun tumorbiopt geen baat hebben bij medicijnen die werken tegen de ER-, PR- en/of de HER2-receptor, omdat de kans groot is dat deze receptoren niet aanwezig zijn in de tumorcellen. Voor deze patiënten kan dan een andere therapie overwogen worden. Omdat de cellen dus αB-crystalline bevatten, zou deze therapie bijvoorbeeld tegen dit eiwit gericht kunnen zijn. Recentelijk is er een peptide ontwikkeld, die de binding tussen αB-crystalline en VEGF verstoort (***Hoofdstuk 7***). Deze peptide bleek de tumorgroei en aanmaak van bloedvaten te kunnen remmen. Mogelijk zou deze aanpak dus gebruikt kunnen worden bij de behandeling van (borst)kanker.

De functie van eiwitten kan worden aangepast door kleine veranderingen aan te brengen, post-translationele modificaties genoemd. De functie van het αB-crystalline-eiwit kan aangepast worden door op drie verschillende posities een fosfaatgroep te plaatsen (fosforylering genoemd), namelijk op serine 19, serine 45 en serine 59 (***Hoofdstuk 1***). Wanneer serine 59 wordt gefosforyleerd, kan αB-crystalline verplaatst worden van het cytoplasma naar de nucleus. Fosforylering van serine 45 leidt ertoe, dat αB-crystalline zich in de kern ophoopt in bepaalde structuren, '*speckles*' genoemd. Hoe αB-crystalline wordt verplaatst naar de kern en wat de functie is van αB-crystalline in de *speckles* was nog niet bekend. In ***Hoofdstuk 6*** hebben we eerst geanalyseerd hoe αB-crystalline in de kern terecht kan komen. Door middel van een techniek die '*yeast two-hybrid screening*' wordt genoemd, hebben we gevonden dat αB-crystalline, met nagebootste fosforylering op de drie eerder genoemde posities (αB-STD) kan binden aan een eiwit dat Gemin3 wordt genoemd. Dit eiwit maakt onderdeel uit van het zogenaamde SMN complex. Van dit complex was al bekend dat het betrokken is bij kernimport van eiwitten. Verlaging van de hoeveelheid Gemin2 eiwit (een ander eiwit uit het SMN complex) en Gemin3 eiwit bleek tot minder αB-STD *speckles* in de celkern te leiden. Om informatie te krijgen over de functie van αB-crystalline in de

celkern hebben we vervolgens bestudeerd wat celstress doet met de distributie van αB-crystalline. We hebben dit gedaan door αB-STD tot overexpressie te brengen in HeLa cellen en deze 45 minuten bij 45^{o}C te verhitten (*heat-shocken*) en daarna weer terug te brengen tot 37^{o}C. Direct en 6 uur na de *heat-shock* was αB-STD diffuus vespreid door de kern. Na 24 uur was αB-STD weer in de *speckles* te vinden. Om the bepalen of αB-crystalline in de kern ook chaperonne activiteit heeft, werd een ander eiwit (luciferase) in de kern tot overexpressie gebracht. Het bleek dat de functie van dit eiwit na een *heat-shock* sneller werd hersteld in aanwezigheid van αB-STD. Deze resultaten suggereren dat gefosforyleerd αB-crystalline in de *speckles* opgeslagen wordt totdat dit eiwit nodig is. Onder stress komt αB-crystalline dan vrij uit de *speckles* en kan het de slecht gevouwen eiwitten binden, zodat deze eiwitten uiteindelijk weer teruggevouwen kunnen worden in de juiste structuur en weer functioneel zijn.

Het is duidelijk dat αB-crystalline een zeer veelzijdig eiwit is, dat zowel in het cytoplasma als in de celkern zijn functie kan uitoefenen. Het is ook evident dat dit eiwit kan bijdragen aan het uitzaaien van (HNSCC) tumoren. In dit proefschrift staan cellulaire processen beschreven, die hierbij betrokken kunnen zijn: verhoging van celmotiliteit, verhoogde uitscheiding van VEGF en het helpen van cellen bij de overleving van hypoxie. De moleculaire mechanismen die hiertoe leiden moeten nog opgehelderd worden. Het is daarom belangrijk dat de bijdrage van αB-crystalline aan deze processen verder bestudeerd wordt.

CURRICULUM VITAE

Chantal van de Schootbrugge werd geboren op 21 augustus 1983 te Nunspeet. In 2001 behaalde zij haar VWO-diploma aan het Nuborgh College Lambert Franckens te Elburg, waarna ze begon aan de studie Moleculaire Levenswetenschappen aan de Katholieke Universiteit Nijmegen, later Radboud Universiteit Nijmegen. Tijdens deze studie heeft ze tweemaal een wetenschappelijke stage gelopen, in 2004/2005 op de afdeling Moleculaire Dierfysiologie onder begeleiding van Prof. G. Martens en in 2005/2006 op de afdeling Autoimmuun Biochemie (het huidige Biomoleculaire Chemie) onder begeleiding van Dr. G. J. M. Pruijn. In 2006 is zij *cum laude* afgestudeerd. Van 2006 tot 2007 heeft ze als onderzoeker in opleiding gewerkt op de afdeling Kindergeneeskunde van het Radboud Universitair Medisch Centrum. Daarna heeft ze van 2007 tot 2012 gewerkt als promovenda op de afdeling Biomoleculaire Chemie van de Radboud Universiteit Nijmegen, onder begeleiding van Prof. G. J. M. Pruijn en Dr. W.C. Boelens in samenwerking met de afdeling Radiotherapie van het Radboud Universitair Medisch Centrum onder begeleiding van Prof. J.H.A.M. Kaanders en Dr. J. Bussink. Gedurende deze periode werd het onderzoek verricht dat is beschreven in dit proefschrift. In de eerste helft van 2013 heeft ze het 'Regulatory Affairs' traineeship gevolgd bij Zwiers Regulatory Consultancy in Oss. Sinds augustus 2013 is ze werkzaam als 'Regulatory Project Leader' bij het College ter Beoordeling van Geneesmiddelen in Utrecht.

PUBLICATIES

van de Schootbrugge C., Boelens W.C. (2011): *Introduction to Small Heat Shock Proteins.* In: Simon S., Arrigo A.P., editors. Small Stress Proteins and Human Diseases. Nova Science Publishers: 1

van de Schootbrugge C.; Bussink J., Span P.N., Sweep F.C., Grenman R., Stegeman H., Pruijn G.J., Kaanders J.H.A.M., Boelens W.C. (2013): *alphaB-crystallin stimulates VEGF secretion and tumor cell migration and correlates with enhanced distant metastasis in head and neck squamous cell carcinoma.* BMC Cancer 13: 128

van de Schootbrugge C., van Asten F., Nagtegaal I.D., Versleijen-Jonkers Y.M., van Laarhoven H.W., Roeffen M.H., Sweep F.C., Bussink J., Kaanders J.H., Pruijn G.J., Boelens W.C., Span P.N. (2013): *αB-crystallin expression is correlated with phospho-ERK1/2 expression in human breast cancer.* Int J Biol Markers 28: 365

den Engelsman J., **van de Schootbrugge C.**, Yong J, Pruijn G.J., Boelens W.C. (2013): *Pseudophosphorylated αB-crystallin is a nuclear chaperone imported into the nucleus with help of the SMN complex.* PLoS One 8: 73489

van de Schootbrugge C., Schults E.M., Bussink J., Span P.N., Grénman R., Pruijn G.J., Kaanders J.H., Boelens W.C. (2014): *Effect of hypoxia on the expression of αB-crystallin in head and neck squamous cell carcinoma.* BMC Cancer 14: 252

DANKWOORD

Zo. Ik ben er klaar mee. Letterlijk en figuurlijk! Maar niet voordat ik de mensen heb bedankt zonder wie ik dit proefschrift niet had kunnen voltooien, door de kennis die ze gedeeld hebben of de morele support die ze geboden hebben.

Beste Wilbert, ik ken bijna geen optimistischer persoon dan jij. Waar ik 'te kritisch' kon zijn of resultaten 'kapot kon analyseren', zag jij altijd een mogelijkheid om verder te kijken, waardoor er nu uiteindelijk toch een boekje ligt. Heel erg bedankt hiervoor! En ik bewonder je enthousiasme voor de wetenschap!

Beste Ger, heel erg bedankt dat ik na mijn stage (bij de 'oude' afdeling Autoimmuun Biochemie) weer aan de slag kon bij de 'nieuwe' afdeling Biomoleculaire Chemie. Een afdeling met zeer divers onderzoek, waardoor er toch altijd weer met een frisse blik naar mijn onderzoeksresultaten werd gekeken. Alle input tijdens de werkbesprekingen en brainstormavonden hebben enorm geholpen!

Beste Lettie, hoe kan iemand nou zoveel weten? Ook bedankt voor alle input die je hebt gegeven!

Hans en Jan, bedankt. Zonder de biopten en UT-SCC cellijnen, die ik heb mogen gebruiken, was een groot deel van mijn onderzoek niet mogelijk geweest. Paul, bedankt voor de prettige samenwerking! Dankzij jou is hoofdstuk 5 van dit proefschrift een feit en kon ik toch aan de 'vier gepubliceerde onderzoekshoofdstukken'-eis voldoen. Ook dank aan alle medewerkers van radiotherapie de me hebben geholpen bij mijn onderzoek.

Lieve Els, het is fijn als mensen aan je denken als het goed gaat, maar nog fijner als iemand dat doet als het niet goed gaat! Het feit dat ik altijd alles tegen je heb kunnen zeggen, zonder erom veroordeeld te worden, heeft heel veel geholpen. Heel erg bedankt voor alle dingen die je voor me hebt gedaan, tijdens mijn 'officiële' promotietijd en erna!

Ex-BMCers Joyce, Sanne, Lonneke, Remon (en Mariska) leuk dat we ook nu nog steeds contact hebben! Dames, de high teas houden we erin! (Prinses) Joyce, ik ben zo blij dat je je droombaan hebt gevonden in Maastricht. Lonneke, na een omzwerving via Italië, gelukkig weer terug in Arnhem. Misschien stranden we weer eens samen als de

treinen vanuit Utrecht weer eens een keer niet rijden ;-) Sanne, heel veel geluk samen met Walter in Mainz en bij BioNTech Diagnostics. Remon en Mariska, hoe kan ik jullie nu niet samen noemen ☺. Alle geluk in jullie prachtige huis in Lithoijen enne, het wordt weer tijd voor een (nachtelijk) dansfeestje :-P Sandy, ook al zit je in het verre Amerika, dankzij Facebook lijkt het toch niet zó ver weg! Raymond, óók al zo ver weg daar in Kiwiland! Maar toch ook niet helemaal weg dankzij alterego 'Blehfaceboek'. Tamara, you seem perfectly happy back in Croatia. I hope to see you again one day, if only for some catching up in our old time favorite restaurant Romagna! Ook alle andere BMC oud-collega's wil ik graag bedanken voor de leuke tijd op het lab én daarbuiten (Aesculaaf, labstap, dagjes uit, kampeertrips, filmpjes, etentjes of borrels): Angelique, Annemarie, Bas, Carla O., Carla W., Geurt, Helma, Ilmar, Judith, Kalok, Marina, Merel, Sander, Siebe en Tim.

Studenten begeleiden was een aangename afwisseling met het labwerk en van jullie heb ik ook weer veel geleerd. Sjoerd, Simone, Floor en Elma, heel erg bedankt hiervoor! Elma, dankzij jouw doorzettingsvermogen hebben we hoofdstuk 4 van dit proefschrift toch kunnen publiceren!

Ook wil ik Alex Zwiers en Karin Ruijtenbeek bedanken, omdat ze mij de kans hebben gegeven het 'Regulatory Affairs' traineeship te volgen bij Zwiers Regulatory Consultancy. Ik heb hier echt een heel leerzame en gezellige tijd gehad, alle medewerkers bedankt hiervoor! In het bijzonder wil ik natuurlijk de twee mede-trainees Fatima en Çiğdem bedanken. Jullie hebben ook zeker wat van mijn proefschriftfrustraties meegekregen... Maar wat hebben we een lol gehad, met als hoogtepunt de bruiloft in Ankara! En uiteindelijk hebben we hier alle drie ook nog eens een superleuke baan aan overgehouden!

Een baan bij het CBG dus. Wat een fijne organisatie om voor te mogen werken! Ik wil daarom mijn (farmacotherapeutische groep-2) collega's bedanken. De RPL'en voor alle tijd die ze in me hebben gestoken om mij het RPL vak te leren (en nog steeds!). Wat een ontzettend veelzijdig beroep, geen dag is hetzelfde. Heerlijk! Natuurlijk ook bedankt voor de gezelligheid, ik voelde me gelijk thuis in de groep. De beoordelaars bedankt voor de ontzettend prettige samenwerking. Door overleg is er zoveel te bereiken. En Jaap voor het vertrouwen om mij als 'jonge' RPL toch al veel verantwoordelijkheid te geven, zoals spreken op de commissie praktijkavond en deelname aan de Wetenschappelijk Advies commissie en Werkgroep Nationaal.

Gelukkig is er naast het werk ook nog zoiets als een sociaal leven, onontbeerlijk! Natuurlijk is er in dit dankwoord dan ook een plekje gereserveerd voor studievriendinnetjes Marij, Teunie, Emmy en Cynthia. Altijd geïnteresseerd hoe het met 'm'n boekie' stond en bereid om me op te beuren als ik het niet meer zag zitten ☺. Ook al zijn we alle vijf heel verschillend, toch brengen we nog steeds heel wat leuke avondjes door met verjaardagen, etentjes en dansjes in Utrecht, Gent en Ibiza!

Renske en Ronald, fijne vrienden van 'Hoogeveldt gang 27'. Ik denk nog altijd met een warm gevoel aan deze tijd terug en geniet nog steeds van onze bijklets- en saunamomenten!

Lenneke, lief vriendinnetje, ook al woon je in het 'verre' Haarlem, we hebben altijd weer de grootste lol als we afspreken! Ook al denken we terug aan 'toen in 2011' ;-).

De 'Nunspeet-gang': Edwin, Richard en Eric! Na al die jaren nog steeds contact! Af en toe een middagje bijkletsen in ons geliefde Nunspeet enne Eric, mijn technomaatje! Wat hebben we toch heerlijke dagen en nachten doorgedanst. Daar ben ik nog làààààààng niet klaar mee!!!

Tim, Lyette, Stephanie, Remco, Leonie en Jeroen, ik kijk alweer uit naar het volgende (bioscoop)filmavondje, 80's/90's feestje of sushi/dans-event!

Joost en Marjon, naast het samenwerken bij het CBG hebben we het daarbuiten ook erg gezellig met bijkletsetentjes/kroegavondjes of dansen (in Groningen). Joost, succes met je 'tweede fulltime baan' studeren en Marjon, ik blijf me verbazen waar je de tijd vandaan haalt voor je duobaan beoordelaar/onderzoeker Dermatologie bij het UMCG!

Thanks Çiğdem (you Dutchy!!!) for being such a wonderful friend! I always enjoy the times we spend chatting, shopping and eating (cannot recall how many times we ate at Sumo Utrecht or Tai Soen any more) and so on! I am glad that Philipp will be coming to Europe soon, and we remain in touch definitely when you are moving across Europe. But first things first, delighted that you are still in The Netherlands and that you have agreed to be my paranymph!

Lieve Michelle, wat hebben we samen al een hoop meegemaakt! Hele leuke, maar ook minder leuke dingen. Maar we slaan ons er altijd weer doorheen ☺ Zoals je al eens hebt opgemerkt: ‘Wij doen niet aan zussendag, wij doen aan zussenjaar!’, van avondjes

kletsen en hangen op de bank, koken, terrassen, avondjes dansen tot zussenweekenden weg, we hebben het altijd gezellig! Ik ben trots dat je je (bijna) 'Master of Arts' mag noemen in Communicatie en Beïnvloeding! Zeker niet makkelijk geweest... ook hier... de laatste loodjes!!!! En ik ben natuurlijk superblij dat je mijn paranimf wilt zijn!

Lieve Bas, ‘pas’ in oktober 2014 op mijn pad gekomen maar het lijkt al zoveel langer ☺ Wat ben ik blij met jou! De laatste loodjes wegen zeker het zwaarst. Jij hebt me zo ontzettend gesteund! Alle keren dat ik in de avonden na werktijd en in de weekenden weer aan de slag moest wist je me altijd weer op te vrolijken! We hebben al zoveel fijne dingen gedaan en meegemaakt en daar komt nog veel meer bij! Maar ook een gewoon avondje thuis voor de buis is heel erg fijn met jou. HVJ!

Lieve pap en mam! Wat ben ik ontzettend gek op jullie! Mam, je bent de meest lieve en verzorgende persoon die ik ken. Je hebt altijd zoveel voor je moeder, broers en zussen moeten doen en dat zonder morren. Daar heb ik heel veel respect voor. En in 2013 ook nog eens je MBO-diploma Verzorgende gehaald (past natuurlijk perfect bij je), fantastisch! En pap, niets is zo moeilijk als veranderen en toch heb je dat voor elkaar gekregen. Heel erg knap! Enne, als we langskomen ligt de kelder altijd weer vol met door jou meegenomen versnaperingen, des Schootbrugges! ‘Hmmmmm, lekker’! We houden allemaal van dezelfde humor en gezelligheid, daarom kom ik nog steeds altijd heel erg graag bij jullie langs! Kletsen, wandelen met de lieve Guc, een spelletje doen of een filmpje kijken, we vervelen ons nooit!

Dit boekje is voor jullie, want wie had dit nu ooit gedacht, lang geleden in 1983…;-)

ISBN 9789462596399